Full-Duplex Relay Based Energy Harvesting Wireless Networks

by

Syed Adil Abbas Kazmi

A Dissertation Submitted to the
Graduate School of Sciences and Engineering
in Partial Fulfillment of the Requirements for
the Degree of

Doctor of Philosophy

in

Electrical and Electronics Engineering

KOÇ ÜNİVERSİTESİ

January, 2022

Full-Duplex Relay Based Energy Harvesting Wireless Networks

Koç University

Graduate School of Sciences and Engineering

This is to certify that I have examined this copy of a doctoral dissertation by

Syed Adil Abbas Kazmi

and have found that it is complete and satisfactory in all respects,

and that any and all revisions required by the final

examining committee have been made.

Committee Members:

Prof. Dr. Sinem Çöleri (Advisor)

Prof. Dr. Ertuğrul Başar

Prof. Dr. Öznur Özkasap

Prof. Dr. Özgür Gürbüz

Prof. Dr. İbrahim Altunbaş

Date:

To my Father, who lost his life fighting Covid; I love you, Papa.

ABSTRACT

Full-Duplex Relay Based Energy Harvesting Wireless Networks
Syed Adil Abbas Kazmi
Doctor of Philosophy in Electrical and Electronics Engineering
January, 2022

According to the recent Ericsson mobility report, 24.6 billion IoT (Internet-of-Things) devices are expected to be installed by 2025. Increasing the lifetime of this massive battery-powered installation can only be achieved by using low power transceivers with energy harvesting capability. For this purpose, we investigate the resource allocation in full-duplex (FD) relay-based wireless powered cooperative communication networks (WPCCN), and Simultaneous Wireless Information and Power Transfer (SWIPT) networks. In the SWIPT network, the nodes are able to receive data and harvest energy to recharge their batteries simultaneously by using the same radio frequency (RF) signal from the hybrid access point (HAP). In WPCCN, energy is transferred in the downlink from the HAP to the nodes and information is transmitted in the uplink from the nodes to the HAP. We consider novel optimization frameworks for the optimization of time allocation, scheduling and relay selection.

In the first part of the thesis, we work on FD-WPCCN. First, we study the transmission time minimization and throughput maximization optimization problems through relay selection. Then, we incorporate the on-off transmission scheme in FD-WPCCN and investigate the transmission time minimization and throughput maximization problems by using scheduling and relay selection.

In the second part of the thesis, we work on the FD-SWIPT network. First, we provide the outage analysis of an FD relay-based system and present the optimization problems for the outage throughput and energy efficiency maximization. Then, we extend the system model to a more practical multi-relay-user FD multiple-input-multiple-output (MIMO) system incorporating self-energy recycling. Self-energy recycling exploits the self-interference that arises due to the FD mode. We present the resource allocation and relay selection optimization framework with the objective of maximizing the sum-throughput in a SWIPT FD MIMO system.

ÖZETÇE

Tam Çift Yönlü Röle Tabanlı Enerji Hasatı Kablosuz Ağlar
Syed Adil Abbas Kazmi
Elektrik ve Elektronik Mühendisliği, Doktora
Ocak 2022

Ericsson mobilite raporuna göre, 2025 yılına kadar 24,6 milyar sensör düğümünün kurulması bekleniyor. Bu devasa pille çalışan kurulumun ömrünü artırmak ancak enerji toplama kapasitesine sahip düşük güçlü alıcı-vericiler kullanılarak elde edilebilir. Bu amaçla, tam çift yönlü (FD) röle tabanlı kablosuz destekli işbirliği iletişim ağlarında (WPCCN) ve Eşzamanlı Kablosuz Bilgi ve Güç Aktarımı (SWIPT) ağlarında kaynak tahsisini araştırıyoruz. SWIPT ağında, düğümler hibrit erişim noktasından (HAP) aynı radyo frekansı (RF) sinyalini kullanarak pillerini aynı anda şarj etmek için veri alabiliyor ve enerji toplayabiliyor. WPCCN'de, HAP'ten düğümlere aşağı bağlantıda enerji aktarılır ve düğümlerden HAP'a giden bağlantıda bilgi iletilir. Zaman ayırma, zamanlama ve geçiş seçiminin optimizasyonu için yeni optimizasyon çerçevelerini göz önünde bulunduruyoruz.

Tezin ilk bölümünde FD-WPCCN üzerinde çalışıyoruz. İlk olarak, röle seçimi yoluyla iletim süresi en aza indirme ve aktarım hızı maksimizasyonu optimizasyonu sorunlarını inceliyoruz. Daha sonra, açık-kapalı iletim şemasını FD-WPCCN'ye dahil ediyoruz ve zamanlama ve röle seçimini kullanarak iletim süresi en aza indirme ve aktarım hızı maksimize etme sorunlarını araştırıyoruz.

Tezin ikinci bölümünde FD-SWIPT ağı üzerinde çalışıyoruz. İlk olarak, FD röle tabanlı bir sistemin kesinti analizini sağlıyoruz ve kesinti verimi ve enerji verimliliği maksimizasyonu için optimizasyon sorunlarını sunuyoruz. Ardından, sistem modelini daha pratik bir çok röle kullanıcılı FD çoklu giriş-çoklu çıkış (MIMO) sistemine kendi kendine enerji geri dönüşümünü içerecek şekilde genişletiyoruz. Kendi kendine enerji geri dönüşümü, FD modu nedeniyle ortaya çıkan kendi kendine enterferanstan yararlanır. Bir SWIPT FD MIMO sisteminde toplam aktarım hızını en üst düzeye çıkarmak hedefiyle kaynak tahsisi ve geçiş seçimi optimizasyon çerçevesini sunuyoruz.

ACKNOWLEDGMENTS

Foremost, I would like to express my gratitude to my supervisor Prof. Sinem Coleri for her continuous support throughout my PhD journey. I am also obliged to the members of my thesis committee Prof. Öznur Özkasap, Prof. Ertuğrul Başar, Prof. Özgür Gürbüz and Prof. İbrahim Altunbaş for their valuable feedback and serving on my thesis defense committee. My heartiest gratitude goes to my parents and sisters for their continuous prayers and encouragement. I would like to thank my friends and office mates who motivated me and provided me a friendly research environment. I would also like to acknowledge Higher Education Commission (HEC) of Pakistan and Scientific and Technological Research Council of Turkey (Tubitak) for financial support.

TABLE OF CONTENTS

LIST OF FIGURES

ABBREVIATIONS

WPCN	Wireless Powered Communication Networks
SWIPT	Simultaneous Wireless Information and Power Transfer
WPCCN	Wireless Powered Cooperative Communication Networks
MIMO	Multiple Input Multiple Output
OFDMA	Orthogonal Frequency Division Multiple Access
RF	Radio Frequency
MTC	Machine Type Communication
HAP	Hybrid Access Point
TDMA	Time-Division Multiple Access
SIC	Self-Interference Cancellation
KKT	Karush-Kuhn-Tucker
FD	Full-Duplex
AF	Amplify-and-forward
DF	Decode-and-forward
EH	Energy Harvesting
HD	Half-Duplex
CSI	Channel State Information
UE	User Equipment
SUDAS	Shared UE-side Distributed Antenna System
MINLP	Mixed Integer Non-Linear Programming Problem
TS	Time-Switching Ratio
EE	Energy Efficiency

Chapter 1

INTRODUCTION

The applications of wireless sensor networks have seen a tremendous increase recently because of the advances and standardization in communication technologies such as Internet of Things (IoT) and machine type communications (MTC) etc. Wireless sensor nodes are capable of sensing, computing and communicating wirelessly and are the backbone of many self controlled and intelligent systems. These networks are expected to support applications in health monitoring, home and industrial automation, unarmed vehicles, cities and traffic management, inter/intra vehicle communication and smart agriculture. A recent Ericsson mobility report states that 24.6 billion sensor nodes are expected to be installed in different fields by 2025. Due to the large number of sensor networks, wireless traffic will grow significantly. Increasing the lifetime of this massive battery dependent installation is a major challenge for the future wireless networks. With the introduction of many innovative and bandwidth hungry applications, the wireless spectrum drought has become more alarming than ever before. Moreover, many of these applications have strict latency and coverage area requirements. In order to overcome these challenges, low power transceivers with energy harvesting capability, networks capable to communicate in full-duplex mode and cooperative (relay-based) communication have been proposed.

The lifetime of a wireless sensor network is battery dependent requiring replacement and recharging, which is either very difficult or infeasible. Getting rid of this dependence not only reduces the size and maintenance cost but also increases the network life. For this purpose, recharging the batteries of sensor nodes through wireless means is the most efficient option. Wireless sensor nodes can harvest energy from various renewable sources such as solar, wind, thermal and radio frequency (RF). The dependence of natural sources like solar, wind on the environmental conditions results in an unpredictable amount of harvested energy, which is not acceptable for time critical wireless network applications. However, RF energy harvesting arises as a competent option due to its long range, controlled energy and small form factor. In RF energy harvesting, radio signals with frequency range 3 kHz-300 GHz are used as a medium to carry energy in the form of electromagnetic radiation. In the literature, two main RF energy harvesting schemes are proposed: Simultaneous Wireless Information and Power Transfer (SWIPT) and Wireless Powered Communication Network (WPCN). In the SWIPT scheme, the nodes are being able to transfer information and harvest energy to recharge their batteries simultaneously by using the same RF signal. In WPCN, energy and information flow separately, i.e., energy flows in downlink and information in uplink. To enhance the network lifetime, throughput and coverage area by assisting the end-user nodes to successfully transmit information, cooperative (relay-based) communication networks have been proposed together with RF energy harvesting capabilities. There are two main type of relays: decode-and-forward (DF), where the relay node first decodes the signal received and then forwards it to the destination; and amplify-and-forward (AF), in which the relay node amplifies the received signal and then sends it to the destination. To overcome the spectrum scarcity issue and to increase the energy harvesting time, full-duplex communications can be used in both relay-based SWIPT and WPCN schemes. However, the main challenge in full-duplex systems is to mitigate the self-interference, where part of the transmitted signal is received by itself. Several self-interference cancellation (SIC) techniques and their practical implementations have been proposed in the literature which placed full-duplex as one of the key transceiving techniques for future wireless networks. Moreover, instead of cancelling the self-interference signal, it can be utilized to harvest energy through the concept of self-energy recycling.

In order to increase the network lifetime, throughput, coverage area, and to overcome the spectrum scarcity issue, resource allocation schemes in which scheduling, relay selection, allocation of transmission times, powers and rates are determined are of paramount importance. This thesis investigates the resource allocation of full-duplex WPCN and SWIPT based relay networks subject to various constraints such as maximum transmit power, energy causality and traffic demand of the users etc. It is organized as different chapters focusing on a variety of problems with different objective functions such as total transmission time minimization and throughput maximization through scheduling and relay selection requirements.

1.1 Organization

The rest of the thesis is organized as follows.

- **Chapter 2** presents the novel optimization framework to determine the time allocation and relay selection with the objective of minimizing the total transmission time duration for an FD-WPCCN. The formulated problem is mixed integer nonlinear programming problem (MINLP), which is difficult to solve for the global optimal solution. We decompose the problem into two sub-problems: time allocation problem for a predetermined relay selection and relay selection problem. For the time allocation problem, we prove that it is convex and present an optimal solution. Then, we propose a heuristic relay selection algorithm utilizing the optimal time allocation problem solution.

  S. A. A. Kazmi, M. S. Iqbal, and S. Coleri, "Total transmission time minimization through relay selection for full-duplex wireless powered cooperative communication networks," Grieco L.A., Boggia G., Piro G., Jararweh Y., Campolo C. (eds) Ad-Hoc, Mobile, and Wireless Networks. ADHOC-NOW, vol. 12338, pp. 257–268, 2020.

- **Chapter 3** presents the optimization framework for the throughput maximization and relay selection of an FD-WPCCN. The formulated problem is MINLP, which is difficult to solve for the global optimum. We decompose the problem into two sub-problems: throughput maximization problem for a predetermined relay selection and relay selection problem. For the throughput maximization problem, we prove that it is convex and present an optimal solution by utilizing Karush-Kuhn-Tucker (KKT) conditions. Then, we propose a heuristic relay selection algorithm based on the idea of selecting a relay for each user with the best channel conditions.

S. A. A. Kazmi, M. S. Iqbal, and S. Coleri, “Relay selection and Throughput Maximization for full-duplex wireless powered cooperative communication networks,” IEEE International Symposium on Personal, Indoor and Mobile Radio Communications, PIMRC 2021.

- **Chapter 4** presents the optimization framework for the throughput maximization through relay selection and scheduling of the users for an on-off transmission scheme based FD-WPCCN. The formulated optimization problem is MINLP, which is difficult to solve for the global optimal solution. As a solution strategy, we first present the polynomial time heuristic relay selection algorithm for a predetermined schedule of the users by studying the characteristics of optimal relay allocation solution of the optimization problem. Then, we propose a polynomial time heuristic scheduling algorithm by investigating the characteristics of the optimal scheduling solution of the optimization problem.

  S. A. A. Kazmi, M. S. Iqbal, and S. Coleri, “Throughput Maximization for On-Off transmission scheme based full-duplex wireless powered cooperative communication networks,” submitted to IEEE International Conference on Communications, ICC 2022.

- **Chapter 5** presents the analysis of the outage probability of an FD-AF relay based SWIPT system, incorporating a non-linear CLC EH model. We formulate the problems of maximizing the system outage throughput and energy efficiency (EE) and optimize the time-switching (TS) ratio. The formulated optimization problems are found to be convex, we utilize golden-section method to find the optimal TS solution.

  S. A. A. Kazmi and S. Coleri, ”Optimization of Full-Duplex Relaying System With Non-Linear Energy Harvester,” in IEEE Access, vol. 8, pp. 201566-201576, 2020, doi: 10.1109/ACCESS.2020.3035005.

- **Chapter 6** presents the resource allocation problem of FD-MIMO relaying system with self-energy recycling. The formulated problem is MINLP, which is difficult to solve for the optimal solution. We decompose the optimization problem into two sub-problems: resource allocation problem and relay selection problem. First, we reduce the resource allocation problem to a convex optimization problem by using the optimality analysis and Taylor series approximation. Then, we solve it for the optimal solution by using the convex optimization techniques. For the relay selection problem, we propose the polynomial time heuristic algorithm based on the idea of iteratively selecting the relay offering the maximum throughput at each time.

S. A. A. Kazmi, M. S. Iqbal, and S. Coleri, "Resource Allocation for Full-Duplex MIMO Relaying System with Self-Energy Recycling," submitted to IEEE Transactions on Wireless Communications.

- **Chapter 7** presents the optimization problem of maximizing the end-to-end achievable information rate of the MIMO-OFDMA system employing SUDAS. It exploits both licensed and unlicensed frequency bands in the system. The formulated problem is MINLP, which is difficult to solve for the optimal solution. We present the heuristic polynomial time algorithm based on the separation of EH and information transmission problems and optimize the interactive time-switching variable.

  S. A. A. Kazmi and S. Coleri Ergen, ”Wireless Information and Energy Transfer for Outdoor to Indoor Multicarrier SUDAS: Poster”, EuCNC, June 2018.

- **Chapter 8** presents the concluding remarks and possible future research directions.

Chapter 2

TOTAL TRANSMISSION TIME MINIMIZATION THROUGH RELAY SELECTION FOR FULL-DUPLEX WIRELESS POWERED COOPERATIVE COMMUNICATION NETWORKS

We consider a relay based full-duplex wireless powered cooperative communication network which consists of a hybrid access point (HAP), N users and K decode-and-forward relays with energy harvesting capability. We propose an optimization framework for relay selection with the objective of minimizing the total transmission time subject to energy causality and user traffic demand constraints. The formulated optimization problem is a mixed integer non-linear programming problem, which is difficult to solve for the global optimal solution in polynomial-time. As a solution strategy, we decompose the proposed optimization problem into two sub-problems: time allocation problem and relay selection problem. We derive the optimal solution of the time allocation problem by using convex optimization techniques. For the relay selection problem, based on the optimality analysis, we propose a polynomial-time heuristic algorithm, which minimizes the total transmission time by allocating the best relay to each user. Through simulations, we illustrate that the proposed algorithm outperforms the conventional predetermined relay allocation scheme and performs very close to the optimal solution for different network densities, HAP power values, and initial battery levels.

2.1 Introduction

In conventional wireless networks, the network lifetime is limited since the wireless devices in the network are powered by replaceable or rechargeable batteries. Energy harvesting (EH) from various renewable sources, such as wind, solar, and radio frequency (RF), has been proposed as a promising solution to prolong the lifetime of such networks.

Among these renewable sources, RF-EH is the most suitable option for future wireless systems due to its controllability, reliability, and lower cost. In the literature, two main RF-EH network models are proposed: Simultaneous Wireless Information and Power Transfer (SWIPT), and Wireless Powered Communication Networks (WPCN). In SWIPT, information and energy are transmitted simultaneously from the access point (AP) to multiple users, whereas in WPCN, only energy flows in the downlink (DL), and users harvest this energy to transmit their information in the uplink (UL).

Relay nodes are incorporated into the RF-EH networks with the goal of enhancing the throughput and network coverage by assisting the end users in their information transmission [1]. There are two main categories of the relays: decode-and-forward (DF), where a relay node first decodes the received signal and then forwards it to the destination; and amplify-and-forward (AF), in which a relay node amplifies the received signal from the source and forwards it to the destination. Initially, relay selection has been studied in SWIPT systems considering a single source, a destination and multiple EH relays [2–6]. The relay selection is proposed based on the available channel state information (CSI) of the single hop, either of the hop from source to relay or from relay to destination (known as partial relay selection (PRS)), or for both the hops, from source to relay and relay to destination, (known as opportunistic relaying (OR)) [2–4]. [5] and [6] consider EH relays, which are equipped with batteries, and present a relay selection problem based on the available energy level of the relays. All the aforementioned relay based SWIPT systems incorporate half-duplex (HD) transmission mode, in which information transmission and reception takes place in non-overlapping time slots. [7] considers the full-duplex (FD) relay based SWIPT system, where a single or multiple relays can be selected based on the greedy RS method that achieves the maximum capacity, whereas [8] studies a two-way FD SWIPT system, where two relay selection schemes to select a single best relay, to minimize the outage probability and maximize the sum capacity respectively are proposed. [9] extends the work of [8], by incorporating both single relay and multiple relays selection schemes in two-way SWIPT system.

In the context of WPCN, initially researchers analyzed the three node model for the relay based system which consists of a source, a relay and a destination, also referred as the wireless powered cooperative communication network (WPCCN). [10] studies this WPCCN, in which both source and relay need to harvest energy from the HAP in the DL, and work cooperatively in the UL. Authors incorporate the AF relaying scheme and present the closed-form expression of the average throughput. The analysis is also extended to multi-relay scenario and CSI based relay selection. [11] derives an approximate closed-form expression for the average throughput of the proposed adaptive transmission (AT) protocol of the three node WPCCN. In the proposed AT protocol, at the beginning of each transmission block, the HAP transfers energy to the source, and HAP and then, the source performs channel estimation to acquire the CSI. Based on the CSI estimation, the HAP adaptively chooses the source to perform UL information transmission either directly or cooperatively through relay. [12] extends the three node WPCCN model to multiple source/user multiple relay network model and presents a joint relay selection, scheduling and power control problem with the objective of minimizing the total duration of wireless power and information transfer for an HD system. To the best of our knowledge, [10] and [12] are the only works in WPCCN, where the relay selection problem is addressed, but they are limited to HD transmission.

In this chapter, we study the multiple relay, multiple users FD-WPCCN, where relays and users are the energy harvesting components and harvest energy from the HAP in the DL. Both the users and the relays incorporate a practical non-linear EH model based on logistic function, whereas all the previous studies incorporated an easy and impractical linear EH model in WPCCN systems. We determine the time allocation and relay selection with the objective of minimizing the total transmission time. The main contributions of this chapter are as follows:

- We present a new optimization framework for an FD-WPCCN system, incorporating the energy causality and traffic demand constraints by using a non-linear EH model for the first time in the literature.

- We formulate the optimization problem to determine the time allocation and relay selection with the objective of minimizing the total transmission time. The formulated problem is MINLP, which is difficult to solve for global optimal solution.

- We decompose the problem into two sub-problems. First, we formulate a time allocation sub-problem for a given relay selection and after proving its convexity, we propose the optimal solution. Then, we extend the problem to the best relay selection problem and propose a polynomial-time heuristic algorithm for the relay selection.

The rest of the chapter is organized as follows. The system model and assumptions are given in Section 2.2. The optimization problem for total transmission time minimization is presented in Section 2.3. In Section 2.4, we present the time allocation problem for a predetermined relay selection. In section 2.5, we present the heuristic relay selection algorithm. The numerical results are provided and discussed in Section 2.6. Finally, Section 2.7 presents the concluding remarks.

2.2 System Model and Assumptions

We consider a cooperative WPCN which consists of a HAP, K DF relays and N users, as depicted in Fig. 2.1. The HAP is operating in an FD mode, whereas the relays and users are operating in HD mode. The HAP is equipped with an FD antenna, which is used for simultaneous wireless energy transfer (WET) in the DL to the relays and users, and wireless information transmission (WIT) in the UL from the users to the HAP via relays. The transmission power of the HAP is assumed to be constant and denoted by P_h. We assume that the channels are block fading and different, i.e., channel gains remain constant during the transmission time and may change independently in the other blocks. DL channel gains from HAP to user i and relay k are denoted by h_i and h_k, respectively. UL channel gains from user i to relay k and from relay k to HAP are denoted by $g_{i,k}$ and g_k, respectively. We assume a practical non-linear energy harvesting model, based on logistic function. The energy harvesting rate of user i is given by

$$C_i = \frac{P_s(\Psi_i - \frac{1}{1+e^{a_i b_i}})}{(1 - \frac{1}{1+e^{a_i b_i}})}, \tag{2.1}$$

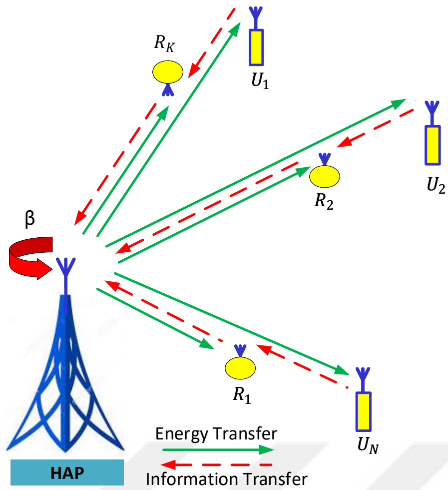

Figure 2.1: Architecture for Wireless Powered Cooperative Communication Network

where Ψ_i=$(1 + e^{-a_i(P_h h_i - b_i)})^{-1}$, and EH rate for relay k is given by

$$C_k = \frac{P_s(\Psi_k - \frac{1}{1+e^{a_k b_k}})}{(1 - \frac{1}{1+e^{a_k b_k}})}, \tag{2.2}$$

where Ψ_k=$(1 + e^{-a_k(P_h h_k - b_k)})^{-1}$, P_s represents the maximal power that energy harvester can harvest, a and b are the positive constants related to the non-linear charging rate with respect to the input power and turn-on threshold, respectively.

We consider time division multiple access as medium access protocol for the UL data transmission from the users to the HAP via relays. The total time is partitioned into scheduling frames, which are further divided into variable-length slots, each allocated to a particular user and its selected relay, as depicted in Fig. 2.2. We assume that the transmission order of the users is predetermined and the relays and users can harvest energy throughout the frame except during information transmission/reception time. The energy harvested after the information transmission can be stored in the battery, resulting in the initial battery level $B_i, i \in \{1, ..., N\}$ and $B_k, k \in \{1, ..., K\}$ for users and relays respectively. We assume that user i and the corresponding relay are transmitting information during time slot i. The transmission time of user i by using relay k is denoted by $\tau_{i,k}$ and transmission time of relay k, to transmit information of user i to HAP, is denoted by τ_k. Therefore, the energy harvesting time of user i till the end of its transmission is given

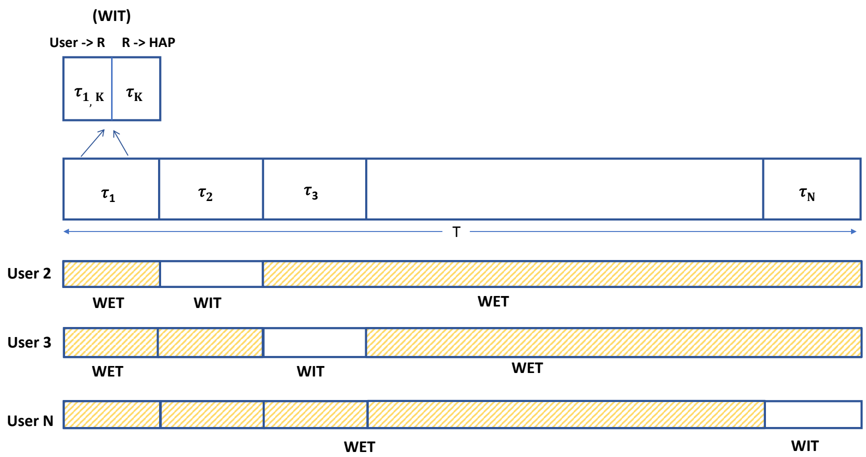

Figure 2.2: A time-slotted transmission block for downlink WET and uplink WIT

by $\sum_{j=1}^{i-1}\sum_{k=1}^{K} s_{j,k}(\tau_{j,k}+\tau_k)$, where $s_{j,k}$ is a binary variable, which takes value 1 if user j transmits information using relay k and zero otherwise. Then the total available energy for user i is given by

$$E_i = B_i + C_i \sum_{j=1}^{i-1}\sum_{k=1}^{K} s_{j,k}(\tau_{j,k}+\tau_k) \tag{2.3}$$

Similarly, the energy harvesting time before the information transmission of relay k is $\sum_{j\in U}\sum_{k=1}^{K} s_{j,k}(\tau_{j,k}+\tau_k)$, where the set U is the set of users, which are scheduled before user i using their corresponding relays. Note that the set U does not contain the users who have selected the same k^{th} relay to communicate to the HAP. The total available energy of the relay k, E_k is given by

$$E_k = B_k + C_k \sum_{j\in U}\sum_{k=1}^{K} s_{j,k}(\tau_{j,k}+\tau_k) \tag{2.4}$$

We assume that user i and relay k must consume all of its available energy in the allocated transmission slot $\tau_{i,k}$ and τ_k, respectively. Then the average transmit power of user i by using relay k is given by

$$P_{i,k} = \frac{E_i}{\tau_{i,k}} \quad \forall i \in \{1,2,\cdots,N\}, \forall k \in \{1,2,\cdots,K\} \tag{2.5}$$

Similarly, the average transmit power of the relay k is given by

$$P_k = \frac{E_k}{\tau_k} \quad \forall k \in \{1, 2, \cdots, K\} \tag{2.6}$$

We assume that user i has traffic demand D_i bits to be transmitted over the scheduling frame. We use continuous transmission rate model and Shannon's channel capacity formula to determine the maximum achievable rate. The instantaneous UL transmission rates from user i to relay k, denoted by $R_{i,k}$ and from relay k to HAP, denoted by R_k, are given by

$$R_{i,k} = \tau_{i,k} W log_2\left(1 + \frac{E_i g_{i,k}}{\tau_{i,k} W N_0}\right) \tag{2.7}$$

$$R_k = \tau_k W log_2\left(1 + \frac{E_k g_k}{\tau_k(\beta P_h + N_0 W)}\right) \tag{2.8}$$

where βP_h is the power of self-interference at the HAP, arises due to FD mode and $N_0 W$ is the noise power, where W is the bandwidth.

The objective of the optimization is to minimize the total transmission time for an FD WPCCN subject to energy causality constraint and users traffic demand. In the following section, we formulate the optimization problem.

2.3 Problem Formulation

In this section, we formulate the optimization problem of the relay selection for total time minimization, denoted by $\mathcal{RS} - \mathcal{TTM}$, as follows:

$\mathcal{RS} - \mathcal{TTM}$

$$minimize \sum_{i=1}^{N} \sum_{k=1}^{K} \tau_{i,k} + \sum_{k=1}^{K} \tau_k \tag{2.9a}$$

subject to

$$\sum_{k=1}^{K} s_{i,k}\tau_{i,k} Wlog_2\Big(1 + \frac{E_i g_{i,k}}{\tau_{i,k} W N_0}\Big) \geq D_i; \forall i \in \{1, ..., N\}, \tag{2.9b}$$

$$\tau_k Wlog_2\Big(1 + \frac{E_k g_k}{\tau_k(\beta P_h + W N_0)}\Big) \geq \sum_{i=1}^{N} D_i s_{i,k}; \forall k \in \{1, ..., K\}, \tag{2.9c}$$

$$\sum_{k=1}^{K} s_{i,k} = 1; \forall i \in \{1, ..., N\}, \tag{2.9d}$$

variables

$$s_{i,k} \in \{0, 1\}; \tau_{i,k}, \tau_k, \geq 0; \forall i \in \{1, ..., N\}, k \in \{1, ..., K\}. \tag{2.9e}$$

The variables of the $\mathcal{RS} - \mathcal{TTM}$ optimization problem are $s_{i,k}$, the relay selection variable, which is a binary variable taking value 1 if user i transmits information by using relay k and zero otherwise for $i \in \{1, ...N\}$, $k \in \{1, ..., K\}$; $\tau_{i,k}$ transmission time of user i by using the relay k, for $i \in \{1, ...N\}$, $k \in \{1, ..., K\}$; and τ_k, the transmission time of relay k to the HAP for $k \in \{1, ..., K\}$.

The objective of the optimization problem is to minimize the total transmission time duration. Eqs. (2.9b) and (2.9c) represent the constraints on satisfying the traffic demand of the users. Eq. (2.9d) guarantees that only one relay is selected for each user.

The $\mathcal{RS} - \mathcal{TTM}$ is MINLP, which is generally hard to solve for the optimal solution. To solve the problem optimally, we decompose the $\mathcal{RS} - \mathcal{TTM}$ into two sub-problems, namely, time allocation problem and relay selection problem. Next, we formulate the time-allocation problem.

2.4 Time Allocation Problem

In this section, we discuss the time allocation problem, denoted by $\mathcal{TAP}$. In the $\mathcal{TAP}$ the users are already allocated the relay, i.e., $s_{i,k}$ are known. The $\mathcal{TAP}$ is formulated as follows:

$\mathcal{TAP}$

$$\text{minimize} \sum_{i=1}^{N}\sum_{k=1}^{K}\tau_{i,k} + \sum_{k=1}^{K}\tau_k \tag{2.10a}$$
$$\text{subject to}$$
$$D_i - \tau_{i,k}Wlog_2\left(1 + \frac{E_i g_{i,k}}{\tau_{i,k}N_0W}\right) \leq 0; \forall i, \forall k, \tag{2.10b}$$
$$D_i - \tau_k Wlog_2\left(1 + \frac{E_k g_k}{\tau_k(\beta P_h + N_0W)}\right) \leq 0; \forall i, \forall k, \tag{2.10c}$$
$$\tau_{i,k}, \tau_k \geq 0; \forall i, \forall k. \tag{2.10d}$$

The variables of the problem are $\tau_{i,k}$, the transmission time of the first hop, from user i to relay k, for $i \in \{1, ...N\}$, $k \in \{1, ..., K\}$ and τ_k, the transmission time of the relay k to HAP, for $k \in \{1, ..., K\}$.

Lemma 1. *$\mathcal{TAP}$ is a convex optimization problem.*

Proof. The objective function of $\mathcal{TAP}$ is a linear function of $\tau_{i,k}$ and τ_k. The constraints in Eqs. (2.10b) and (2.10c) are convex functions as the hessian of both functions are positive semi-definite. Therefore, $\mathcal{TAP}$ is a convex optimization problem. □

Since $\mathcal{TAP}$ is a convex optimization problem, there is a unique optimal solution for the problem. In the following, we provide the optimality conditions of the optimization problem.

Lemma 2. *In the optimal solution of $\mathcal{TAP}$, the constraints in Eqs. (2.10b) and (2.10c) should hold with equality.*

Proof. The proof is by contradiction. Suppose that in an optimal solution $\tau = \{\tau^*_{1,k}, \tau^*_{2,k}, \cdots, \tau^*_{N,k}\}$ are the allocated transmission times of users such that $\tau^*_{i,k}Wlog_2\left(1 + \frac{g_{i,k}E_i}{\tau^*_{i,k}WN_0}\right) > D_i$. The function $f(x) \triangleq xlog(1 + z/x)$, where z is a constant, is a monotonically increasing function of x for $x > 0$. Therefore, for any user i, we can always find a $\tau'_{i,k}$ such that $\tau'_{i,k}Wlog_2\left(1 + \frac{g_{i,k}E_i}{\tau'_{i,k}WN_0}\right) = D_i$ and it is clear that $\tau'_{i,k} < \tau^*_{i,k}$. This is a contradiction. In a similar way, we can prove that Eq.(2.10c) should hold with equality. □

Based on Lemma 2, the problem $\mathcal{TAP}$ can be solved for a unique set of transmission times and the solution is presented in Theorem 1.

Theorem 1. *In the optimal solution of $\mathcal{TAP}$, the transmission time of user i is given by*

$$\tau_{i,k} = \frac{1}{\frac{-W}{D_i \ln(2)} \boldsymbol{W}(\frac{-D_i \ln(2)}{W\gamma_{i,k}} \exp(\frac{-D_i \ln(2)}{W\gamma_{i,k}})) + \frac{1}{\gamma_{i,k}}}, \tag{2.11}$$

where ***W****(.) is a well known Lambert function [13], and $\gamma_{i,k}$ is given by*

$$\gamma_{i,k} = \frac{g_{i,k} E_i}{N_0 W}. \tag{2.12}$$

Proof. As per Lemma 2, the constraint given in Eq. (2.10b) should hold with equality, i.e.,

$$D_i - \tau_{i,k} W log_2\Big(1 + \frac{g_{i,k}\gamma_{i,k}}{\tau_{i,k}}\Big) = 0. \tag{2.13}$$

Eq. (2.13) can then be rearranged as follows:

$$1 = (1 + \frac{\gamma_{i,k}}{\tau_{i,k}}) \exp\Big(\frac{-D_i \ln(2)}{W\tau_{i,k}}\Big). \tag{2.14}$$

We rewrite the Eq. (2.14) in the form of $Y = Xe^X$ as

$$\frac{-D_i \ln(2)}{W\gamma_{i,k}} \exp\Big(\frac{-D_i \ln(2)}{W\gamma_{i,k}}\Big) = \Big(\frac{-D_i \ln(2)}{W\gamma_{i,k}} - \frac{-D_i \ln(2)}{W\tau_{i,k}}\Big) exp\Big(\frac{-D_i \ln(2)}{W\gamma_{i,k}} - \frac{-D_i \ln(2)}{W\tau_{i,k}}\Big). \tag{2.15}$$

Eq. (2.15) is a standard form for $Y = Xe^X$ and its solution is $X = W(Y)$, Then after some simple mathematics, $\tau_{i,k}$ is obtained as given in Eq. (2.11). □

Since, in the decode-and-forward relay network, user and relay transmit their information in non-overlapping transmission times, we can treat both entities separately. The transmission time of the relays is given as presented in the following theorem.

Theorem 2. *In the optimal solution of $\mathcal{TAP}$, the transmission time of relay k is given by*

$$\tau_k = \frac{1}{\frac{-W}{D_i \ln(2)} \boldsymbol{W}(\frac{-D_i \ln(2)}{W\gamma_k} \exp(\frac{-D_i \ln(2)}{W\gamma_k})) + \frac{1}{\gamma_k}}, \tag{2.16}$$

where,

$$\gamma_k = \frac{g_k E_k}{\beta P_h + N_0 W}. \tag{2.17}$$

Proof. Theorem 2 can be proved in a similar way as Theorem 1 by solving Eq. (2.10c) and proof is skipped for brevity. □

Now, as we have solved the $\mathcal{TAP}$ problem, the relay selection problem is presented in the following section.

2.5 Relay Selection

The goal of this section is to determine the relay selection for each user such that the total transmission time is minimized. In section 2.4, we presented the optimal transmission time allocation for a given relay allocation, i.e., $s_{i,k}$ were known for $i \in \{1, ...N\}$, $k \in \{1, ..., K\}$. On the other hand, the total transmission time can be further minimized by optimizing the relay selection for each user. For instance, allocating a relay to the user with better channel conditions and smaller distance over any random relay will significantly reduce the transmission time of the users. A straightforward approach to this problem can be brute-force search, i.e., enumerate all the possible relay combinations and then pick the combination with minimum transmission time. However, the computational complexity of this approach is exponential due to K^N possible combinations of the relays. Therefore, we propose a polynomial time heuristic algorithm based on the minimization of the total transmission time through the allocation of the best relay to each user. For a single user i, let $\tau_{i,k}$ be the transmission time of the first hop, from user to relay k and τ_k be the transmission time from relay k to HAP. Then $argmin_{k\in\{1,2,\cdots,K\}}(\tau_{i,k} + \tau_k)$ will be the optimal relay that gives the minimum transmission time for the single user. As the users are transmitting data in a sequence, the relay selection is updated online for each user as due to different energy harvesting rates, users may select different relay at different decision times. Based on this we propose the following heuristic algorithm.

The Minimum Length Relay Selection Algorithm (MLRSA), as given in Algorithm 1, is described in detail next. The algorithm starts by initializing $\mathcal{R}$, $\tau_{i,k}(\mathcal{R})$, $\tau_k(\mathcal{R})$, $t(\mathcal{N})$

Algorithm 1 Minimum Length Relay Selection Algorithm (MLRSA)

1: **input:** set of users $\mathcal{N}$ and relays $\mathcal{K}$
2: **output:** Relay selection $\mathcal{R}$, set of user transmission times $\tau_{i,k}$, set of relay transmission times τ_k, schedule length $t(\mathcal{N})$
3: $\mathcal{R} \leftarrow \emptyset$, $\tau_{i,k}(\mathcal{R}) \leftarrow 0$, $\tau_k(\mathcal{R}) \leftarrow 0$, $t(\mathcal{N}) \leftarrow 0$
4: **for** $i = 1 : |\mathcal{N}|$ **do**
5:     Calculate $\tau_{i,k}, \tau_k, \forall k \in \{1, ..., K\}$
6:     $m \leftarrow \text{argmin}_{k \in \mathcal{K}} \, (\tau_{i,k} + \tau_k)$,
7:     $\mathcal{R} \leftarrow \mathcal{R} + \{m\}$,
8:     $\tau_{i,k} \leftarrow \tau_{i,k} + \{\tau_{i,m}\}$,
9:     $\tau_k \leftarrow \tau_k + \{\tau_m\}$,
10:     $t(\mathcal{N}) \leftarrow t(\mathcal{N}) + \tau_{i,m} + \tau_m$,
11: **end for**

to an empty set (Line 3). For each user i of the system, the relay that offers the minimum transmission time is selected (Line 6). Then, the set $\mathcal{R}$ is updated with the selected relay (Line 7). $\tau_{i,k}(\mathcal{R})$ is updated by adding the transmission time of the user i to the selected relay m (Line 8) and $\tau_k(\mathcal{R})$ by adding the transmission time of relay m to HAP (Line 9). Finally, $t(\mathcal{N})$ is updated by adding the transmission times of both the hops i.e, $\tau_{i,m}$ and τ_m (Line 10). Algorithm terminates when all the users in the system are being assigned to the best relays. The computational complexity of MLRSA is $O(N \times K)$.

2.6 Performance Analysis

In this section, we evaluate the performance of the proposed algorithm. Simulations are carried out in MATLAB, averaged over 1000 independent random network realizations. The attenuation in the channel is calculated by using both large scale and small scale fading. To model the large scale fading, we used $PL(d, dB) = PL(d_0, dB) + 10\alpha log_{10}(d/d_0) + Z$ where, $PL(d, dB)$ is the path loss at distance d in dB, d_0 is the reference distance and path loss at reference distance $d_0 = 1m$ is taken as $30dB$, the term α is the path loss exponent and is taken as 2.76. Z is a zero mean Gaussian random variable with standard deviation σ=4 . The parameters used in the simulations are W=1 MHz; D_i is 100 bits for $i \in \{1, ...N\}$ and $\beta = -80dB$ [14]. For the non-linear EH model, $P_s = 7mW$, $a = 1500$ and $b = .0022$.

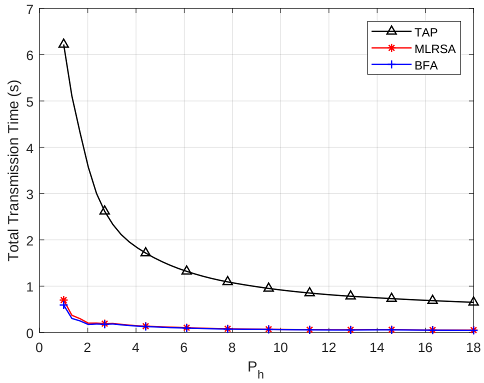

Figure 2.3: Total transmission time vs. HAP transmit power P_h

2.6.1 Transmission Time versus HAP Power P_h

Fig. 2.3 illustrates the total transmission time for different values of HAP transmit power P_h. The total transmission time duration decreases with the increasing transmit power since higher HAP power allows the relays and the users to harvest more energy and complete their transmission in shorter time as long as they can transmit with higher transmit powers. After a certain value of P_h, the total transmission time becomes almost constant due to the saturation region of all the users and relays and any further increase in the HAP power will not improve the energy harvesting rate. The proposed MLRSA outperforms the predetermined relay selection scheme (TAP) and performs very close to the optimal solution (BFA).

2.6.2 Transmission Time versus the number of users

Fig. 2.4 illustrates the effect of the network size on the total transmission time. As the number of users increase in the system, the total transmission time increases. When the network size keeps increasing, any further addition of a user results in very small increase in the total transmission time.

2.6.3 Transmission Time versus battery level of the nodes

Fig. 2.5 shows the total transmission time for different values of battery levels of the relays and the users. Total transmission time decreases as the energy in the battery of the

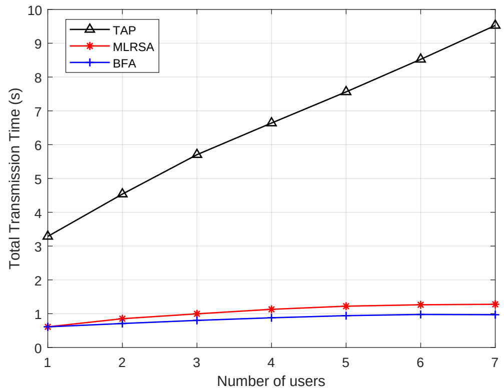

Figure 2.4: Total transmission time vs. the number of users in the system

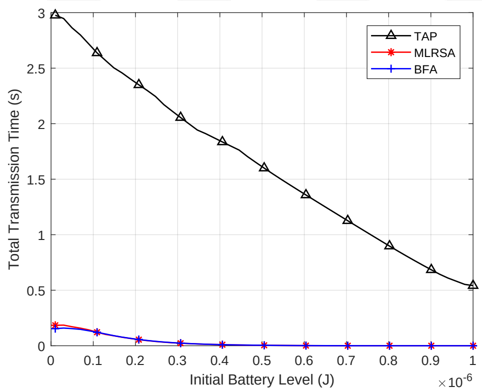

Figure 2.5: Total transmission time vs. the initial battery level of the relays and the users

nodes increases. It is because of the fact that higher initial battery level helps the users to complete their transmissions in shorter time. The MLRSA outperforms the conventional predetermined relay selection (TAP) and performs close to the optimal BFA.

2.7 Conclusion and Future Work

In this chapter, we have investigated the total transmission time minimization of the FD-WPCCN system through relay selection. We formulate an MINLP problem for the subject. To solve the problem efficiently, we decompose the problem into two sub-problems, namely, time allocation and relay selection problem. We derive the optimal solution of the time allocation problem by using convex optimization techniques and present the polynomial-time heuristic algorithm for the relay selection problem. Through simulations, we show that the proposed algorithm performs very close to the optimal solution. We aim to incorporate multi-antenna system in the future.

Chapter 3

RELAY SELECTION AND THROUGHPUT MAXIMIZATION FOR FULL-DUPLEX WIRELESS POWERED COOPERATIVE COMMUNICATION NETWORKS

Cooperative communication using energy harvesting (EH) nodes promises significant improvement in network throughput, coverage, and reliability. This chapter studies a full-duplex (FD) wireless powered cooperative communication network (WPCCN), in which the users communicate to a hybrid access point (HAP) via decode-and-forward (DF) EH relay nodes. We present an optimization framework for the relay selection problem with an objective of maximizing the sum throughput of the FD-WPCCN, for the first time in the literature. The formulated optimization problem is a mixed integer non-linear programming problem (MINLP), which is difficult to solve for global optimal solution. As a solution strategy, we first analyze the problem for a given relay allocation and prove that it is a convex problem. We solve the problem for the optimal solution by using the Karush-Kuhn-Tucker conditions. Then, for the relay selection problem, we present a polynomial-time heuristic algorithm based on the allocation of relay with the best channel conditions to each user. Through extensive simulations, we show that the proposed algorithm performs close to the optimal solution for various network parameters such as different HAP transmission power values, network sizes, and initial battery level of the nodes. We observe that the sum throughput of the network can be increased significantly by using a proper relay selection technique.

3.1 Introduction

The lifetime of a conventional wireless network is limited, because the nodes are dependent on rechargeable or replaceable batteries. To prolong the lifetime of such energy constrained networks, EH techniques have been proposed from the sources such as wind, solar, vibration and radio frequency (RF). Among these sources, RF energy harvesting arises as the most suitable option due to its long range, lower cost, and control on the energy being transferred [15]. The relay based RF-EH wireless networks have been exploited by the researchers to enhance the network throughput and coverage area by helping the end terminals in their signal transmission with efficient energy management [16]. There are two main types of RF energy harvesting wireless network models. Simultaneous Wireless Information and Power Transfer (SWIPT) [17] and Wireless Powered Communication Network, referred as WPCN [18].

Specifically, in WPCCN, the relay and user nodes are powered by the transferred energy from the HAP in the downlink (DL). Then, they transmit their information signal by using the harvested energy in the uplink (UL), to the HAP. [10,11,19] study a simple three node WPCCN, operating in half-duplex (HD) mode, in which the relay and user nodes first harvest energy in the DL, and then work cooperatively to transmit the user's information in the UL. Specifically, [10] derives the closed-form expression for the average throughput of the three node HD-WPCCN. It also extends the three node model to multi-relay scenario, and proposes a relay selection algorithm based on available channel state information (CSI) of the system. [11] presents an approximate closed-form expression for the throughput of an adaptive transmission (AT) protocol. In the AT protocol, HAP charges the source and then, they together estimate the CSI. Based on the channel state estimation, the AP chooses the source to transmit information either with or without using a relay. [19] studies the impact of EH relay position on the link outage performance of a three node WPCCN. [12] studies a multi-relay multi-user HD-WPCCN and presents a joint relay selection, scheduling and power control problem with the objective to minimize the total duration of wireless information and power transfer. However, [10] and [12] are the only works in WPCCN that investigate the relay selection problem and are based on the HD mode of transmission. Recently, our works [20] (Chapter 2) and [21] study an FD-WPCCN, for the first time. The throughput performance achieved by the FD-WPCCN is always better than its HD counterpart due to the HAP's ability of simultaneous EH and information transmission. [20] studies a relay selection and transmission time minimization problem, considering the multi-relay multi-user FD-WPCCN. [21] studies a scheduling and relay selection problem in FD-WPCCN, with the objective of total time minimization, for an on-off transmission scheme. However, both of these works consider only the transmission time minimization problem.

In this chapter, we study an optimization problem of throughput maximization for a multi-relay multi-user FD-WPCCN, incorporating a realistic non-linear energy harvesting model based on logistic function. The original contributions of this chapter are as follows:

- We formulate an optimization problem with the objective of maximizing the sum throughput of the FD-WPCCN through relay selection, for the first time in the literature.
- The formulated problem is a mixed integer non-linear programming problem, which is difficult to solve for the global optimal solution. Therefore, we first solve the given relay allocation problem for the optimal solution by exploiting the convexity of the problem. Then, we present the polynomial time heuristic algorithm for relay selection based on the allocation of a relay to each user with the best channel conditions.
- Through extensive simulations, we demonstrate that the proposed algorithm significantly outperforms the conventional scheme while performing very close to the optimal solution.

The rest of the chapter is organized as follows. In Section 3.2, we present the system model and assumptions. In section 3.3, we formulate an optimization problem for the relay selection of the FD-WPCCN, with the objective of maximizing the throughput of the system. Section 3.4 presents the solution of the formulated problem for a predetermined relay allocation. In section 3.5, we present the polynomial-time heuristic relay selection algorithm. Section 3.6 evaluates the performance gain of the proposed algorithm through simulations. In section 3.7, we conclude our work and discuss the future direction.

3.2 System Model

We consider an FD-WPCCN, as shown in Fig. 2.1. It consists of a single FD antenna HAP, L HD DF relays and N HD users. The FD antenna of the HAP is used for transmitting energy to the relay and user nodes in the DL, and receiving information in the UL from the users through relays, simultaneously. The relays and users depend on the energy harvested from the HAP, which they store in their batteries. The initial battery levels of the relays and users at the start of time frame are denoted by $B_l, l \in \{1, ..., L\}$, and $B_n, n \in \{1, ..., N\}$, respectively. The transmission power of the HAP is denoted by P_h.

We assume that the channel gains are constant during the transmission time frame, i.e., they are block fading. We consider that the total time duration for the operation of the system is divided into multiple scheduling frames of unit length. Every frame is further divided into multiple time slots allocated to the relay and user nodes for information transmission. We assume that the transmission order of the users is known [18], [20]. We incorporate a more realistic non-linear energy harvesting model based on a logistic function [22], in which the energy harvesting rate of user n and relay l, is given by

$$C_x = \frac{P_s(\Psi_x - \frac{1}{1+e^{a_x b_x}})}{(1 - \frac{1}{1+e^{a_x b_x}})}, \tag{3.1}$$

where $x \epsilon [n, l]$, $\Psi_x = \frac{1}{(1+e^{-a_x(P_h h_x - b_x)})}$, h_l and h_n are the channel coefficients of the first and second hop i.e., from the HAP to relay l and user n, in the DL, respectively; P_s represents the maximum saturated power achieved due to large input power values; constants a and b are linked to the circuit specifications of the energy harvester such as input power, capacitance, resistance, and diode turn-on threshold.

The HD relays and users cannot harvest energy when transmitting or receiving information. Harvested energy after the information transmission of any node can be stored in the battery for future use. The information transmission time from user n to relay l in the UL is denoted by $\tau_{n,l}$, whereas transmission time of relay l is denoted by τ_l. The total available energy of user n and relay l is given by

$$E_n = B_n + C_n \sum_{i=1}^{n-1} \sum_{l=1}^{L} s_{i,l}(\tau_{i,l} + \tau_l) \tag{3.2}$$

where $\sum_{i=1}^{n-1} \sum_{l=1}^{L} s_{i,l}(\tau_{i,l} + \tau_l)$ represent the time in which user n is harvesting energy, $s_{i,l}$ is a binary relay selection variable, which is either 1 or 0, depending on whether a relay l is assigned to user n or not.

$$E_l = B_l + C_l \sum_{i \in S} \sum_{l=1}^{L} s_{i,l}(\tau_{i,l} + \tau_l) \tag{3.3}$$

where $\sum_{i \in S} \sum_{l=1}^{L} s_{i,l}(\tau_{i,l} + \tau_l)$ is the energy harvesting time of relay l before it transmits information, the set S contains the users, scheduled before user n with their allocated relays. However, the users that have been allocated the same l^{th} relay before to assist the information transmission to the HAP are not included in the set. We assume that user n and relay l consume all of its harvested energy in their respective information transmission time slots. Based on this, the transmit powers of the two hops are given by

$$P_{n,l} = \frac{E_n}{\tau_{n,l}} \tag{3.4}$$

$$P_l = \frac{E_l}{\tau_l} \tag{3.5}$$

The instantaneous throughput from user n to relay l and from relay l to the HAP is denoted by $R_{n,l}$ and R_l, respectively and is given by

$$R_{n,l} = \tau_{n,l} W log_2\Big(1 + \frac{E_n g_{n,l}}{\tau_{n,l} W N_0}\Big) \tag{3.6}$$

$$R_l = \tau_l W log_2\Big(1 + \frac{E_l g_l}{\tau_l(\beta P_h + N_0 W)}\Big) \tag{3.7}$$

where $g_{n,l}$ and g_l are the channel coefficients from user n to relay l and from relay l to HAP, respectively; βP_h is the self-interference power; $N_0 W$ is the noise power, and W is the system bandwidth.

The end-to-end throughput of the two-hop DF relay based WPCCN is given as [23]

$$R = min\{R_{n,l}, R_l\} \tag{3.8}$$

3.3 Optimization Framework

This section presents the joint optimization framework of the relay selection and throughput maximization. It is denoted by $\mathcal{RS}-\mathcal{TMP}$, and is presented as follows:

$\mathcal{RS}-\mathcal{TMP}$

$$max \sum_{n=1}^{N}\sum_{l=1}^{L} s_{n,l}\ min\{R_{n,l}, R_l\} \tag{3.9a}$$

subject to

$$\sum_{n=1}^{N}\sum_{l=1}^{L} \tau_{n,l} + \sum_{l=1}^{L} \tau_l \leq 1, \tag{3.9b}$$

$$\sum_{l=1}^{L} s_{n,l} = 1; \forall n \in \{1, ..., N\}, \tag{3.9c}$$

variables

$$s_{n,l} \in \{0, 1\}; \tau_{n,l}, \tau_l, \geq 0; \forall n \in \{1, ..., N\}, l \in \{1, ..., L\}. \tag{3.9d}$$

The $\mathcal{RS}-\mathcal{TMP}$ optimization problem has three decision variables, namely, $\tau_{n,l}$, τ_l, the transmission times of the two hops, and $s_{n,l}$, the binary relay selection variable, which is 1 if relay l is selected for user n and 0 otherwise.

The objective of the optimization problem is to maximize the sum throughput of the system. Eq. (3.9b) represents the constraint that indicates the normalized schedule length of 1 is assigned to the users. Eq. (3.9c) guarantees that only one relay assists each user for the information transmission. The $\mathcal{RS}-\mathcal{TMP}$ is a mixed integer non-linear programming problem. Therefore, to solve the MINLP problem, in the next section, we first present the optimal solution of the $\mathcal{RS}-\mathcal{TMP}$ for a predetermined relay allocation, and then study the optimal brute-force and heuristic best relay selection algorithms.

3.4 Throughput Maximization Problem for a known relay selection

In this section, we present the throughput maximization problem for a predetermined relay allocation scheme i.e., $s_{n,l}$ are known. The novelty of this problem is to optimize the transmission times of both the hops with the objective of sum throughput maximization. The problem is denoted by $\mathcal{TMP}$, and is presented as follows:

$\mathcal{TMP}$

$$max \sum_{n=1}^{N} \sum_{l=1}^{L} min\{R_{n,l}, R_l\} \tag{3.10a}$$

$$subject\ to$$

$$\sum_{n=1}^{N} \sum_{l=1}^{L} \tau_{n,l} + \sum_{l=1}^{L} \tau_l \leq 1, \tag{3.10b}$$

$$variables$$

$$\tau_{n,l}, \tau_l \geq 0; \forall n, \forall l. \tag{3.10c}$$

Lemma 3. *$\mathcal{TMP}$ is a convex optimization problem.*

Proof. The objective function of $\mathcal{TMP}$ is concave as hessian of both the functions are negative semi-definite and minimum of two concave functions is a concave function. Moreover, the constraint in Eq. (3.10b) is linear w.r.t. $\tau_{n,l}$ and τ_l. Therefore, $\mathcal{TMP}$ is a convex problem. □

There exists an optimal solution, which is unique, for $\mathcal{TMP}$, since it is a convex optimization problem. However, for simplicity, we first handle the $min\{R_{n,l}, R_l\}$ function of the objective function. Then, we incorporate the Karush-Kuhn-Tucker (KKT) conditions to find the optimal solution. Since the sum throughput performance of DF relaying system is limited by the link with lower signal-to-noise (SNR) ratio, $\mathcal{TMP}$ is optimized only when $\sum_{n=1}^{N} \sum_{l=1}^{L} R_{n,l} = \sum_{l=1}^{L} R_l$. Therefore, the $\mathcal{TMP}$ is equivalent to a problem having $\sum_{n=1}^{N} \sum_{l=1}^{L} R_{n,l} + \sum_{l=1}^{L} R_l$ as an objective function with an additional constraint $\sum_{n=1}^{N} \sum_{l=1}^{L} R_{n,l} = \sum_{l=1}^{L} R_l$. Therefore, the transformed $\mathcal{TMP}$ is written as:

$\mathcal{T}-\mathcal{TMP}$

$$max \sum_{n=1}^{N}\sum_{l=1}^{L} R_{n,l} + \sum_{l=1}^{L} R_l \tag{3.11a}$$

subject to

$$\sum_{n=1}^{N}\sum_{l=1}^{L} \tau_{n,l} + \sum_{l=1}^{L} \tau_l \leq 1, \tag{3.11b}$$

$$\sum_{n=1}^{N}\sum_{l=1}^{L} R_{n,l} = \sum_{l=1}^{L} R_l, \tag{3.11c}$$

variables

$$\tau_{n,l}, \tau_l \geq 0; \forall n, \forall l. \tag{3.11d}$$

To analyze the KKT conditions of $\mathcal{T}-\mathcal{TMP}$, the Lagrangian function of the problem is written as:

$$L = \sum_{n=1}^{N}\sum_{l=1}^{L} \tau_{n,l} W log_2\Big(1 + \frac{E_n g_{n,l}}{\tau_{n,l} W N_0}\Big) + \sum_{l=1}^{L} \tau_l W log_2\Big(1 + \frac{E_l g_l}{\tau_l(\beta P_h + W N_0)}\Big) - \mu(\sum_{n=1}^{N}\sum_{l=1}^{L} \tau_{n,l} + \sum_{l=1}^{L} \tau_l - 1)$$
$$-\phi\Big(\sum_{n=1}^{N}\sum_{l=1}^{L} \tau_{n,l} W log_2\Big(1 + \frac{E_n g_{n,l}}{\tau_{n,l} W N_0}\Big) - \sum_{l=1}^{L} \tau_l W log_2\Big(1 + \frac{E_l g_l}{\tau_l(\beta P_h + W N_0)}\Big)\Big) \tag{3.12}$$

where $\mu \geq 0$ and $\phi \geq 0$ are the Lagrange multipliers corresponding to constraints.

Theorem 2: In $\mathcal{T}-\mathcal{TMP}$, the transmission times of user n and relay l are given by

$$\tau_{n,l} = \frac{-\gamma_{n,l}\mathbf{W}(-e^{-}(\frac{\mu ln(2)}{(1-\phi)W} + 1))}{1 + \mathbf{W}(-e^{-}(\frac{\mu ln(2)}{(1-\phi)W} + 1))} \tag{3.13}$$

$$\tau_l = \frac{-\gamma_l\mathbf{W}(-e^{-}(\frac{\mu ln(2)}{(1-\phi)W} + 1))}{1 + \mathbf{W}(-e^{-}(\frac{\mu ln(2)}{(1-\phi)W} + 1))} \tag{3.14}$$

where $\mathbf{W}(.)$ is a Lambert function [13], the terms $\gamma_{n,l}$ and γ_l are given by

$$\gamma_{n,l} = \frac{g_{n,l}E_n}{N_0 W}. \tag{3.15}$$

$$\gamma_l = \frac{g_l E_l}{(\beta P_h + N_0 W)}. \tag{3.16}$$

Proof. To solve for the transmission times of user n and relay l, we take the derivative of Lagrangian function L with respect to $\tau_{n,l}$ and τ_l, respectively. First, we derivate L w.r.t to $\tau_{n,l}$, which is given as

$$\frac{\partial L}{\partial \tau_{n,l}} = \frac{(1-\phi)}{ln(2)}\Big(\Big(\frac{g_{n,l}E_n}{\tau_{n,l}N_0 W} + 1\Big) - \frac{W g_{n,l} E_n}{W N_0 \tau_{n,l}(\frac{g_{n,l}E_n}{\tau_{n,l}N_0 W} + 1)}\Big) - \mu = 0 \tag{3.17}$$

which can be written as

$$-e^{(\frac{-\mu \ln(2)}{(1-\phi)W}+1)} = -\Big(\frac{\tau_{n,l}}{\gamma_{n,l} + \tau_{n,l}}\Big)e^{(\frac{-\tau_{n,l}}{\gamma_{n,l}+\tau_{n,l}})} \tag{3.18}$$

Since $X = W(Y)$ is the solution of $Y = Xe^X$, after some manipulations, $\tau_{n,l}$ is obtained as given in Eq. (3.13). The expression for transmission time of relay l can be proved similarly by taking the derivative of L with respect to τ_l and is skipped for brevity. □

To update the multipliers μ and ϕ, we adopt the gradient method [24]. The rules of updating multipliers are given as

$$\mu(j+1) = \Big[\mu(j) + \epsilon_\mu\Big(\sum_{n=1}^{N}\sum_{l=1}^{L}\tau_{n,l} + \sum_{l=1}^{L}\tau_l - 1\Big)\Big]^+ \tag{3.19}$$

$$\phi(j+1) = \Big[\phi(j) + \epsilon_\phi\Big(\sum_{n=1}^{N}\sum_{l=1}^{L}\tau_{n,l} W log_2\Big(1 + \frac{E_n g_{n,l}}{\tau_{n,l} W N_0}\Big) - \sum_{l=1}^{L}\tau_l W log_2\Big(1 + \frac{E_l g_l}{\tau_l(\beta P_h + W N_0)}\Big)\Big)\Big]^+ \tag{3.20}$$

where ϵ_μ and ϵ_ϕ are the step sizes at the j^{th} iteration. In the following, we present the algorithm for the evaluation of optimal transmission times $\tau_{n,l}$ and τ_l, named as Transmission Times Evaluation Algorithm (TTEA). The algorithm takes the set of users N and predetermined relays L as inputs, and returns the optimal $\tau_{n,l}$, τ_l, $R_{n,l}$, and R_l results. It starts by initializing the lagrange multipliers μ and ϕ and iteration index j to 0 (Line 1). In each iteration, the values of $\tau_{n,l}$ and τ_l are updated (Line 3). Then, the corresponding $R_{n,l}$

and R_l are updated using the values of $\tau_{n,l}$ and τ_l (Line 4). In Line 5, μ and ϕ are updated, using $\tau_{n,l}$ and τ_l. The TTEA algorithm keeps updating $\tau_{n,l}$, τ_l, $R_{n,l}$, and R_l values iteratively until μ and ϕ converge.The computational complexity of TTEA algorithm is $O(N \times L \times J)$ for a network of N users and L relays, where J is the number of iterations until the algorithm converges. In order to guarantee that the TTEA algorithm convergences, $\epsilon_\mu(j)$ and $\epsilon_\phi(j)$ must satisfy $\sum_{j=1}^{\infty} \epsilon(j) = \infty$ and $lim_{j\to\infty}\epsilon(j) = 0$.

Algorithm 2 Transmission Times Evaluation (TTEA) Algorithm

input: users N and relays L
output: $R_{n,l}$,$\tau_{n,l}$, R_l, τ_l, $\forall n$, $\forall l$

1: set $j \leftarrow 0$ and initialize $\mu(j)$, $\phi(j)$,
2: **repeat**
3: update $\tau_{n,l}$ and τ_l according to Eqn. (3.13) and Eqn. (3.14),
4: update the corresponding $R_{n,l}$ and R_l according to Eqn. (3.6) and Eqn. (3.7),
5: update $\mu(j+1)$ and $\phi(j+1)$ according to Eqn. (3.19) and Eqn. (3.20),
6: $j \leftarrow j+1$
7: **until** μ and ϕ converge
8: obtain the values $\tau_{n,l}$, τ_l, and corresponding $R_{n,l}$ and R_l.

3.5 Best Relay Selection Algorithm (BRS)

In this section, we present the heuristic polynomial-time sub-optimal best relay selection algorithm (BRS). The throughput of the FD-WPCCN can be increased further by selecting a better relay for each user. An optimal solution of the relay selection problem is to incorporate brute force search (BFA) algorithm. In BFA, we evaluate all the possible relay-user combinations and select the combination with the maximum sum throughput. The computational complexity of BFA is exponential due to L^N possible combinations of the relay-user, where L and N are the total number of relays and users, respectively. Due to the exponential computational complexity of BFA, we propose BRS as a heuristic algorithm. It is based on assigning a relay to the user that offers the best channel to noise (CNR) ratio, taking into account both channel links of the network i.e., from user to relay, and from relay to HAP, respectively.

The BRS Algorithm, as given in Algorithm 3, is described in detail as follows. It

Algorithm 3 Best Relay Selection (BRS) Algorithm

input: users N and relays L

output: Relay selection $\mathcal{R}$, transmission times $\tau_{n,l}$, τ_l, throughput $R_{n,l}$, R_l, $\forall n$, $\forall l$

1: **for** $n = 1 : |\mathcal{N}|$ **do**
2: Calculate $\alpha_{n,l}, \alpha_l$, $\forall l$
3: $z \leftarrow argmax_{l \in L}\ \{min(\alpha_{n,l}, \alpha_l)\}$,
4: $\mathcal{R} \leftarrow \mathcal{R} + \{z\}$,
5: **end for**
6: Execute the TTEA algorithm using the relay set $\mathcal{R}$, and get the outputs $\tau_{n,l}$, τ_l, $R_{n,l}$, R_l, $\forall n, \forall l$

starts by taking the total number of N users, and L relays as inputs and returns the relay allocation $\mathcal{R}$, transmission times $\tau_{n,l}$, τ_l, throughput $R_{n,l}$, and R_l as outputs. Then, for every user in the network, it calculates the CNR of both the hops with all the relays l, respectively (Line 2), and allocates a relay to the current user with the highest $\{min(\alpha_{n,l}, \alpha_l)\}$ (Line 3), where $\alpha_{n,l} = \frac{g_{n,l}}{N_o W}$ and $\alpha_l = \frac{g_l}{\beta P_h + N_o W}$ be the CNR of the two hops using the relay l, respectively. After allocating relays to all the users in the network, TTEA algorithm is executed to get the outputs (Line 6). The computation time complexity of BRS is $O(N \times L) + O(N \times L \times J)$, for a network of N users and L relays.

3.6 Performance Evaluation

In this section, we compare the throughput performance of the proposed BRS and TTEA algorithms to the optimal BFA.

The simulations are obtained in MATLAB and are based on Monte Carlo simulations, averaged over 1000 random network realizations. For large scale fading, we used the model given as

$$PL(d, dB) = PL(d_0, dB) + 10\alpha log_{10}(d/d_0) + Z \tag{3.21}$$

where, $PL(d, dB)$ is the path loss in dB at distance d, d_0 is the reference distance, α is the path loss exponent, Z is a zero mean Gaussian random variable with standard deviation σ. The parameters used are W=1 MHz; β=-80 dB; d_o=1 m; PL(d_o)=30 dB; α=2.76; σ=4 [14]. For the non-linear EH model based on logistic function, $P_s = 7mW$, $a = 1500$

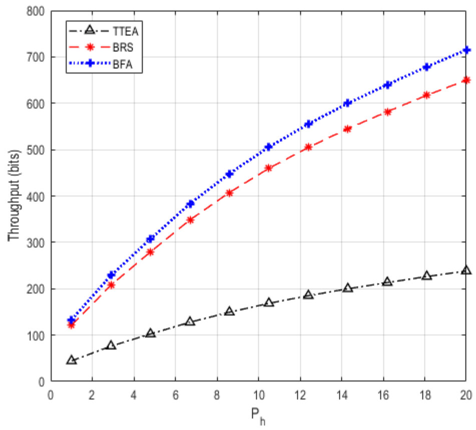

Figure 3.1: Sum throughput of the algorithms for different HAP transmit power P_h

and b = .0022. We assume a network of N=4 users, and L=4 relays, P_h= 1 dB, and initial battery levels B_n=B_l=10e^{-8} J, unless otherwise stated.

3.6.1 Throughput versus HAP power P_h

Fig. 3.1 illustrates the sum throughput of a network for varying HAP power P_h values. As P_h increases, throughput of the system increases. It is because the relays and users can harvest more energy with increasing P_h values. After a certain value of HAP power, the throughput becomes almost constant. This is due to the saturation region of the non-linear energy harvester of the relays and the users. Specifically, as P_h increases, the EH circuit saturates, and throughput of the network becomes almost constant. The proposed BRS algorithm performs close to the optimal BFA solution, despite offering a very low computational complexity as compared to BFA. It outperforms the predetermined relay allocation TTEA, showing the significance of appropriate relay selection in the network.

3.6.2 Throughput versus the number of users

Fig. 3.2 shows the throughput performance of the TTEA and BRS algorithms in comparison to optimal, denoted by BFA, for different network densities. We observe that the sum throughput increases with the network size, as expected. With the increase of each user in the network, throughput increase yielded by BRS is large compared to TTEA. This ob-

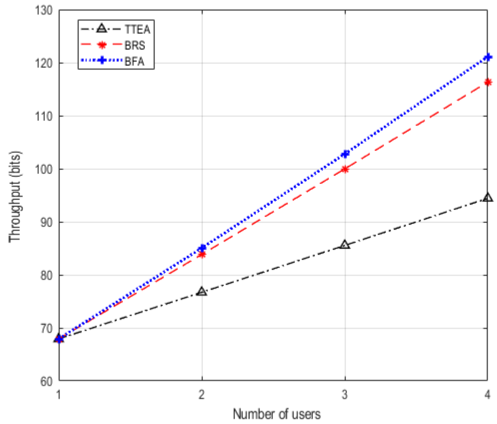

Figure 3.2: Sum throughput of the algorithms for varying network sizes

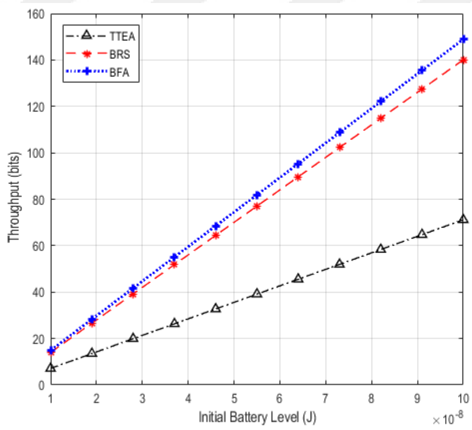

Figure 3.3: Sum throughput for different battery levels of the nodes

servation shows the significance of appropriate relay selection in BRS as compared to the predetermined relay allocation in TTEA. Moreover, throughput achieved by the proposed BRS algorithm performs very close to the optimal solution BFA.

3.6.3 Throughput versus battery levels of the nodes

Fig. 3.3 shows the throughput for different initial battery levels of the relays and users. Throughput increases as the battery level of the nodes increases. It is because higher battery levels allow the users to transmit their information in short time durations and with higher rates. The proposed BRS algorithm performs very close to the optimal BFA, followed by the TTEA scheme.

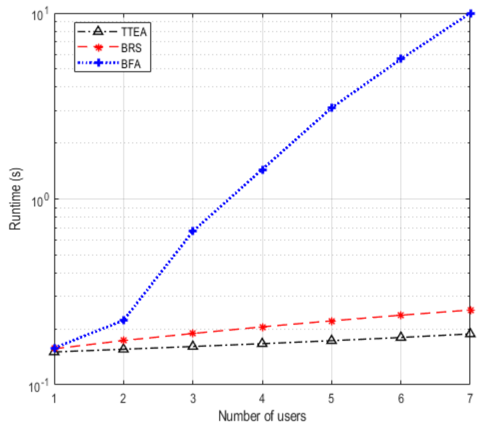

Figure 3.4: Run time of the algorithms for different network densities

3.6.4 Run time versus Network Density

Fig. 3.4 shows the runtime of the proposed algorithms for different network densities. With the addition of nodes in the network, the runtime of optimal BFA increases exponentially, whereas add minimal burden to the proposed BRS and predetermined TTEA. The significance of incorporating the proposed BRS is that it achieves very close throughput performance to the optimal BFA, but with very less computational complexity, as observed in this section.

3.7 Conclusion and Future Works

In this chapter, we investigate the relay selection problem to maximize the sum throughput of the FD-WPCCN. The formulated problem is MINLP. First, we present the optimal solution of the throughput maximization problem by studying its properties for a predetermined relay allocation. We then propose a polynomial time heuristic BRS algorithm for the relay selection. We compare the performance of the proposed algorithms through simulations. In future, we will study multi-antenna WPCCN.

Chapter 4

THROUGHPUT MAXIMIZATION FOR ON-OFF TRANSMISSION SCHEME BASED FULL-DUPLEX WIRELESS POWERED COOPERATIVE COMMUNICATION NETWORKS

Higher network throughput, increased coverage area and reliability are some of the significant improvements promised by the energy harvesting (EH) cooperative communication. This chapter considers a two-hop full duplex (FD) multi-relay multi-user wireless powered cooperative communication network (WPCCN), in which the EH capable relays and users transmit their information to an energy broadcasting hybrid access point (HAP). We present an optimization framework for the relay selection and scheduling of the users. The objective is to maximize the sum throughput of FD-WPCCN, considering an on-off transmission scheme, in which the relays and users either transmit at a constant power or remain silent. The formulated optimization problem is a mixed integer nonlinear programming problem, which is difficult to solve for the global optimum. As a solution strategy, we first present the polynomial time heuristic relay selection algorithm for a predetermined schedule of the users by studying the characteristics of optimal relay allocation solution of the optimization problem. Then, we propose a polynomial time heuristic scheduling algorithm by investigating the characteristics of the optimal scheduling solution of the optimization problem. Through extensive simulations, we evaluate the performance of the proposed algorithms for different HAP power values, network sizes, battery levels of the nodes, and transmit power values of the relays and the users. We compare the proposed algorithms with the optimal and another benchmark algorithm and observe that throughput can be increased by selecting an appropriate relay and optimal transmission order of the users.

4.1 Introduction

Cooperative communication, in which one or more intermediate relay nodes assist the information transmission between a source and destination has the potential to increase the network coverage area, system throughput, and reliability of the transmission [25]. According to the recent ericsson report, 24.6 billion sensors are expected to be installed by 2025, which are mostly battery dependent. For this purpose, researchers proposed an interesting idea of harvesting energy from various environmental sources such as wind, solar, vibration, and radio frequency (RF) signals [26]. Among them, RF energy harvesting is the most efficient solution due to its reliability, and controllability [15]. There are two main types of RF energy harvesting wireless network models. Simultaneous Wireless Information and Power Transfer (SWIPT) [17] and Wireless Powered Communication Network, referred as WPCN [27]. Specifically in WPCN, a HAP transmits the energy signal to the destination nodes, i.e., sensors, which then transmit their information using the harvested energy, to the HAP.

In the context of relay based WPCN, also known as wireless powered cooperative communication network (WPCCN), authors initially study a simple three node model, consisting of a HAP, a relay and a user [10, 11, 19]. In these WPCCN works, the relay and user are the EH nodes, which harvest energy in the downlink (DL) from the HAP, and transmit the information in the uplink (UL) to the HAP. Specifically, [10] derives the closed form expression of the average throughput. [11] presents an approximate closed-form expression for the throughput of an adaptive transmission (AT) protocol, whereas [19] investigates the impact of EH relay position on the link outage performance. In addition, [10] also investigates a multi-relay scenario and proposes a relay selection scheme based on channel state information (CSI) of the system. [12] extends the three node model to multi-relay multi-user scenario, with an objective to minimize the time duration for information and energy transfer. However, the aforementioned studies consider a half-duplex (HD) model. More recently, [20] and [28] consider an FD multi-relay multi-user WPCCN, with the objectives of transmission time minimization and throughput maximization through relay selection, respectively. The performance gain achieved by the FD WPCCN is always better than the HD counterpart due to the HAP's ability of simultaneous information and energy transfer.

Generally, in RF EH networks, the EH rates are very small, which necessitates simple and low power consuming circuitry. In this scenario, an on-off transmission scheme is very efficient which requires simple power amplifiers and low processing cost. [29–31] study a single hop multi-user WPCN based on on-off transmission scheme. In [29, 30], authors analyze the average error and outage probability in a single user system, whereas [31] studies a multi-user system with the objective to minimize the schedule length and maximize the sum throughput. Currently, [21] investigates the scheduling and relay selection problem for an on-off transmission based FD-WPCCN to minimize the schedule length.

In this chapter, we present an optimization framework for the scheduling and relay selection problem, with the objective of maximizing the sum throughput of the multi-relay multi-user FD-WPCCN, considering an on-off transmission scheme, for the first time in the literature. The main contributions of this chapter are as follows:

- We consider an FD-WPCCN, with HAP and decode-and-forward (DF) relays both operating in FD mode, for the first time in literature. The relays and users harvest energy from the HAP, by using a non-linear energy harvesting model which is based on a logistic function, and transmit information utilizing on-off transmission scheme.

- We formulate an optimization problem with the objective of maximizing the sum throughput of the FD-WPCCN through relay selection and scheduling of the users.

- The formulated optimization problem is a mixed integer non-linear programming problem which is in general hard to solve for the global optimum. To solve the problem, we decompose it into two sub-problems: relay selection problem and scheduling problem. We first propose a polynomial time heuristic relay selection algorithm by studying the characteristics of the optimal solution of optimization problem, for a known schedule of the users. It is based on the idea of selecting a relay for the user with the minimum difference of transmission times between the two hops. Then, we present the heuristic scheduling algorithm by investigating the characteristics of the optimal scheduling solution of the original problem. The scheduling algorithm is based on the idea of prioritizing the users with the maximum throughput performance.

- We evaluate the performance of the proposed algorithms through simulations and compare them with the other benchmark scheme. We observe that the throughput can be increased significantly by choosing appropriate relays and schedule of the users.

The rest of the chapter is organized as follows. In Section 4.2, we present the system model and assumptions. In section 4.3, we formulate the optimization problem and present the polynomial-time heuristic algorithms for the formulated optimization problem. Section 4.4 evaluates the performance gain of the proposed algorithms through simulations. Section 4.5 presents the concluding remarks and future directions.

4.2 System Model and Assumptions

We consider a WPCCN architecture, as shown in Fig. 4.1. It consists of a single HAP, K relays and N users. The HAP and relays are equipped with single FD antenna, whereas single antenna users operate in HD mode. The FD antenna of the HAP is used for simultaneous information and energy transfer in the UL and DL, respectively. The FD antenna of the relay works in a way that it receives and transmits information from the user to the HAP simultaneously. The HAP is transmitting a constant power denoted by P_h, whereas relays and users harvest energy from the HAP in the DL. The UL channel gains from user n to relay i, and from relay i to HAP are denoted by $g_{n,i}$, and g_i, respectively. The DL channel gains from HAP to relay i and user n are represented by h_i and h_n, respectively. We assume a non-linear energy harvesting model based on logistic function, in which the

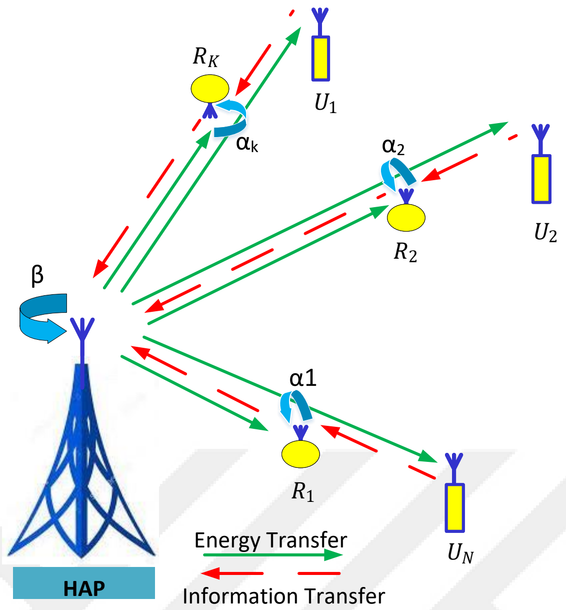

Figure 4.1: Full-Duplex Wireless Powered Cooperative Communication Network

energy harvesting rate of user n is given as

$$C_n = \frac{P_s(\Psi_n - \frac{1}{1+e^{a_n b_n}})}{(1 - \frac{1}{1+e^{a_n b_n}})}, \tag{4.1}$$

where $\Psi_n = \frac{1}{(1+e^{-a_n(P_h h_n - b_n)})}$. The energy harvesting rate of relay i is expressed as

$$C_i = \frac{P_s(\Psi_i - \frac{1}{1+e^{a_i b_i}})}{(1 - \frac{1}{1+e^{a_i b_i}})}, \tag{4.2}$$

where $\Psi_i = \frac{1}{(1+e^{-a_i(P_h h_i - b_i)})}$, P_s represents the maximum saturation power achieved by the energy harvesting circuit due to large input power values, constants a and b are linked to the circuit specifications.

We consider block fading channels, i.e., the channel gains remain constant within the time frame and may vary from frame to frame. The total time duration is divided into various scheduling frames. Each scheduling frame is further divided into slots of variable lengths which are allocated to the users and their selected relays. We assume that the relays and users can harvest energy from the HAP throughout the time duration except when they are transmitting information to the HAP in the UL. The harvested energy can be stored in their batteries with initial battery levels $B_i, i \in \{1, ..., K\}$, and $B_n, n \in \{1, ..., N\}$, respectively. The available energy for user n is given by

$$E_n = B_n + C_n \sum_{l=1}^{n-1} \sum_{i=1}^{K} x_{l,i}(t_{l,i} + t_i) \tag{4.3}$$

where $\sum_{l=1}^{n-1} \sum_{i=1}^{K} x_{l,i}(t_{l,i} + t_i)$ represent the energy harvesting time duration for the user n, $x_{l,i}$ is a binary variable for the relay selection, which is either 1 or 0, depending on whether a relay i is assigned to user n or not, $t_{l,i}$ is the information transmission time of user l to relay i, and t_i is the information transmission time of relay i to HAP. The available energy for relay i is given by

$$E_i = B_i + C_i \sum_{n \in S} \sum_{i=1}^{K} x_{n,i}(t_{n,i} + t_i) \tag{4.4}$$

where $\sum_{n \in S} \sum_{i=1}^{K} x_{n,i}(t_{n,i} + t_i)$ is the energy harvesting time of relay i before its information transmission time. The set S contains the users, scheduled before user n with their allocated relays. However, those users which have been allocated the same i^{th} relay before are not included in this set.

We assume a constant on-off transmission power model, in which all the relays and users in the system have a constant transmission power, denoted by P_{max}. The throughput from the user n to relay i is expressed as

$$R_{n,i} = t_{n,i} W log_2 \left(1 + \frac{g_{n,i} P_{max}}{\alpha_i P_{max} + N_0 W}\right) \tag{4.5}$$

where $t_{n,i}$ is the information transmission time of user n to relay i, $\alpha_i P_{max}$ is the self-interference power at each relay i, $i \in \{1, ..., K\}$, arises due to the FD mode. $N_0 W$ is the noise power, and W is the system bandwidth. The transmission throughput of relay i is given as

$$R_i = t_i W log_2 \left(1 + \frac{g_i P_{max}}{\beta P_h + N_0 W}\right) \tag{4.6}$$

where t_i is the transmission time of relay i to HAP, and βP_h is the self-interference power at the HAP. The end-to-end throughput is expressed as [32]

$$R = min\{R_{n,i}, R_i\} \tag{4.7}$$

4.3 Optimization Framework

4.3.1 Throughput Maximization Problem

In this subsection, we formulate the joint optimization problem for scheduling and relay selection with the objective of maximizing the sum throughput of the system. It is denoted by $\mathcal{TM}-\mathcal{SRP}$, and is presented as follows: $\mathcal{TM}-\mathcal{SRP}$

$$max \sum_{n=1}^{N}\sum_{i=1}^{K} x_{n,i}\, min\{R_{n,i}, R_i\} \tag{4.8a}$$

subject to

$$\sum_{n=1}^{N}\sum_{i=1}^{K} t_{n,i} + \sum_{i=1}^{K} t_i \leq 1, \tag{4.8b}$$

$$E_n - t_{n,i}P_{max} \geq 0; \forall n \in \{1,..,N\} \tag{4.8c}$$

$$E_i - t_iP_{max} \geq 0; \forall i \in \{1,..,K\} \tag{4.8d}$$

$$\sum_{i=1}^{K} x_{n,i} = 1; \forall n \in \{1,..,N\} \tag{4.8e}$$

$$s_{mn} + s_{nm} = 1; \forall m,n \in \{1,..,N\} \tag{4.8f}$$

variables

$$t_{n,i}, t_i, \geq 0; \forall n,i; x_{n,i} \in \{0,1\}; s_{mn} \in \{0,1\}; \tag{4.8g}$$

The decision variables of the $\mathcal{TM}-\mathcal{SRP}$ are $x_{n,i}$, a binary relay selection variable, which takes value 1 if user n is assigned to relay i, and 0 otherwise; $t_{n,i}$ and t_i, the transmission times of the two hops i.e., from user n to relay i, and relay i to HAP; and s_{mn}, a binary scheduling variable, which is 1 if user m transmits before user n, and 0 otherwise.

The objective of the $\mathcal{TM}-\mathcal{SRP}$ is to maximize the sum throughput, as given in Eqn. (4.8a). Eqn. (4.8b) represents a normalized schedule length of 1 to transmit information. Eqns. (4.8c) and (4.8d) represent the energy causality constraints of the users and relays, respectively. Energy causality guarantees that the consumed energy must be less than or equal to the available energy. Eqn. (4.8e) ensures that only one relay assists a particular user in its information transmission. Eqn. (4.8f) represents a scheduling constraint, i.e., if user m transmits its information first, then some other user n cannot transmit before user m.

The $\mathcal{TM}-\mathcal{SRP}$ is a mixed integer non-linear programming problem, which is in general difficult to solve for global optimal solution. As a solution strategy, we first propose a polynomial-time heuristic relay selection algorithm for a predetermined schedule of the users, by incorporating the characteristics of the optimal solution of $\mathcal{TM}-\mathcal{SRP}$. After the relay selection, we present the heuristic scheduling algorithm by exploiting the properties of the optimal solution of $\mathcal{TM}-\mathcal{SRP}$.

4.3.2 Relay Selection Algorithm

In this subsection, we propose a polynomial-time heuristic relay selection algorithm for a predetermined schedule of the users. We observe that the $\mathcal{TM}-\mathcal{SRP}$ is a mixed integer non-linear programming problem, and is very difficult to solve for the global optimal solution. One approach to solve $\mathcal{TM}-\mathcal{SRP}$ is the exhaustive search, in which we enumerate all the possible transmission order of the users and the relay-user combinations, and then select the scenario yielding the maximum throughput value. However, this solution is intractable due to $\mathcal{O}(K^N \times N!)$ computational complexity, where K^N represents the possible relay-user combinations and $N!$ is the possible transmission orders of the users. On the other hand, the predetermined schedule and relay selection problem, i.e., s_{mn} and $x_{n,i}$ are given, is a convex optimization problem. Therefore, to overcome this exponential computational complexity of the optimal exhaustive search and to better understand the optimization problem, we first study the characteristics of the optimal relay allocation solution of $\mathcal{TM}-\mathcal{SRP}$, in the following discussion.

Since the DF relays in the network operate in FD mode of transmission, each relay achieves the maximum throughput performance gain when assigned to a user with the minimum transmission time difference of the two hops. Suppose, for a user n, $\Delta_i = |t_{n,i} - t_i|$ and $\Delta_k = |t_{n,k} - t_k|$ be the difference of transmission time of the two hops using relays i and k, respectively. If $\Delta_k > \Delta_i$, the throughput performance achieved by the user n via relay

i is better as compared to the performance via relay k i.e., $min\{R_{n,i}, R_i\} > min\{R_{n,k}, R_k\}$. Specifically, for a user n to transmit the same number of bits, over the two hops using relay i, the transmission time difference of the hops from user n to relay i and from relay i to the HAP should be minimum to achieve the maximum end-to-end throughput.

Based on the above discussion, we propose a polynomial-time heuristic relay selection algorithm for a predetermined schedule of the users, referred as Best Relay and Predetermined Schedule (BRPS), in Algorithm 4. It is based on the idea of selecting a relay for each user with the minimum transmission time difference of the two hops i.e., $|t_{n,i} - t_i|$, where $t_{n,i} = \frac{E_{n,i}}{P_{max}}$ and $t_i = \frac{E_i}{P_{max}}$.

The BRPS Algorithm 4 is described in detail as follows. It takes the set of relays K and users N as input, and returns the set of selected relays $\mathcal{R}$ for all the users as output. For each user n in the system, it calculates $t_{n,i}$ and t_i, for all the relays, respectively (Line 2), and allocates a relay to the user which provides minimum $|t_{n,i} - t_i|$ (Line 3). The BRPS Algorithm terminates when all the users are being allocated the relays. The computational complexity of BRPS is $\mathcal{O}(N)$.

Algorithm 4 Best Relay and Predetermined Schedule (BRPS) Algorithm

input: relays $\mathcal{K}$ and predetermined scheduled users $\mathcal{N}$
output: Relay selection set $\mathcal{R}$

1: **for** $n = 1 : |\mathcal{N}|$ **do**
2: Calculate $t_{n,i}, t_i, \forall i$
3: $z \leftarrow argmin_{i \in K} (|t_{n,i} - t_i|)$,
4: $\mathcal{R} \leftarrow \mathcal{R} + \{z\}$,
5: **end for**

After the relay selection algorithm BRPS, the problem reduces to a scheduling problem. In the next subsection, we present the polynomial time heuristic scheduling algorithm by discussing the properties of $\mathcal{TM} - \mathcal{SRP}$.

4.3.3 Scheduling Algorithm

In this subsection, we propose a polynomial-time heuristic scheduling algorithm, referred as Best Relay and Best Schedule (BRBS), for the relay-user set obtained from BRPS algorithm. For this purpose, we first present the optimal scheduling property of $\mathcal{TM} - \mathcal{SRP}$

in the following Lemma.

Lemma 4. *In the optimal solution of $\mathcal{TM}-\mathcal{SRP}$, for any two users n and m, and $R_n > R_m$, if $t_n = 0$, then $t_m = 0$, where $R_l = min\{R_{l,i}, R_i\}$, $t_l = min\{t_{l,i}, t_i\}$, and $l \in [n, m]$.*

Proof. The lemma can be proved by contradiction. Suppose that $t^* = [t_1^*, t_2^*, ..., t_N^*]$ represent the set of optimal transmission time of the users. In this optimal set, t_n^*=0 and t_m^* >0 for some users n and m with rates $R_n > R_m$. Now, for some positive $t' > 0$, which do not violate the energy causality constraint of user n, we can divide the transmission time of user m into time slots having lengths $t_m^* - t'$ and t', respectively. We can allocate $t_m^* - t'$ to user m, and t' to user n, which in turn increases the throughput by an amount $t'(R_n - R_m)$. The term $t'(R_n - R_m)$ is strictly positive. This is a contradiction. □

Based on Lemma 4, the high rate users in the network must be prioritized to transmit the information and the final schedule must not necessarily contain all the users of the network. The final schedule can be any subset of the users, as long as it achieves the objective i.e., to maximize the throughput. Moreover, it is possible that the maximum throughput user i.e., $max_{i \in \mathcal{R}}\ \{min(R_{n,i}, R_i)\}$ can occupy the entire frame length T, where $\mathcal{R}$ is the set of relays allocated to the users by using BRPS Algorithm.

In the following, we present the BRBS Algorithm. The BRBS algorithm takes the set of users $\mathcal{N}$, sorted in decreasing order of transmission rates with their selected relays $\mathcal{R}$ obtained from the BRPS algorithm, and transmission times $t_{n,i}$, t_i. It returns the schedule set $\mathcal{S}$ and resulting sum throughput $R(\mathcal{S})$ of the system. It starts by initializing the unallocated time T to 1 (Line 1). In each step, BRBS allocates the maximum feasible transmission time to the maximum rate user (Line 4). Note that it starts allocating time from the end of the scheduling frame T, so that the users with higher rates can harvest more energy. It keeps updating unallocated transmission time T (Line 5), and terminates if T becomes 0 at any step (Line 6). Otherwise, it schedules all the users accordingly, and the remaining unallocated time is considered as t_o (Line 9), which represent the energy harvesting or waiting time until the first user in the network starts transmitting. Finally, BRBS algorithm returns the schedule set $\mathcal{S}$ and the corresponding sum throughput $R(\mathcal{S})$. The computational complexity of BRBS is $\mathcal{O}(N)$.

Algorithm 5 Best Relay and Best Schedule (BRBS) Algorithm

input: set of users $\mathcal{N}$ sorted in decreasing order of transmission rates with their selected relay set $\mathcal{R}$, $t_{n,i}$, t_i, $\forall n$, $\forall i \epsilon \mathcal{R}$
output: schedule set $\mathcal{S}$, throughput $R(\mathcal{S})$

$T = 1$
for $n = 1 : |\mathcal{N}|$ **do**
    obtain the corresponding $t_{n,i}$ and t_i,
    $t_n \leftarrow min\{(t_{n,i}, t_i), T\}$,
    $T \leftarrow T - t_n$,
    if $T = 0$ **then** break,
    end if
end for
$t_o \leftarrow T$,
Obtain $\mathcal{S} \leftarrow \{1, 2, ..., n\}$
Obtain $R(\mathcal{S}) \leftarrow \sum_{l=1}^{n} t_l r_l$

4.4 *Performance Evaluation*

In this section, we evaluate the throughput performance of the proposed heuristic algorithms BRBS and BRPS, and compare them to the optimal BFA solution which is exponential time complex and other polynomial time heuristic algorithm as benchmark, namely, PRPS; predetermined relay and predetermined schedule. As the name suggests, in PRPS, we assume a predetermined relay allocation and predetermined schedule of the users. Moreover, in the simulations, for fair comparison, we terminate all the algorithms once the condition $T = 1$s is achieved. The simulations are obtained in MATLAB and are averaged over 1000 random network realizations. For large scale fading, we used the model given as

$$PL(d, dB) = PL(d_0, dB) + 10\alpha log_{10}(d/d_0) + Z \tag{4.9}$$

where, $PL(d, dB)$ is the path loss in dB at distance d, d_0 is the reference distance, α is the path loss exponent. Z is a zero mean Gaussian random variable, and its standard deviation is σ. We assume a network of N=10 users, HAP power value P_h=1W, P_{max}=10^{-3}W, battery levels $B_i = B_n = 1e^{-8}$, unless otherwise stated. The other simulation parameters are W=1 MHz; β=-80 dB; d_o=1 m; PL(d_o)=30 dB; α=2.76; and σ=4 [14]. For the non-

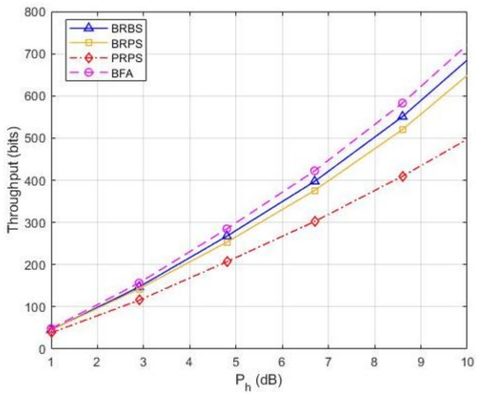

Figure 4.2: Throughput of the algorithms for different HAP transmit power values P_h

linear EH model based on logistic function, $P_s = 5mW$, $a = 1500$ and $b = .0022$.

4.4.1 Throughput versus HAP power P_h

Fig. 4.2 illustrates the throughput performance of the algorithms for different HAP power P_h values. The throughput of the system increases with the increasing HAP power. It is due to the fact that higher P_h values allow the relays and users to harvest more energy in less time, thus increasing the throughput. The proposed BRBS algorithm performs close to the optimal BFA solution. Note that the optimal BFA is exponential time complex, whereas the proposed BRBS has polynomial time complexity. BRBS performance is followed by the BRPS in which we assume the predetermined schedule of the users and perform the relay allocation only. The benchmark PRPS algorithm in which we assume the predetermined schedule and relay allocation, achieves the least performance gain, showing the significance of determining an appropriate relay and optimal schedule of the users.

4.4.2 Throughput versus P_{max}

Fig. 4.3 shows the throughput performance of the algorithms for different P_{max} values. We observe that the throughput decreases with increasing P_{max}. It is because the relays and users need more time to harvest energy to afford information transmission at high P_{max} values, which results in an increased unallocated initial harvesting time, and therefore,

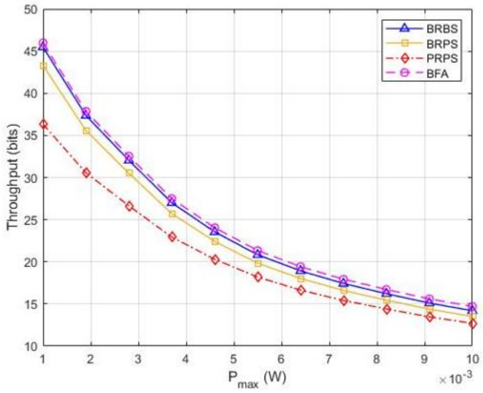

Figure 4.3: Throughput of the algorithms for different values of P_{max}

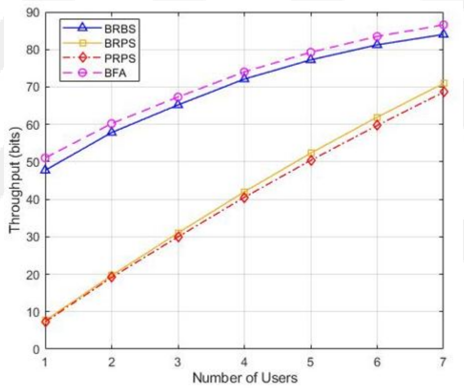

Figure 4.4: Throughput for different network densities

decrease in allocated transmission time for the users. The proposed BRBS algorithm performs very close to the optimal BFA and outperforms other heuristic BRPS and PRPS algorithms, showing the significance of determining an appropriate relay and optimal schedule of the users.

4.4.3 Throughput versus network size

Fig. 4.4 compares the throughput performance of the proposed BRBS and BRPS algorithms as compared to the optimal BFA and benchmark PRPS schemes for different network sizes. We observe that the throughput increases with the network size, as expected. With the increasing network size, the better throughput performance achieved by

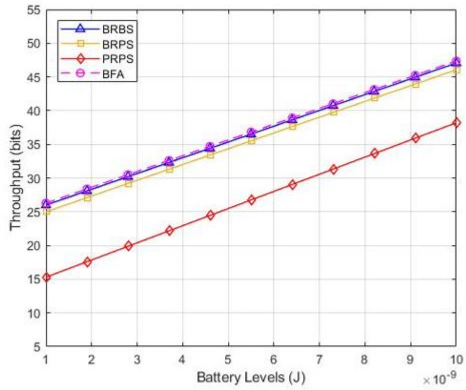

Figure 4.5: Throughput of the algorithms for different initial battery levels

the proposed BRBS algorithm as compared to BRPS shows the significance of scheduling of the users in the network. Moreover, the BRPS achieves better performance gain as compared to the benchmark PRPS signifies the importance of appropriate relay selection for the users in the network. Note that the polynomial time BRBS algorithm performs very close to the exponential time complex optimal BFA solution.

4.4.4 Throughput versus battery levels of the nodes

Fig. 4.5 shows the throughput for different initial battery levels of the nodes i.e., relays and users, in the network. We observe that the throughput increases with the increasing battery levels. Higher battery levels allow the nodes to transmit their information in shorter time durations, which in turn increases the throughput of the system. The proposed BRBS algorithm performs very close to the optimal BFA solution followed by BRPS and PRPS algorithms, respectively.

4.5 Conclusion and Future Works

In this chapter, we investigate the throughput maximization problem through appropriate relay selection and scheduling of the users of the FD-WPCCN. The formulated optimization problem is a mixed integer non-linear programming problem. To solve the problem, we divide the problem into two sub-problems: relay selection and scheduling problem. First, for a predetermined schedule, we present the polynomial time heuristic relay selection algorithm by discussing the characteristics of the original optimization problem. Then, we extend the problem to the scheduling problem and present the polynomial time heuristic scheduling algorithm. We evaluate the performance of the proposed algorithms through simulations and observe that the throughput of the system can be significantly increased by using appropriate relays and optimal schedule of the users in the network. In future, we will incorporate multiple hybrid access points in our system.

Chapter 5

OPTIMIZATION OF FULL-DUPLEX RELAYING SYSTEM WITH NON-LINEAR ENERGY HARVESTER

Simultaneous wireless information and power transfer (SWIPT) is a promising technique to prolong the lifetime of energy constrained relay-based systems. Most of the existing literature on relay-based SWIPT systems incorporate linear energy harvesting (EH) model. This chapter incorporates a non-linear EH model into the full-duplex (FD) amplify-and-forward (AF) relay-based system for the first time in the literature. We consider a practical non-linear energy harvester model namely constant-linear-constant (CLC) EH model, which takes into account the sensitivity and saturation characteristics of the EH circuit. First, the end-to-end outage probability of the system is derived for the time-switching (TS) based relay protocol. To prevent the outage performance degradation, the outage throughput and energy efficiency (EE) of the system is maximized by optimizing the TS parameter. Since the formulated problems are convex in nature, the golden-section method is used to find the optimal TS solution. Numerical results reveal the significance of employing a non-linear EH model by demonstrating the difference of the proposed model from the traditional linear EH model system and importance of using full-duplex relay by showing large performance gain over half-duplex relay-based (HDR) system, in terms of outage probability, throughput, and EE.

5.1 Introduction

Beyond 5*th* generation (5G) wireless communication systems face huge challenges for high data rates, reliability, and energy efficiency of communication [33]. Cooperative relaying, where a source node transmits a data signal to the destination, a third node overhears it and relays the signal to the destination as well, is an efficient technique to provide reliable transmission, high throughput and long coverage [34, 35]. On the other hand, in recent years, energy harvesting (EH) from various renewable sources such as wind, solar, and radio frequency (RF) has been realized as a potential solution to prolong the lifetime of energy constrained communication networks [36]. Among these renewable sources, harvesting energy from the radio frequency (RF) is an efficient option for future wireless systems because of its controllability, reliability, and lower cost [15]. Since RF signals can carry both energy and information, simultaneous wireless information and power transfer (SWIPT), which is a combination of wireless information transfer and wireless power transfer (WPT) has received the great attention from the researchers recently [37]. In many applications of SWIPT, wireless powered relaying is one typical application scenario for cooperative systems, in which the energy constrained intermediate relay nodes rely on the harvested energy from RF signals of the source to assist its communication to the destination. There are two types of relay commonly being used, amplify-and-forward (AF) [38], where a relay node amplifies the received signal from the source and sends it to the destination and decode-and-forward (DF) [39], where a relay node first decodes the received signal and then sends it to the destination. For energy harvesting and information transmission, the relay nodes use two prominent architectures, namely, time-switching (TS) and power-splitting (PS) protocols [37], [40]. In TS-based SWIPT protocol, the relay harvests power from an energy signal sent by the source and receives the source transmitted information signal in two different time phases, whereas, in PS-based SWIPT, the received source signal is split into two signal streams to perform energy harvesting and information processing.

Initially, SWIPT-aided two-hop relaying systems incorporate half-duplex (HD) transmission and traditional linear energy harvesting (EH) model [38–43]. The traditional linear EH model assumes that the output power of an energy harvester is linearly dependent on its input power. [40] derives the analytical expressions for the outage probability and ergodic capacity of an HD-AF relay-based system incorporating the TS and PS protocols, whereas [38] studies the system of [40] in the presence of interference at the relay and destination. In [41], the authors investigate the outage performance of an HD-AF relay-based system with PS protocol in the presence of a direct link between source and destination, whereas [42] incorporates the adaptive relaying (AR) protocol based on TS-PS protocol in HD-AF relay-based system. In [39], the authors derive the analytical expressions of the achievable throughput and ergodic capacity of an HD-DF relaying network for both TS and PS schemes. [43] studies an energy efficiency maximization (EEM) optimization problem for the multi-user multi-carrier energy-constrained HD-AF multi-relay network under the total source transmit power budget and energy-causality constraints. However, the limitation of the aforementioned relaying SWIPT systems to HD transmission results in loss of spectral efficiency. Therefore, full-duplex (FD) relaying, which utilizes the scarce frequency spectrum more efficiently by supporting simultaneous signal transmission and reception at the same frequency band, has been exploited.

FD relaying SWIPT systems with a linear EH model are investigated in [9, 44–53]. The throughput of the FD-AF and DF relaying system based on a TS receiver structure is investigated in [44]. Later on, [45] extended the work of [44] to the FD multi-antenna system. In [46], the authors study the outage probability of the FD-DF relay system incorporating the PS protocol, whereas in [47] the outage probability and throughput of FD-AF relay system incorporating TS protocol are analyzed under the QoS constraints. [9] discusses the problem of relay selection in FD two-way communication system whereas, [48] analyzes the outage performance of four different energy harvesting schemes based on two-way communication FD relay system. [49] studies the outage performance for the SWIPT FD-EH relay system, with the relay node subjected to co-channel interference (CCI), under PS protocol. [50] analyzes the outage probability of the EH-based FD AF and DF relay system in α-μ environment, under TS protocol. [51] studies an FD-AF multiple relay system employing SWIPT receivers operating in interference channels under PS protocol and presents power allocation problem using game theory. [52] presents the problem of maximizing the energy efficiency of an FD-AF MIMO-OFDM system with self-energy recycling, whereas [53] analyzes an FD-AF MIMO relay system based on antenna switching with self energy recycling and presents the problem of maximizing the spectral efficiency. The above mentioned full-duplex systems are all based on the conventional linear EH model. As stated above, the linear EH model assumes that the output power of the energy harvester is linearly dependent on its input power. However, the components of the EH circuit in a real system are non-linear, and the traditional linear EH model is unrealistic. As a result, researchers start to study the practical non-linear EH models based on RF signals [22, 32, 54–73].

The non-linear EH model based on sigmoid function has been studied in [22, 54–62], where as authors in [63–68] incorporates the non-linear EH model based on a linear-constant (LC) function. [69] studies the non-linear EH model based on a quadratic function and [70, 71] on a polynomial function obtained by a Taylor series expansion of the diode output in the rectifier. These non-linear EH models incorporate only the saturation effect of the EH circuit. Only recently, the authors in [32, 72, 73] incorporate the sensitivity characteristic of the EH circuit in modeling non-linear models which is known as constant-linear-constant (CLC) model. Considering the sensitivity characteristic is important for EH circuits containing diodes.

The developed non-linear EH models are being used in the design and analysis of various SWIPT systems [56–62], [64–68], [71], [32]. For the non-linear EH model relay-based systems specifically, based on the sigmoid function [22], [61] study the PS scheme for the HD-AF relay-based system in the presence of a direct link between source and destination, where as [62] studies the resource allocation and relay selection in a two-hop AF relay-assisted HD multi-user orthogonal frequency division multiple access (OFDMA) network with PS scheme. Based on LC model, [64] calculates the outage capacity of the HD-AF relay system with TS protocol, whereas [65] deduces the expression of the secret outage probability in the HD multi-DF relay-based system with PS protocol. The outage probability of the HD-DF relay-based system incorporating PS protocol under the imperfect channel is presented in [66]. [67] studies the dynamic PS schemes for the HD-AF relay-based system under the perfect and imperfect channel scenario. In [68], the authors derive the expressions for the outage probability of the HD-DF relay system in the interference-limited environment. [72] studies the two way communication rate regions under fixed and mobile relays based on CLC function. However, the systems mentioned above are limited to HD mode of transmission. Authors in [32] study the outage performance and QoS optimization of a full-duplex relay system with a constant-linear-constant (CLC) energy harvesting model, considering both the finite sensitivity and saturation characteristics of the EH circuit. Based on the TS scheme, the authors incorporate the DF relay to co-operate between the source and destination.

Motivated by the previous works, this chapter incorporates a non-linear EH model into an FD-AF relay-based system for the first time in literature. We consider a practical CLC EH model, which takes into account both the sensitivity and saturation characteristics of the EH circuit [73], [32]. The main contributions of this chapter are as follows:

- We provide the analysis of the outage probability of an FD-AF relay-based system incorporating a non-linear constant-linear-constant (CLC) EH model, considering both the sensitivity and saturation characteristics of the EH circuit for the first time in the literature.

- We optimize the TS scheme to maximize the system outage throughput and EE under the non-linear EH model. The formulated optimization problems are observed to be convex. Therefore, we exploit the golden-section method to find the optimal TS solution.

- The numerical results reveal that the performance of the proposed system under the non-linear EH model is different from the linear model system and illustrates the importance of using FD relay by showing significant performance gain over an HDR system incorporating both linear and non-linear EH models.

The rest of this chapter is organized as follows. Section 5.2 presents the system model and the non-linear energy harvesting model. In Section 5.3, the outage probability analysis of an FD-AF relaying system is analyzed. Section 5.4 and 5.5 present the optimization problems of maximizing the outage throughput and energy efficiency (EE) of the system and their solutions, whereas, in Section 5.6, numerical results are presented. Section 5.7 concludes the chapter.

5.2 System Model

We consider a two-hop wireless communication system, where the information is transferred from the source node S to the destination node D, through an energy constrained in-

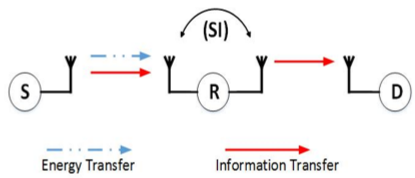

Figure 5.1: Full-duplex AF relay-based EH system

termediate relay node R, as shown in Fig. 5.1. Source and destination nodes are equipped with a single antenna, whereas relay contains two antennas (one receive antenna and one transmit antenna). We choose AF relay because of its following advantages. 1. Lower implementation and computational complexity. 2. Less delay at the relay terminal. 3. Transparent to the modulation/coding used by the source node. We assume that the AF relay operates in FD transmission mode and harvests energy from the source node. Due to the environmental limitations, we assume that there is no direct link between the source and destination, and communication can only be established via a cooperative relay node. We assume that the channel state information (CSI) is available to all the nodes. We obtain CSI by channel estimation in the training phase. First, the relay and destination transmit their own pilot signals, respectively. Hence, the CSI of source-relay link is obtained at the source, and CSI of relay-destination link is obtained at the relay. Then, the relay forwards CSI indicator to the source to indicate the CSI of relay-destination and self-interference link. Hence, CSI of all links in a two-hop FD relaying system is acquired at the source.

We assume that h_1 and h_2 denote the channel coefficients of the source-to-relay and relay-to-destination links, respectively, and h_R denotes the self-interference channel coefficient. The channels are quasi-static non-frequency selective Rayleigh fading, so the PDF and CDF of h_k ($k \epsilon (1), (2), (R)$) can be written as

$$f_{|h_k|^2}(x) = \frac{1}{\lambda_k} e^{-\frac{x}{\lambda_k}} \tag{5.1}$$

$$F_{|h_k|^2}(x) = 1 - e^{-\frac{x}{\lambda_k}} \tag{5.2}$$

where λ_k denotes the mean value of $|h_k|^2$.

5.2.1 Time-Switching (TS) Protocol

Relay's receiver architecture is based on time-switching (TS) protocol [44, 45], [47]. The framework of TS is presented in Fig. 5.2, where the time slot T is divided into two phases, where the relay works in HD mode in the first time slot but FD mode in the second time slot. The first phase is of duration αT. This phase is used to transfer energy from the source to the relay. The second phase is of $(1-\alpha)T$ duration and is used to transfer the information from the source to the destination via a relay. The relay operates in FD mode in the second phase, i.e., receives the information from the source and transmits the information to the destination simultaneously. We consider a harvest-use strategy, where we assume that all the energy harvested by the relay in αT time fraction is used to transmit information to the destination in $(1-\alpha)T$ time fraction. For simplicity, we normalize the time period T to be equal to 1. We assume the usage of TS protocol because it outperforms PS protocol at low signal-to-noise-ratios and high transmission rates [40]. During the energy harvesting phase, the signal received at the relay at time t is

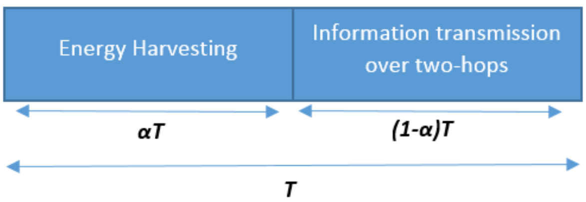

Figure 5.2: Block diagram of relay receiver architecture based on TS protocol

$$z_R(t) = h_1\sqrt{P_s}x_s(t) + n_R(t) \tag{5.3}$$

where P_s represents the transmission power at the source node, x_s is the normalized transmitted signal with $E(|x_s(t)|^2)$=1 for all t, $n_R(t)$ is the additive white Gaussian noise at relay at time t, $CN \sim (0, \sigma_R^2)$.

During the information transmission phase, the signal received at the relay is

$$y_R(t) = h_1\sqrt{P_s}x_s(t) + h_R\sqrt{P_R}x_R(t) + n_R(t) \tag{5.4}$$

where $h_R \sqrt{P_R} x_R(t)$ is the self-interference signal due to the FD mode of the relay. After receiving the signal from the source node, the AF relay multiplies it with an amplification gain G_R and then forwards the signal to the destination. Hence, the signal at the destination at time t is given by

$$y_D(t) = h_2 G_R y_R(t) + n_D(t) \tag{5.5}$$

$$y_D(t) = h_2 G_R h_1 \sqrt{P_s} x_s(t) + h_2 G_R h_R \sqrt{P_R} x_R(t) + h_2 G_R n_R(t) + n_D(t) \tag{5.6}$$

where $n_D(t)$ is the additive white Gaussian noise at the destination at time t, $CN \sim (0, \sigma_D^2)$ and amplification factor G_R is expressed as

$$G_R = \sqrt{\frac{P_R}{P_s|h_1|^2 + P_R|h_R|^2 + \sigma_R^2}} \tag{5.7}$$

Considering Eqn. 5.6, the end-to-end signal-to-noise ratio SNR of the system, after some algebraic manipulations, can be express as in [74]

$$\gamma = \frac{P_s P_R |h_1|^2 |h_2|^2}{P_R^2 |h_2|^2 |h_R|^2 + P_R |h_R|^2 \sigma_D^2 + P_s |h_1|^2 \sigma_D^2} \tag{5.8}$$

The end-to-end rate of the system can be expressed as

$$R = (1 - \alpha) \log_2(1 + \gamma) \tag{5.9}$$

5.2.2 *Constant-Linear-Constant (CLC) EH Model*

In this work, we consider the non-linear EH model known as CLC. It takes into account the sensitivity and saturation characteristics of the EH circuit. Fig. 5.3 shows the harvested power for different input power values for two EH models, namely, linear EH model and CLC non-linear EH model [32, 73]. For the CLC EH model, when the input power is below the sensitivity value P_{min}, the EH circuit does not harvest any energy. When the input power becomes greater then P_{min}, the circuit operates in linear fashion but when it reaches the saturation value P_{th}, the output power of the harvester becomes constant.

Therefore, the transmission power of the relay can be expressed as

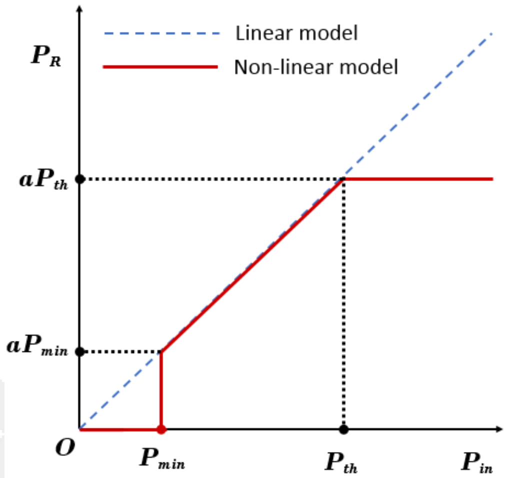

Figure 5.3: Constant-Linear-Constant (CLC) based non-linear EH model

$$P_R = \begin{cases} 0, & P_s|h_1|^2 < P_{min} \\ \frac{\eta P_s |h_1|^2 \alpha}{1-\alpha}, & P_{min} \leq P_s|h_1|^2 \leq P_{th} \\ \frac{\eta P_{th} \alpha}{1-\alpha}, & P_s|h_1|^2 > P_{th} \end{cases} \tag{5.10}$$

where, η is the energy conversion efficiency. The existence of these three regions in the P_R expression results in three regions in SNR expressions. This is the main challenge we have to tackle in this study. Therefore, the end-to-end SNR can be expressed respectively as

$$\gamma = \begin{cases} 0, & P_s|h_1|^2 < P_{min} \\ \frac{P_s|h_1|^2|h_2|^2}{aP_s|h_1|^2|h_2|^2|h_R|^2+|h_R|^2\sigma_D^2+\frac{\sigma_D^2}{a}}, & P_{min} \leq P_s|h_1|^2 \leq P_{th} \\ \frac{P_s|h_1|^2|h_2|^2}{aP_{th}|h_2|^2|h_R|^2+|h_R|^2\sigma_D^2+\frac{P_s|h_1|^2\sigma_D^2}{aP_{th}}}, & P_s|h_1|^2 > P_{th} \end{cases} \tag{5.11}$$

where $a = (\frac{\eta\alpha}{1-\alpha})$.

5.3 Outage Analysis of FD-AF Relaying System

An outage in the system happens when the rate is smaller than the target rate R_{th}. Therefore, outage probability can be defined as

$$P_{op} = Pr(R < R_{th}) = Pr(\gamma < \gamma_{th}) \tag{5.12}$$

where $\gamma_{th} = 2^{R_{th}} - 1$ represents the target SNR of the system. Considering the existence of three regions in the end-to-end SNR expressions of Eqn. (5.11) of the system, we can derive

$$P_{op} = 1 - I_1 - I_2 - I_3 \tag{5.13}$$

where

$$I_1 = Pr(\gamma > \gamma_{th}, P_s|h_1|^2 < P_{min}) \tag{5.14}$$

$$I_2 = Pr(\gamma > \gamma_{th}, P_{min} \leq P_s|h_1|^2 \leq P_{th}) \tag{5.15}$$

$$I_3 = Pr(\gamma > \gamma_{th}, P_s|h_1|^2 > P_{th}) \tag{5.16}$$

Now, we calculate I_1, I_2, and I_3 separately.

- $I_1 = Pr(\gamma > \gamma_{th}, P_s|h_1|^2 < P_{min})$

For the case of I_1, the input power $P_s|h_1|^2$ is below the sensitivity level P_{min}, the relay does not harvest energy, due to which information cannot be transferred to the destination. Hence $I_1 = 0$.

- $I_2 = Pr(\gamma > \gamma_{th}, P_{min} \leq P_s|h_1|^2 \leq P_{th})$

After some algebraic manipulations, I_2 in Eqn. (5.15) can be written as,

$$I_2 = Pr\Big(|h_1|^2 > C, A \leq |h_1|^2 \leq B\Big) \tag{5.17}$$

where $A = \frac{P_{min}}{P_s}, B = \frac{P_{th}}{P_s} and\ C = \frac{\gamma th(|h_R|^2\sigma_D^2 + \frac{\sigma_D^2}{a^2})}{P_s|h_2|^2(1-a\gamma_{th}|h_R|^2)}$

We can divide I_2 into two further cases, namely when $C \leq A$ and $A < C \leq B$. Now, we solve for these two cases.

Case I : Note that when $C \leq A$, Eqn. (5.17) becomes

$$I_{2.1} = Pr(C \leq A, A \leq |h_1|^2 \leq B) \tag{5.18}$$

Putting the expressions of A,B, and C, and considering the fact that $|h_1|^2$ and $|h_2|^2$ are independent random variables, we can write $I_{2.1}$ as,

$$I_{2.1} = Pr\left(|h_2|^2 > \frac{\gamma_{th}(|h_R|^2\sigma_D^2 + \frac{\sigma_D^2}{a})}{(1 - a\gamma_{th}|h_R|^2)P_{min}}\right)Pr(A \leq |h_1|^2 \leq B) \tag{5.19}$$

$I_{2.1}$ can be further classified into two cases depending on the fact that $|h_2|^2$ is a positive value.

$$I_{2.1} = \begin{cases} Pr\left(|h_2|^2 < \frac{\gamma_{th}(|h_R|^2\sigma_D^2 + \frac{\sigma_D^2}{a})}{(1-a\gamma_{th}|h_R|^2)P_{min}}\right), & |h_R|^2 < \frac{1}{a\gamma th} \\ Pr\left(|h_2|^2 > \frac{\gamma_{th}(|h_R|^2\sigma_D^2 + \frac{\sigma_D^2}{a})}{(1-a\gamma_{th}|h_R|^2)P_{min}}\right) = 1, & |h_R|^2 > \frac{1}{a\gamma th} \end{cases} \tag{5.20}$$

Therefore, $I_{2.1}$ can be calculated as

$$I_{2.1} = \left\{1 - \Big[\int_0^{\frac{1}{a\gamma_{th}}} F_{|h_2|^2}\left(\frac{\gamma_{th}(x\sigma_D^2 + \frac{\sigma_D^2}{a})}{(1 - a\gamma_{th}x)P_{min}}\right)f_{|h_R|^2}(x)dx + \int_{\frac{1}{a\gamma_{th}}}^{\infty} f_{|h_R|^2}(x)dx\Big]\right\}\Big[F_{|h_1|^2}(B) - F_{|h_1|^2}(A)\Big] \tag{5.21}$$

After solving the integral in Eqn. (5.21) by standard integral evaluation method, we get

$$I_{2.1} = \Big[\frac{1}{\lambda_R}\int_0^{\frac{1}{a\gamma_{th}}} e^{-\left(\frac{\gamma_{th}(x\sigma_D^2 + \frac{\sigma_D^2}{a})}{(1-a\gamma_{th}x)P_{min}\lambda_2} + \frac{x}{\lambda_R}\right)}dx\Big][F_{|h_1|^2}(B) - F_{|h_1|^2}(A)] \tag{5.22}$$

Since, there is no closed-form expression for the integral $\frac{1}{\lambda_R}\int_0^{\frac{1}{a\gamma_{th}}} e^{-\left(\frac{\gamma_{th}(x\sigma_D^2+\frac{\sigma_D^2}{a})}{(1-a\gamma_{th}x)P_{min}\lambda_2}+\frac{x}{\lambda_R}\right)}dx$, we employ Gaussian-Chebyshev quadrature [75] to achieve an approximation of $I_{2.1}$ as

$$I_{2.1} \approx \left[\frac{\pi}{2\lambda_R a\gamma_{th}N}\sum_{n=1}^{N}\sqrt{1-a_n}f(b_n)\right]\left[e^{-\frac{A}{\lambda_1}}-e^{-\frac{B}{\lambda_1}}\right] \tag{5.23}$$

where N is a parameter that determines the trade off between complexity and accuracy, a_n=$cos\frac{2n-1}{2N}\pi$, and b_n= $\frac{1}{2a\gamma_{th}}[a_n+1]$.

Case II : When $A < C \le B$, I_2 becomes

$$I_{2.2} = Pr(A < C \le B, C \le |h_1|^2 \le B) \tag{5.24}$$

Putting the expressions for A, B and C, and after some algebraic manipulations, we can write $I_{2.2}$ as

$$I_{2.2} = Pr\left(\frac{\gamma th(|h_R|^2\sigma_D^2+\frac{\sigma_D^2}{a})}{P_s|h_2|^2(1-a\gamma_{th}|h_R|^2)} < |h_1|^2 \le B, \frac{\gamma th(|h_R|^2\sigma_D^2+\frac{\sigma_D^2}{a})}{(1-a\gamma_{th}|h_R|^2)P_{th}} \le |h_2|^2 \le \frac{\gamma th(|h_R|^2\sigma_D^2+\frac{\sigma_D^2}{a})}{(1-a\gamma_{th}|h_R|^2)P_{min}}\right) \tag{5.25}$$

We can further classify $I_{2.2}$ on the basis of the value of random variable $|h_R|^2$ as

$$\begin{cases} \int_0^{\frac{1}{a\gamma_{th}}}\left\{\int_F^G\int_E^B f_{|h_1|^2}(x)f_{|h_2|^2}(y)dxdy\right\}f_{|h_R|^2}(z)dz, & |h_R|^2 < \frac{1}{a\gamma th} \\ 0, & |h_R|^2 > \frac{1}{a\gamma th} \end{cases} \tag{5.26}$$

Therefore, $I_{2.2}$ can be written as

$$I_{2.2} = \int_0^{\frac{1}{a\gamma_{th}}}\left\{\int_F^G\int_E^B f_{|h_1|^2}(x)f_{|h_2|^2}(y)dxdy\right\}f_{|h_R|^2}(z)dz \tag{5.27}$$

where $E = \frac{\gamma_{th}\left(|h_R|^2\sigma_D^2+\frac{\sigma_D^2}{a}\right)}{P_s y\left(1-a\gamma_{th}|h_R|^2\right)}$, $F = \frac{\gamma_{th}\left(|h_R|^2\sigma_D^2+\frac{\sigma_D^2}{a}\right)}{P_{th}\left(1-a\gamma_{th}|h_R|^2\right)}$, $G = \frac{\gamma_{th}\left(|h_R|^2\sigma_D^2+\frac{\sigma_D^2}{a}\right)}{P_{min}\left(1-a\gamma_{th}|h_R|^2\right)}$ and $\left\{\int_F^G\int_E^B f_{|h_1|^2}(x)f_{|h_2|^2}(y)dxdy\right\}$ is the joint CDF of $|h_1|^2$ and $|h_2|^2$. The integral in Eqn. (5.27) can be solved by incorporating Gaussian-Chebyshev quadrature approximation. After solving, we get Eqn. (5.28).

$$I_{2.2} \approx e^{-\frac{B}{\lambda_1}}\Bigg[\frac{-\pi}{2\lambda_R a\gamma_{th}N}\sum_{n=1}^{N}\sqrt{1-a_n}f_1(b_n)+\frac{\pi}{2\lambda_R a\gamma_{th}N}\sum_{n=1}^{N}\sqrt{1-a_n}f_2(b_n)\Bigg]+ \frac{1}{\lambda_2\lambda_R}\int_{0}^{\frac{1}{a\gamma_{th}}}\Big((\frac{G-F}{2})\sum_{n=1}^{N}\frac{\pi}{N}\sqrt{1-a_n}f(b_n)\Big)e^{-\frac{z}{\lambda_R}}dz \quad (5.28)$$

Since, the Gaussian approximation lies inside the integral in Eqn. (5.28), we can not find the final closed-form approximation without integral.

- $I_3 = Pr(\gamma > \gamma_{th}, P_s|h_1|^2 > P_{th})$

For the case of I_3, when the input power $P_S|h_1|^2$ is greater than the threshold level P_{th}, putting the expression for γ, and after some algebraic manipulations, Eqn. (5.16) becomes

$$I_3 = Pr(|h_1|^2 > D, |h_1|^2 > B) \quad (5.29)$$

where $D = \left(\frac{\gamma_{th}(aP_{th}^2|h_2|^2|h_R|^2+|h_R|^2\sigma_D^2)}{P_s\left(|h_2|^2-\frac{\gamma_{th}\sigma_D^2}{aP_{th}}\right)}\right)$. We can further classify I_3 into two cases described below. Case I : Note that when $D < B$, Eqn. (5.29) becomes

$$I_{3.1} = Pr(|h_1|^2 > B, D < B) \quad (5.30)$$

After incorporating the expressions of B and D and the fact that $|h_1|^2$ and $|h_R|^2$ are independent random variables, we can write $I_{3.1}$ as,

$$I_{3.1} = Pr(|h_1|^2 > B)Pr\left(|h_R|^2 < \frac{P_{th}(|h_2|^2-\frac{\gamma_{th}\sigma_D^2}{aP_{th}})}{\gamma_{th}(aP_{th}|h_2|^2+\sigma_D^2)}\right) \quad (5.31)$$

We can futher divide $I_{3.1}$ based on the fact that $|h_R|^2$ is a positive value.

$$I_{3.1} = \begin{cases} Pr\left(|h_R|^2 > \frac{P_{th}(|h_2|^2-\frac{\gamma_{th}\sigma_D^2}{aP_{th}})}{\gamma_{th}(aP_{th}|h_2|^2+\sigma_D^2)}\right) = 1, & |h_2|^2 < \frac{\gamma_{th}\sigma_D^2}{aP_{th}} \\ Pr\left(|h_R|^2 < \frac{P_{th}(|h_2|^2-\frac{\gamma_{th}\sigma_D^2}{aP_{th}})}{\gamma_{th}(aP_{th}|h_2|^2+\sigma_D^2)}\right), & |h_2|^2 > \frac{\gamma_{th}\sigma_D^2}{aP_{th}} \end{cases} \quad (5.32)$$

Therefore, we can write $I_{3.1}$ as Eqn. (5.33).

$$I_{3.1} = \Bigg[\int_{0}^{\frac{\gamma_{th}\sigma_D^2}{aP_{th}}} f_{|h_2|^2}(x)dx + \int_{\frac{\gamma_{th}\sigma_D^2}{aP_{th}}}^{\infty} F_{|h_R|^2}\Big(\frac{P_{th}(x-\frac{\gamma_{th}\sigma_D^2}{aP_{th}})}{\gamma_{th}(aP_{th}x+\sigma_D^2)}\Big) f_{|h_2|^2}(x)dx\Bigg]\Bigg[1 - F_{|h_1|^2}(B)\Bigg] \quad (5.33)$$

After solving the integral in Eqn. (5.33) by using the standard integral evaluation method, we get

$$I_{3.1} = \Bigg[1 - \frac{1}{\lambda_2}\int_{\frac{\gamma_{th}\sigma_D^2}{aP_{th}}}^{\infty} e^{-\left(\frac{P_{th}(x-\frac{\gamma_{th}\sigma_D^2}{aP_{th}})}{\gamma_{th}(aP_{th}x+\sigma_D^2)\lambda_R}+\frac{x}{\lambda_2}\right)}dx\Bigg]\Bigg[e^{-\frac{B}{\lambda_1}}\Bigg] \quad (5.34)$$

Since there is no closed-form expression for the integral $\int_{\frac{\gamma_{th}\sigma_D^2}{aP_{th}}}^{\infty} e^{-\left(\frac{P_{th}(x-\frac{\gamma_{th}\sigma_D^2}{aP_{th}})}{\gamma_{th}(aP_{th}x+\sigma_D^2)\lambda_R}+\frac{x}{\lambda_2}\right)}dx$, and due to infinite limit, we can not approximate through Gaussian-Chebyshev quadrature.
Case II : When $D > B$, I_3 can be written as

$$I_{3.2} = Pr(|h_1|^2 > D, D > B) \quad (5.35)$$

After some algebraic manipulations, we can write $I_{3.2}$ as Eqn. (5.36).

$$I_{3.2} = Pr\Bigg(|h_1|^2 > \frac{\gamma_{th}(aP_{th}|h_2|^2|h_R|^2 + |h_R|^2\sigma_D^2)}{P_s\Big(|h_2|^2 - \frac{\gamma th\sigma_D^2}{aP_{th}}\Big)}, |h_R|^2 > \frac{P_{th}\Big(|h_2|^2 - \frac{\gamma th\sigma_D^2}{aP_{th}}\Big)}{\gamma_{th}(aP_{th}|h_2|^2 + \sigma_D^2)}\Bigg) \quad (5.36)$$

By observing Eqn. (5.36), we can further classify $I_{3.2}$ on the basis of $|h_2|^2$.

$$\begin{cases} 0, & |h_2|^2 < \frac{\gamma_{th}\sigma_D^2}{aP_{th}} \\ \int_{\frac{\gamma_{th}\sigma_D^2}{aP_{th}}}^{\infty} \Big\{\int_J^{\infty}\int_I^{\infty} f_{|h_1|^2}(x)f_{|h_R|^2}(y)dxdy\Big\} f_{|h_2|^2}(z)dz, & |h_2|^2 > \frac{\gamma_{th}\sigma_D^2}{aP_{th}} \end{cases} \quad (5.37)$$

Therefore, $I_{3.2}$ can be written as,

$$I_{3.2} = \int\limits_{\frac{\gamma_{th}\sigma_D^2}{aP_{th}}}^{\infty} \left\{ \int\limits_{J}^{\infty} \int\limits_{I}^{\infty} f_{|h_1|^2}(x) f_{|h_R|^2}(y) dxdy \right\} f_{|h_2|^2}(z) dz \tag{5.38}$$

where $I = \frac{\gamma_{th}\left(y\sigma_D^2 + yaP_{th}|h_2|^2\right)}{P_s\left(|h_2|^2 - \frac{\gamma_{th}\sigma_D^2}{aP_{th}}\right)}$, and $J = \frac{P_{th}\left(|h_2|^2 - \frac{\gamma_{th}\sigma_D^2}{aP_{th}}\right)}{\gamma_{th}\left(aP_{th}|h_2|^2 + \sigma_D^2\right)}$ and $\left\{ \int\limits_{J}^{\infty} \int\limits_{I}^{\infty} f_{|h_1|^2}(x) f_{|h_R|^2}(y) dxdy \right\}$ is the joint CDF of $|h_1|^2$ and $|h_R|^2$. After solving the integral,

$$I_{3.2} = e^{-\frac{B}{\lambda_1}} \int_{\frac{\gamma_{th}\sigma_D^2}{aP_{th}}}^{\infty} \frac{e^{-\left(\frac{P_{th}(z - \frac{\gamma_{th}\sigma_D^2}{aP_{th}})}{\gamma_{th}\lambda_R(aP_{th}z + \sigma_D^2)} + \frac{z}{\lambda_2}\right)}}{\left(\frac{\gamma_{th}\lambda_R(aP_{th}z + \sigma_D^2)}{(z - \frac{\gamma_{th}\sigma_D^2}{aP_{th}})P_s\lambda_1} + 1\right)} dz \tag{5.39}$$

Since there is no closed-form expression of the above integral and due to infinite limit, we can not find the approximation.

Finally, we can calculate outage probability P_{op} by calculating $I_{2.1}$, $I_{2.2}$, $I_{3.1}$, and $I_{3.2}$, and putting them into Eqn. (5.13).

5.4 Outage Throughput Maximization Problem

In this section, we maximize the end-to-end outage throughput of the FD-AF relaying system. The optimization problem can be expressed as [32]

$$\max_{\alpha} \quad R = (1 - P_{op})(1 - \alpha)R_{th} \tag{5.40}$$

$$s.t \qquad 0 \le \alpha \le 1$$

where R_{th} is the target rate. We observe that the objective function of the problem (5.40) is concave w.r.t. α. Therefore, the problem is convex and the solution is unique. To find the optimal TS solution, we use line search method like golden-section method [76]. The optimization algorithm based on golden-section method is presented in Algorithm 6. The optimal maximum throughput algorithm based on golden-section method is described as follows. We first describe the interval to be searched $\alpha \in [0,1]$, accuracy to be achieved

$\sigma = e^{-7}$, and golden-ratio $\epsilon = 0.618$. We then calculate α_o and $\tilde{\alpha_o}$ and throughput values $R(\alpha_o)$ and $R(\tilde{\alpha_o})$. Depending on the function values or whether the convergence criteria is fulfilled, we keep updating the interval until we get the optimal α. The complexity of

---

Algorithm 6 Optimal Maximum Througput Algorithm

Initialization: $\epsilon = 0.618$, $a_o = 0$, $b_o = 1$, $k = 0$, $\sigma = e^{-7}$
$\alpha_o \leftarrow a_o + (1-\epsilon)(b_o - a_o)$
$\tilde{\alpha_o} = a_o + \epsilon(b_o - a_o)$
Calculate $R(\alpha_o)$ and $R(\tilde{\alpha_o})$
for $\forall k$ do
  if $R(\alpha_o) > R(\tilde{\alpha_o})$ then
    if $\mid \tilde{\alpha_k} - a_k \mid \leq \sigma$
      $\alpha^*_{op} = \alpha_k$
      Break
    else
      $a_{k+1} \leftarrow a_k$, $b_{k+1} \leftarrow \tilde{\alpha_k}$, $R(\tilde{\alpha_{k+1}}) \leftarrow R(\alpha_k)$
      $\tilde{\alpha_{k+1}} \leftarrow \alpha_k$
      $\alpha_{k+1} \leftarrow a_{k+1} + (1-\epsilon)(b_{k+1} - a_{k+1})$
      Calculate $R(\alpha_{k+1})$
      Continue
    end if
  else
    if $\mid b_k - \alpha_k \mid \leq \sigma$ then
      $\alpha^*_{op} \leftarrow \tilde{\alpha_k}$
      Break
    else
      $a_{k+1} \leftarrow \alpha_k$, $b_{k+1} \leftarrow b_k$, $R(\alpha_{k+1}) \leftarrow R(\tilde{\alpha_k})$
      $\alpha_{k+1} \leftarrow \tilde{\alpha_k}$
      $\tilde{\alpha_{k+1}} \leftarrow a_{k+1} + \epsilon(b_{k+1} - a_{k+1})$
      Calculate $R(\tilde{\alpha_{k+1}})$
      Continue
    end if
  end if
end for
Return α^*_{op} and $R(\alpha^*_{op})$

---

golden-section method is $O(\log \frac{1}{\sigma})$, the number of iterations golden-section method takes to converge is $\left\lceil C log\left(\frac{L}{\sigma}\right)\right\rceil$, where C=$(log(\frac{1}{\epsilon}))^{-1}$, L is the length of interval given by (b_o-a_o). In the golden search method, two function evaluations are made at the first iteration and then only one function evaluation is made for each subsequent iteration.

5.5 Energy efficiency (EE) Maximization Problem

In this section, we maximize the EE of the FD-AF relay-based EH system and find the optimal value of time fraction α. The EE of the system is given as

$$EE = \frac{R}{P_S} \tag{5.41}$$

The optimization problem is expressed below

$$\max_{\alpha} \quad EE = \frac{(1 - P_{op})(1 - \alpha)R_{th}}{P_s} \tag{5.42}$$

$$s.t \qquad 0 \leq \alpha \leq 1$$

where EE is the ratio of end-to-end outage throughput to the total consumed power in the system. We observe that the above problem is convex. To find the optimal solution, we use golden-section method similar to Algorithm 6.

5.6 Numerical Results and Discussions

The goal of this section is to present the numerical results based on analytical expressions developed and verify the analysis through Monte-Carlo simulations. We assume that all the channels undergo Rayleigh fading. The attenuation in the channel is calculated by using both large scale and small scale fading. To model the large scale fading, following model is used.

$$PL(d, dB) = PL(d_0, dB) + 10\beta log_{10}\left(\frac{d}{d_0}\right) + Z \tag{5.43}$$

Where, $PL(d, dB)$ is the path loss at distance d in dB, d_0 is the reference distance and path loss at reference distance $d_0 = 1m$ is taken as $70dB$, the term β is the path loss exponent and is taken as 3. Z is a zero mean Gaussian random variable with standard deviation $\sigma = 4$. For the simulations, unless otherwise specified, we set the parameters as follows [32]: We set the maximum transmit power of the source node to P_s = 30 dBm; energy conversion efficiency to $\eta = 0.7$; the sensitivity and saturation values of the EH circuit to

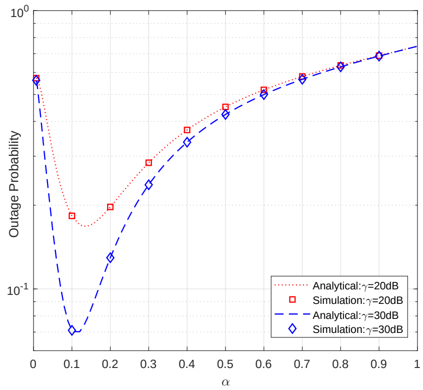

Figure 5.4: Outage probability for different values of time fraction α, where η = 0.7, P_s= 30 dBm.

P_{min} = 17 dBm and P_{th} = 29 dBm, respectively; noise variance to $\sigma_D^2 = \sigma_R^2 = \sigma^2 = 0.01$; target rate to R_{th} = 3bps/Hz; and the average channel gains $\lambda_1 = \lambda_2 = \lambda_i$ to 1. For convenience we define SNR $\gamma = \frac{P_s}{\sigma^2}$.

5.6.1 Outage Probability and Throughput versus $\boldsymbol{\alpha}$ *for different SNR* ($\boldsymbol{\gamma}$)

Fig. 5.4 shows the outage probability for different values of time fraction α and for different SNR (γ). When we increase α, outage probability decreases, but when α reaches to a certain value, outage probability starts increasing. It is due to the trade-off of energy harvesting and information transmission phases. More specifically, when α increases, energy harvesting at relay increases which in turn increases the transmission power at the relay. Due to which, outage probability decreases to the minimum. However, when α keeps increasing, the information processing time phase decreases which increases outage probability. It can be observed that high SNR achieves better performance as compared to low SNR.

Fig. 5.5 shows the outage throughput for different α values and for different γ. The outage throughput first increases and then decreases with increasing α. It is because of the trade-off of energy and information transmission phases. For high SNR value γ = 30 dB, the system achieves higher outage throughput as compared to γ = 20dB.

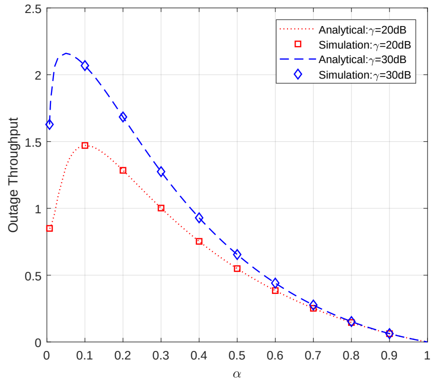

Figure 5.5: Outage throughput for different values of time fraction α, where η = 0.7, P_s = 30 dBm.

5.6.2 *Outage Throughput for different values of* $\boldsymbol{\alpha}$ *under different EH Model*

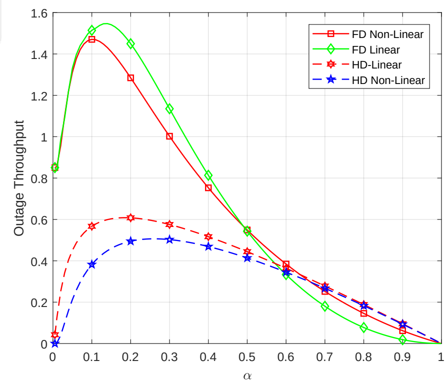

Figure 5.6: Outage throughput for different EH models, where $\sigma_D^2 = \sigma_R^2$ = 0.01, η = 0.7, P_s = 30 dBm.

Fig. 5.6 shows the outage throughput for different α and different EH models. The optimal α found for non-linear FD model is around 0.1, which is in accordance with the literature [32]. The optimal outage throughput in the non-linear FD model is smaller than that of a linear model. It is because of the non-linear behavior of the practical energy harvesting (EH) circuit, where we consider the sensitivity and saturation characteristics. It can be observed that the optimal α in a linear model is different from the one in non-linear and is not practical. When α reaches to a certain value, the outage throughput of the non-linear model becomes higher than the linear model, which is because of the saturation

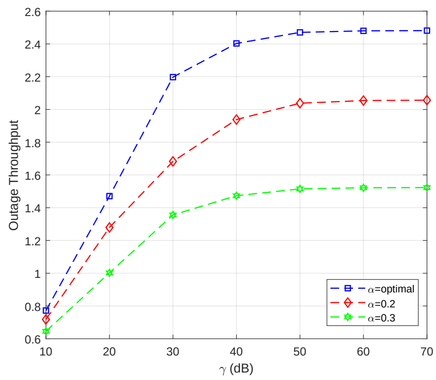

Figure 5.7: Outage Throughput for different SNR γ, where $\eta = 0.7$, $P_s = 30$ dBm.

effect of the non-linear model. With increasing α, the transmission power of the relay keeps increasing in a linear model which means the self-interference keeps increasing and hence the throughput decreases. Due to saturation, the transmission power of the relay becomes constant in the non-linear model and so is the self-interference, therefore after a certain α, the throughput of the non-linear model becomes higher than the linear model. Moreover, it can be observed that FD system achieves better performance gain as compared to the HD system. In the HD system, the outage throughput of the non-linear model is smaller than the linear model, which is because, in the non-linear model, transmission power at the relay is limited and hence the outage probability in non-linear model is larger than the linear EH model system.

Fig. 5.7 shows the outage throughput for different γ and different values of α. As γ increases, outage throughput first increases and then becomes steady. It is because of the saturation effect of the non-linear EH circuit. Specifically, as γ keeps increasing, the EH circuit saturates, and as a result, the outage throughput of the system becomes steady. It can be seen from the figure that optimal α achieves better throughput as compared to other α values.

5.6.3 Comparison of Linear and Non-Linear Model

Fig. 5.8 compares the proposed non-linear FD model with the linear model. We analyze our non-linear system on optimal time fraction (α^*) found from the linear model and plot

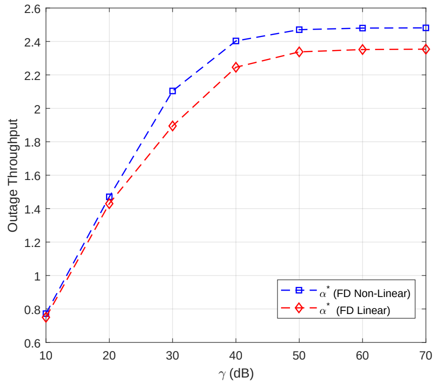

Figure 5.8: Outage Throughput for different values of SNR (γ) by incorporating optimal α^* of linear model.

the outage probability for different values of γ. It can be observed that by incorporating α^* of linear model, we achieve less throughput for a given (γ) as compared to the throughput we achieved on α^* of non-linear system. This result ensures the advantage and practicality of using the non-linear EH model over the linear EH model system.

5.6.4 Optimal Outage Throughput for different values of Self-Interference

Fig. 5.9 shows the optimal outage throughput versus self-interference λ_r of FD non-linear system with different values of γ and half-duplex non-linear system. As the strength of self-interference increases, outage throughput in the full-duplex system decreases. However, in a half-duplex system, there is no change in system performance. It is because self-interference does not exist in HD systems.

5.6.5 Energy Efficiency for different values of α and γ

Fig. 5.10 shows the energy efficiency (EE) for different values of α and different EH models. As observed for the outage throughput, the optimal EE in the non-linear FD model is different from that of a linear model. It is because of the non-linear behavior of the practical energy harvesting (EH) circuit, where we consider the sensitivity and saturation characteristics. The optimal α found for linear EH model is also different from the non-linear model, and is not practical. Moreover, FD system achieves better performance gain

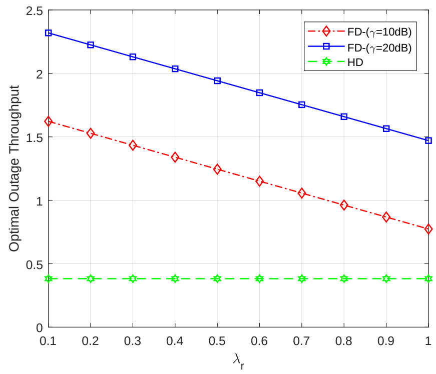

Figure 5.9: Outage throughput for different values of self-interference λ_R, where $\eta = 0.7$, $P_s = 30$ dBm.

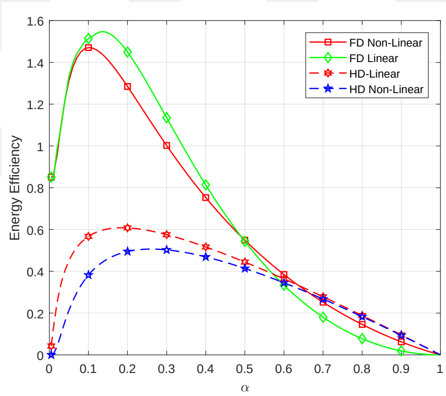

Figure 5.10: EE for different values of α and EH Models, where $\sigma_D^2 = \sigma_R^2 = 0.01$, $\eta = 0.7$, $P_s = 30$ dBm.

in terms of EE than the HD system.

Fig. 5.11 shows EE for different values of γ and different α. It can be seen that as γ increases, energy efficiency of the system increases, but becomes steady as γ reaches to a certain value. It is because of the saturation characteristic of the EH circuit. It can be observed from the figure that optimal α gives better performance in terms of EE as compared to other arbitrary α values. We get similar results in Figs. 5.6 and 5.7 to Figs. 5.10 and 5.11, respectively, because of the value of P_s used in the simulations.

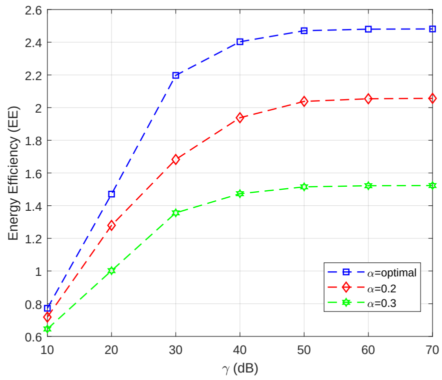

Figure 5.11: EE versus SNR γ for different α, where $\eta = 0.7$, $P_s = 30$ dBm.

5.7 Conclusion and future works

This chapter presented a practical non-linear EH model, which takes into account the sensitivity and saturation characteristics of the EH circuit. Based on this model, we provided the outage probability analysis of an FD-AF relay-based system. To optimize the system performance, we presented an optimal solution of the TS parameter to maximize the outage throughput and EE of the system based on the golden-section method. Numerical results suggested that the proposed FD non-linear EH system outperforms the other existing systems including linear FD, linear and non-linear HD systems. This work can be further extended by incorporating power-splitting (PS) protocol, multi-antenna systems, Nakagami fading channels and more accurate non-linear EH models. Multi-antenna systems can be studied in the context of antenna-selection, and beamform designing for SWIPT. More accurate non-linear EH models can capture the increase in the received power between minimum threshold and saturation points by the use of a high-order polynomial and include the decrease in the received power after saturation.

Chapter 6

RESOURCE ALLOCATION FOR FULL-DUPLEX MIMO RELAYING SYSTEM WITH SELF-ENERGY RECYCLING

Cooperative communication using energy harvesting (EH) relay nodes promises significant improvement in throughput, coverage, and reliability. Self-energy recycling, in which the relay nodes simultaneously harvest energy from the source and their own transmitted signal, has been demonstrated to significantly increase the total harvested energy. In this chapter, we present an optimization framework for the resource allocation and relay selection in a two-hop full-duplex (FD) multi-relay multi-user multiple-input-multiple-output (MIMO) network by incorporating self-energy recycling at the relays, for the first time in the literature. The objective is to maximize the sum-throughput by jointly optimizing the dynamic time slot durations, power control and relay selection. The formulated problem is a mixed integer non-linear programming problem, which is difficult to solve for the global optimal solution in polynomial-time. As a solution strategy, we decompose the optimization problem into two sub-problems: resource allocation problem and relay selection problem. First, we reduce the resource allocation problem to a convex optimization problem by using the optimality analysis and Taylor series approximation. Then, we solve it for the optimal solution by using the convex optimization techniques. For the relay selection problem, we propose the polynomial-time heuristic algorithm based on the idea of iteratively selecting the relay offering the maximum throughput at each time rather than only considering the channel conditions in conventional relay selection algorithms. Through extensive simulations, we demonstrate that the proposed dynamic time FD-MIMO system increases the throughput by 30% as compared to the conventional FD-MIMO utilizing static time protocol for harvesting power at the relay, and by a factor of 2.4 over the FD-MIMO system without self-energy recycling at the relays, respectively. Moreover, the proposed polynomial-time relay selection algorithm performs very close to the optimal solution, and outperforms previously proposed polynomial-time conventional heuristic algorithms which consider only the channel characteristics of the system and predetermined relay allocation.

6.1 Introduction

Radio frequency (RF) energy harvesting (EH) technique has recently drawn significant attention of the research community due to its long range, low cost, and full control on the transferred energy [15, 77]. Since RF signals can carry both energy and information, the researchers have proposed two RF-EH design models named as Simultaneous Wireless Information and Power Transfer (SWIPT) [37], and Wireless Powered Communication Networks [18, 78–80]. In SWIPT, the energy and information are transferred simultaneously from the source to multiple network nodes. In WPCN, the energy flows from the source to multiple users in the downlink (DL), and users harvest this energy to transmit their information to the source in the uplink (UL).

Cooperative relaying is used to increase the network throughput, coverage area and energy efficiency while reducing the fading effects by assisting the information delivery from a source node to a user node via one or several intermediate nodes, referred to as relay nodes [1, 25, 81–83]. Recently, cooperative communication (i.e., relaying) is investigated for RF-EH networks to improve the network performance in terms of reliability and efficiency [16, 77]. In relay based SWIPT networks, the relay nodes harvest energy from the source and assist the end users by relaying their information. In the literature, two types of relays are commonly used, amplify-and-forward (AF) [38], in which a relay node first amplifies the received signal from the source and then sends it to the user, and decode-and-forward (DF) [39], in which the relay decodes the signal from the source and then sends to the user. For the purpose of simultaneous information and energy transfer, relay nodes use two protocols named as: Time-switching based relaying (TSR), and power-splitting based relaying (PSR) protocols [37, 40]. In TSR-based SWIPT protocol, the relay harvests power from an energy signal sent by the source and receives the source transmitted information signal in two different time phases, whereas, in PSR-based SWIPT, the received source signal is split into two signal streams to perform energy harvesting and information decoding.

The early research on SWIPT-aided relaying networks mainly focuses on half-duplex (HD) transmission mode and traditional linear EH model incorporating either TSR or PSR protocols [38–43, 84–86]. Specifically, [40] derives the analytical expressions for the outage probability and ergodic capacity of an HD-AF relay-based system incorporating the TSR and PSR protocols, whereas [38] studies the system of [40] in the presence of interference at the relay and destination. In [39], the authors derive the analytical expressions of the achievable throughput and ergodic capacity of an HD-DF relaying network for both TSR and PSR protocols. [84] discusses the impact of spatially random relays on the outage probability of an HD-DF relay system using PSR, whereas [85] studies the average signal-to-noise (SNR) ratio, outage and throughput of an HD-AF relay system incorporating TSR protocol. In [86], authors derive the sum rate expressions of a multiway massive MIMO AF relay network using both TSR and PSR. In [41], the authors investigate the outage performance of an HD-AF relay-based system with PSR protocol in the presence of a direct link between source and destination, whereas [42] incorporates the adaptive relaying (AR) protocol based on TSR-PSR protocol in HD-AF relay-based system. [43] studies an energy efficiency maximization (EEM) optimization problem for the multi-user multi-carrier energy-constrained HD-AF multi-relay network incorporating TSR protocol. However, all the aforementioned studies incorporate a traditional linear EH model. The linear EH model assumes that the output power of the energy harvester is linearly dependent on its input power. It cannot capture the turn-on effect at low input power nor the saturation effect at high input power. The components of the EH circuit in a real system are non-linear, and the traditional linear EH model is impractical. Researchers start to study the SWIPT-aided HD relay-based system with practical non-linear EH model [22,62,64,66,72]. Based on the logistic function based EH model, [22] study the PSR scheme for the HD-AF relay-based system in the presence of a direct link between source and destination, whereas [62] studies the resource allocation and relay selection in a two-hop AF relay-assisted HD multi-user orthogonal frequency division multiple access (OFDMA) network with PSR scheme. Based on linear-constant (LC) EH model, [64] calculates the outage capacity of the HD-AF relay system with TSR protocol. In [66], the outage probability of the HD-DF relay-based system incorporating PSR protocol under the imperfect channel is presented. [72] studies the two way communication rate regions under fixed and mobile relays based on constant-linear-constant (CLC) function based EH model. The above mentioned works incorporating either linear or non-linear EH model are all based on HD transmission mode which results in loss of spectral performance.

FD relaying uses the limited frequency spectrum more efficiently by supporting simultaneous signal transmission and reception at the relay. FD relay-based SWIPT systems incorporating linear EH model are investigated in [8, 44–51, 87]. Based on TSR protocol, [44] and [45] maximize the system throughput for the FD-AF,DF relay system considering a single antenna, and the FD-DF relay considering a multi-antenna system, respectively. [46] and [47] study the outage probability of the FD-DF and FD-AF relay systems using PSR and TSR protocols, respectively. In [8] and [48], authors discuss the problem of relay selection, and analyze the outage performance of four different energy harvesting schemes in a two-way communication FD relay system. Based on PSR, [49] studies the outage performance for the FD-DF relay system with the relay node subjected to co-channel interference (CCI), whereas [51] studies the power allocation problem in the FD-AF multi-relay system with interfering channels. [50] analyzes the outage probability of the EH-based FD-AF and DF relay system under TSR protocol. [87] study the relay selection for the FD-AF multi-relay system using TSR. Considering non-linear EH model, [32] and [88] study the outage performance for a relay-based system considering CLC EH model for a FD-DF and FD-AF relay model, respectively. Although, FD relaying provides better spectral efficiency as compared to the HD counterpart, in these studies, the resulted self-interference due to the FD mode of the relay is considered as an undesired element.

In FD-EH relaying system, the self-interference signal can be utilized for EH through self-energy recycling [24, 52, 89–91]. For this purpose in contrast to previous studies, the authors in [90] propose a novel protocol named as symmetric time based FD protocol (S-FR), in which the source transmits the information signal to the relay in the first time slot, while the relay forwards the re-encoded information signal to the destination and concurrently harvests wireless energy originated from both the source and the relay's self-interference in the second time slot. Specifically, [89] and [90] incorporate S-FR and study the throughput performance in a single-user single-relay MIMO-to-multiple-input-single-output (MISO) and MISO-MISO channel setup, respectively. [52] and [91] study the throughput performance of a single-relay-user system in MIMO-MIMO channel setup with S-FR. However, the authors in [52, 89–91] incorporate linear EH model and S-FR, in which the time duration for both the hops is assumed equal and constant. To further enhance the system performance, [24] proposes a dynamic time-slot FD protocol (A-FR) for the MISO-to-single-input-single-output (SISO) channel, incorporating a non-linear EH model with the objective of maximizing the spectral efficiency of the FD single-relay system. The dynamic time-slots of the A-FR enhance the utilization of the degrees of freedom and improve the system performance. Note that relay selection is an efficient approach to achieve the spatial diversity and to increase the system performance. Several relay selection schemes were proposed in HD/FD-linear/non-linear EH SWIPT systems [8, 43, 62, 84, 87]. Therefore, considering the performance gains of the appropriate relay selection, dynamic time-slot durations of A-FR and practicality of non-linear EH model, we propose to incorporate the A-FR in a multi-relay, multi-user MIMO FD-DF relaying system with a non-linear EH model. Note that, none of the above works consider relay selection in a multi-relay multi-user system with A-FR.

In this chapter, we study the resource allocation and relay selection problem in a MIMO multi-user multi wireless-powered FD-DF relay system, employing dynamic time self-energy recycling, for the first time in the literature. The contributions of the chapter are as follows:

- We present an optimization framework for the resource allocation and relay selection for a MIMO FD-DF multi-relay multi-user system, with the objective of maximizing the sum-throughput, by jointly optimizing the dynamic time slot durations, transmission powers of the source and relays, and relay selection, for the first time in the literature.
- The formulated optimization problem is a mixed integer non-linear programming

problem, which is difficult to solve for global optimum. As a solution strategy, we decompose the original problem into resource allocation problem and relay selection problem. We reduce the resource allocation problem, i.e., time and power allocation problem for the predetermined relay allocation, to a convex optimization problem based on the analysis of the optimality conditions and usage of the Taylor series approximation of the harvested power. Then, by using the Lagrange Multiplier method, we present the solution for the time and power variables.

- For the relay selection problem, we propose a polynomial-time heuristic algorithm based on the iterative relay selection for each user that results in throughput maximization of the network unlike previously proposed conventional relay selection algorithms that consider the channel characteristics only.

- Through extensive simulations, we compare the proposed heuristic relay selection algorithm with the optimal brute-force algorithm (BFA), and the other two conventional relay selection algorithms, namely, Opportunistic Relay Selection (ORS) and Partial Relay Selection (PRS). We observe that the proposed algorithm performs better than the predetermined relay allocation, and conventional heuristic algorithms considering the channel characteristics only, and performs very close to the optimal BFA, which has very high computational time complexity. We also demonstrate that the A-FR protocol based FD-MIMO system outperforms the conventional FD-MIMO system which utilizes S-FR protocol for harvesting power by a 30% throughput increase over S-FR. It also outperforms the system which does not incorporate the self-energy recycling process at the relays, by a factor of 2.4 in throughput performance.

The rest of the chapter is organized as follows. Section 6.2 presents the system model and assumptions. In Section 6.3, we formulate an optimization problem for the relay selection and resource allocation of FD-DF relay based MIMO system. Section 6.4 presents the solution of the formulated problem for a predetermined relay allocation. In Section 6.5, we present the heuristic relay selection algorithm. Section 6.6 evaluates the performance gain of the proposed algorithms through extensive simulations. Section 6.7 concludes our work.

6.2 System Model

We consider a two hop wireless-power aided MIMO relaying system which consists of a source, M relays and K users, where $M \geq K$. The source, relays, and users are all equipped with N antennas, where $N > 1$. Due to environmental limitations, we assume that there is no direct link between the source and users, i.e., the communication always takes place via relays [8, 24, 32, 44–47, 88, 89]. We assume that the relays are operating in an FD mode and are completely dependent on the energy harvested from the RF signal transmitted by the source [24,40,88]. The source node transmits at power P for every user k. The relays incorporate A-FR protocol [24] for the information transmission and energy harvesting. We consider time division multiple access as medium access protocol, and assume that the schedule of the users is known. The total time frame is partitioned into time-slots, each of which is allocated to a particular user k and its allocated relay m. Each time-slot is further divided into two variable-length time-slots $\tau_1^{m,k}$ and $\tau_2^{m,k}$, according to A-FR protocol, as shown in Fig. 6.1. In the time slot $\tau_1^{m,k}$, the source transmits the information signal to the relay m for user k. In slot $\tau_2^{m,k}$, the relay m transmits the received information signal to the user k, whereas the source transmits the energy signal to the relay m. This FD relay operation also introduces the self-interference at the relays, in which a part of the transmitted signal is received back at the relays. The relays are capable of energy-recycling [24, 52, 89–91], in which the self-interference signal is used to harvest the energy. We assume that the complete channel state information (CSI) is available [24, 32, 44–46, 88]. The CSI can be obtained through the training process and fed back to the source at the start of each scheduling frame [24, 88]. During the time slot $\tau_1^{m,k}$, the data symbol vector $r^{m,k}$ for user k using relay m is precoded at the source as

$$x^{m,k} = P^{m,k} r^{m,k}, \tag{6.1}$$

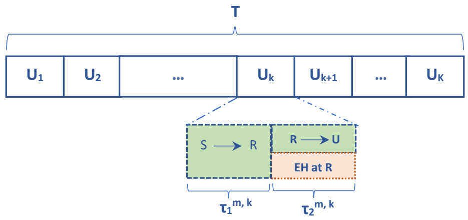

Figure 6.1: Transmission block incorporating dynamic FD protocol (A-FR)

where $x^{m,k}$ is the information signal transmitted by the source to the relay m, $P^{m,k}$ is the precoding matrix adopted by the source. The signal received at relay m for user k is given by

$$y^{m,k} = H_1^{m,k} x^{m,k} + n^m, \tag{6.2}$$

where $H_1^{m,k}$ is the $N \times N$ MIMO channel matrix of the first-hop i.e., between the source and relay m hop, for the user k and captures the joint effect of path loss, shadowing and multi-path fading. n^m is the additive white Gaussian noise (AWGN) vector with distribution $CN \sim (0, \Sigma_m)$ at relay m, where Σ_m is the $N \times N$ diagonal covariance matrix with each diagonal element given by N_o.

In the time slot $\tau_2^{m,k}$, the relay m decodes the received information signal vector from the source, using a processing matrix $F^{m,k}$ and forwards it to the user k. The final signal received at user k is given by

$$z^{m,k} = H_2^{m,k} F^{m,k} y^{m,k} + n^k, \tag{6.3}$$

where $H_2^{m,k}$ is the $N \times N$ MIMO channel matrix between relay m and user k, and n_k is the additive white Gaussian noise vector at user k with distribution $CN \sim (0, \Sigma_k)$.

During the time slot $\tau_2^{m,k}$, the relay m harvests energy from the source. We assume a practical non-linear EH model based on logistic function [22, 62], which takes into account the sensitivity and saturation characteristics of the EH circuit. Due to FD mode, the relay m also harvests energy from its own self interference signal. The energy harvesting rate of relay m, based on non-linear logistic function is given as

$$P_m = \frac{\frac{P_{sat}}{1+e^{(-a((P_{in})-b))}} - P_{sat}\Omega}{1-\Omega}, \tag{6.4}$$

where P_{in} is the input power at the relay m; P_{sat} denotes the maximum saturated EH power due to an excessively large input power; $\Omega = \frac{1}{1+e^{ab}}$ ensures a zero input zero output response for EH circuit; and the parameters a and b are related to the detailed circuit specifications such as the resistance, capacitance, and diode turn-on voltage, and can be determined by curve-fitting.

We incorporate singular value decomposition (SVD) [92] of the channel matrix $H_1^{m,k}$ to convert the $N \times N$ MIMO channel into N parallel SISO channels. Using SVD, the channel matrix can be written as

$$H_1^{m,k} = U_1^{m,k} \wedge_1^{m,k} (V_1^{m,k})^H, \tag{6.5}$$

where $U_1^{m,k}$, $V_1^{m,k}$, are unitary matrices, $\wedge_1^{m,k}$ is a diagonal matrix with main diagonal elements diag($\wedge_1^{m,k}$) = $\left[\sqrt{(\gamma_{s,1}^{m,k})},\ \sqrt{(\gamma_{s,2}^{m,k})},\ ...,\ \sqrt{(\gamma_{s,N}^{m,k})}\right]$, where $\gamma_{s,n}^{m,k}$ is the channel-to-noise ratio (CNR) of the source-to-relay m link for user k on spatial channel n. Based on channel decomposition by SVD, the precoding matrix at the source is given by [93]

$$P^{m,k} = V_1^{m,k} \wedge_p^k, \tag{6.6}$$

where $\wedge_p^k$ is a $N \times N$ diagonal matrix with diagonal elements diag($\wedge_p^k$) = $\left[\sqrt{(p_{s,1}^{m,k})},\ \sqrt{(p_{s,2}^{m,k})},\ ...,\ \sqrt{(p_{s,N}^{m,k})}\right]$. Variable $p_{s,n}^{m,k}$ is the equivalent transmit power of the source-to-relay m link for user k on spatial channel n. The SVD of $H_2^{m,k}$ is given by

$$H_2^{m,k} = U_2^{m,k} \wedge_2^{m,k} (V_2^{m,k})^H, \tag{6.7}$$

where $U_2^{m,k}$, $V_2^{m,k}$ are unitary matrices, $\wedge_2^{m,k}$ is a $N \times N$ diagonal matrix with main diagonal elements diag($\wedge_2^{m,k}$) = $\left[\sqrt{(\gamma_{r,1}^{m,k})},\ \sqrt{(\gamma_{r,2}^{m,k})},\ ...,\ \sqrt{(\gamma_{r,N}^{m,k})}\right]$, $\gamma_{r,n}^{m,k}$ is the CNR of the relay m to user k link on spatial channel n. Based on this, the relay processing matrix is given by [93]

$$F^{m,k} = V_2^{m,k} \wedge_F^k (U_1^{m,}k)^H, \tag{6.8}$$

where $\wedge_F^k$ is a $N \times N$ diagonal matrix, $\text{diag}(\wedge_F^k) = \left[\sqrt{(p_{r,1}^{m,k})},\ \sqrt{(p_{r,2}^{m,k})},\ ...,\ \sqrt{(p_{r,N}^{m,k})} \right]$, $p_{r,n}^{m,k}$ is the equivalent transmit power of the relay m to user k link on spatial channel n. After SVD, the energy harvesting rate of relay m is given as

$$P_m = \frac{\frac{P_{sat}}{1+e^{(-a((\sum_{k=1}^K \sum_{n=1}^N p_{s,n}^{m,k}\gamma_{s,n}^{m,k} + p_{r,n}^{m,k}\gamma_{LI})-b))}} - P_{sat}\Omega}{1-\Omega}, \tag{6.9}$$

where $P_{in} = (\sum_{k=1}^K \sum_{n=1}^N p_{s,n}^{m,k}\gamma_{s,n}^{m,k} + p_{r,n}^{m,k}\gamma_{LI})$; and γ_{LI} represents the self-interference CNR of the relay's own signal.

6.3 Optimization Framework

This section presents the mathematical formulation for sum-throughput maximization through relay selection and resource allocation (i.e., joint time and power optimization) of a two hop wireless-powered FD-DF relay system. The formulated optimization problem is denoted by $\mathcal{RA}-\mathcal{RSP}$ and given as follows:

$\mathcal{RA}-\mathcal{RSP}$

$$\begin{aligned} max \sum_{k=1}^{K} \Big\{ \min\Big(\sum_{m=1}^{M}\sum_{n=1}^{N} \frac{\tau_1^{m,k}}{T} s^{m,k} log_2(1 + p_{s,n}^{m,k}\gamma_{s,n}^{m,k}), \\ \sum_{m=1}^{M}\sum_{n=1}^{N} \frac{\tau_2^{m,k}}{T} s^{m,k} log_2(1 + p_{r,n}^{m,k}\gamma_{r,n}^{m,k})\Big)\Big\} \end{aligned} \tag{6.10a}$$

subject to

$$\sum_{m=1}^{M}\sum_{n=1}^{N} s^{m,k} p_{s,n}^{m,k} \le P;\ \ \forall k \in \{1,2,...,K\}, \tag{6.10b}$$

$$\sum_{k=1}^{K}\sum_{n=1}^{N} s^{m,k} p_{r,n}^{m,k} + p_c \le P_m;\ \ \forall m \in \{1,2,...,M\}, \tag{6.10c}$$

$$\sum_{m=1}^{M} s^{m,k} \le 1;\ \ \forall k \in \{1,2,...,K\}, \tag{6.10d}$$

$$\sum_{k=1}^{K} s^{m,k} \leq 1; \quad \forall m \in \{1, 2, ..., M\}, \tag{6.10e}$$

$$\sum_{k=1}^{K}\sum_{m=1}^{M} \tau_1^{m,k} + \sum_{k=1}^{K}\sum_{m=1}^{M} \tau_2^{m,k} = T, \tag{6.10f}$$

variables

$$s^{m,k} \epsilon \{0, 1\}, p_{s,n}^{m,k}, p_{r,n}^{m,k}, \tau_1^{m,k}, \tau_2^{m,k} \geq 0; \quad \forall n, \forall m, \forall k; \tag{6.10g}$$

The decision variables of the $\mathcal{RA}-\mathcal{RSP}$ are $\tau_1^{m,k}$, $\tau_2^{m,k}$, the time-slot durations for the EH and information transmission of the dynamic FD protocol, respectively; $p_{s,n}^{m,k}$ represent the transmission power of the source to relay m for user k over parallel sub channel n, whereas $p_{r,n}^{m,k}$ represents the transmission power of relay m to user k over parallel channel n; $s^{m,k}$, relay selection binary variable that takes value 1 if relay m is allocated to user k and 0 otherwise; p_c represents the circuit power at the relay.

The objective of the optimization problem is to maximize the sum-throughput of the FD-DF relay based MIMO system as given by Eqn. (6.10a). Eqn. (6.10b) indicates that the transmission power of the source is upper bounded by the available power P for every user k, whereas Eqn. (6.10c) shows that the transmission power of the relay is upper bounded by the total power harvested by the relay m as expressed in Eqn. (6.9). Eqns. (6.10d) and (6.10e) guarantee that only one unique relay is allocated to each user for information transmission. Eqn. (6.10f) indicates that the sum of all $\tau_1^{m,k}$ and $\tau_2^{m,k}$ must be equal to the total time duration T.

The $\mathcal{RA}-\mathcal{RSP}$ is a mixed integer non-linear programming problem, which is difficult to solve for global optimum [20]. As a solution strategy, we decompose the $\mathcal{RA}-\mathcal{RSP}$ problem into resource allocation (time and power allocation) $\mathcal{RAP}$ and relay selection problems. In $\mathcal{RAP}$, we study the optimal solution of resource allocation for a pre-determined relay allocation. To solve $\mathcal{RAP}$ in a low computational complexity, we exploit techniques like transformation of the minimum objective function, and Taylor series approximation to handle the constraint involving non-linear EH expression. After incorporating the above technique and approximation, we observe that the $\mathcal{RAP}$ is a convex optimization problem. Therefore, we solve it using the Lagrange multiplier method for an optimal solution. After optimally solving the $\mathcal{RAP}$, we present the relay selection problem and propose a polynomial-time heuristic relay selection algorithm based on the maximization of the sum-throughput by allocating the best relay to each user.

6.4 Resource Allocation Problem

In this section, we investigate the resource allocation, i.e., time and power allocation problem, for a predetermined relay selection, denoted by $\mathcal{RAP}$, and its solution strategy. For this purpose, first we reduce the original optimization problem to a convex optimization problem by transforming the minimum objective function and using the Taylor Series approximation of the harvested power at the relay. We then propose the optimal solution strategy of the $\mathcal{RAP}$ based on Lagrange multiplier method. Finally, we present the iterative algorithm to obtain the optimal solution of the $\mathcal{RAP}$.

6.4.1 Reduction to Convex Optimization Problem

In this subsection, we reduce the original optimization problem to a convex optimization problem, denoted by $\mathcal{RAP}$. We assume that the relay selection i.e., the variables $s^{m,k}$ are known. First, we transform the minimum objective function of $\mathcal{RA}-\mathcal{RSP}$. The throughput of the two hop DF relay system is always limited by its bottleneck link: the system performance is maximized when the throughput of the first hop becomes equal to that of the second hop, i.e., $\sum_{m=1}^{M}\sum_{n=1}^{N}\frac{\tau_1^{m,k}}{T}log_2(1+p_{s,n}^{m,k}\gamma_{s,n}^{m,k}) = \sum_{m=1}^{M}\sum_{n=1}^{N}\frac{\tau_2^{m,k}}{T}log_2(1+p_{r,n}^{m,k}\gamma_{r,n}^{m,k})$, for every user k. Therefore, the objective function of the $\mathcal{RA}-\mathcal{RSP}$ is equivalent to maximizing $\sum_{k=1}^{K}\sum_{m=1}^{M}\sum_{n=1}^{N}\frac{\tau_1^{m,k}}{T}log_2(1+p_{s,n}^{m,k}\gamma_{s,n}^{m,k})+\sum_{k=1}^{K}\sum_{m=1}^{M}\sum_{n=1}^{N}\frac{\tau_2^{m,k}}{T}log_2(1+p_{r,n}^{m,k}\gamma_{r,n}^{m,k})$ with an additional constraint $\sum_{m=1}^{M}\sum_{n=1}^{N}\frac{\tau_1^{m,k}}{T}log_2(1+p_{s,n}^{m,k}\gamma_{s,n}^{m,k}) = \sum_{m=1}^{M}\sum_{n=1}^{N}\frac{\tau_2^{m,k}}{T}log_2(1+p_{r,n}^{m,k}\gamma_{r,n}^{m,k}), \forall k$ [24].

After transforming the objective function, the difficulty lies in Eqn. (6.10c) in $\mathcal{RA}-\mathcal{RSP}$, which involves the expression for logistic based non-linear EH function. To handle this, we incorporate the first order Taylor series approximation of P_m, which is given as [24]

$$P_m \leq \overline{P_m} = P_m(\boldsymbol{p_s}^{(j)}, \boldsymbol{p_m}^{(j)}) + \sum_{k=1}^{K}\sum_{n=1}^{N} \nabla_{p_{s,n}^{m,k}} P_m(\boldsymbol{p_s}^{(j)}, \boldsymbol{p_m}^{(j)})(p_{s,n}^{m,k} - p_{s,n}^{m,k(j)}) + \sum_{k=1}^{K}\sum_{n=1}^{N} \nabla_{p_{r,n}^{m,k}} P_m(\boldsymbol{p_s}^{(j)}, \boldsymbol{p_m}^{(j)})(p_{r,n}^{m,k} - p_{r,n}^{m,k(j)}), \tag{6.11}$$

where ∇ denotes the derivation calculation and j denotes the iteration index. After eliminating the $s^{m,k}$ variable, transforming the objective function and incorporating the Taylor series approximation, the mathematical formulation for the $\mathcal{RAP}$ is given by

$\mathcal{RAP}$

$$maximize \sum_{k=1}^{K}\sum_{m=1}^{M}\sum_{n=1}^{N} \frac{\tau_1^{m,k}}{T} log_2(1 + p_{s,n}^{m,k}\gamma_{s,n}^{m,k}) + \sum_{k=1}^{K}\sum_{m=1}^{M}\sum_{n=1}^{N} \frac{\tau_2^{m,k}}{T} log_2(1 + p_{r,n}^{m,k}\gamma_{r,n}^{m,k}) \tag{6.12a}$$

subject to

$$\sum_{m=1}^{M}\sum_{n=1}^{N} p_{s,n}^{m,k} \leq P; \quad \forall k \in \{1, 2, ..., K\}, \tag{6.12b}$$

$$\sum_{k=1}^{K}\sum_{n=1}^{N} p_{r,n}^{m,k} + p_c \leq \overline{P_m}; \quad \forall m \in \{1, 2, ..., M\}, \tag{6.12c}$$

$$\sum_{k=1}^{K}\sum_{m=1}^{M} \tau_1^{m,k} + \sum_{k=1}^{K}\sum_{m=1}^{M} \tau_2^{m,k} = T, \tag{6.12d}$$

$$\sum_{m=1}^{M}\sum_{n=1}^{N} \frac{\tau_1^{m,k}}{T} log_2(1 + p_{s,n}^{m,k}\gamma_{s,n}^{m,k}) = \sum_{m=1}^{M}\sum_{n=1}^{N} \frac{\tau_2^{m,k}}{T} log_2(1 + p_{r,n}^{m,k}\gamma_{r,n}^{m,k}); \quad \forall k \in \{1, ..., K\}, \tag{6.12e}$$

Lemma 5. *$\mathcal{RAP}$ is a convex optimization problem.*

Proof. Using Eqn. (6.12e), $\tau_1^{m,k}$ and $\tau_2^{m,k}$ are given by

$$\tau_1^{m,k} = \frac{\tau_2^{m,k} \sum_{n=1}^{N} log_2(1 + p_{r,n}^{m,k}\gamma_{r,n}^{m,k})}{\sum_{n=1}^{N} log_2(1 + p_{s,n}^{m,k}\gamma_{s,n}^{m,k})}, \tag{6.13}$$

$$\tau_2^{m,k} = \frac{\tau_1^{m,k} \sum_{n=1}^{N} log_2(1 + p_{s,n}^{m,k}\gamma_{s,n}^{m,k})}{\sum_{n=1}^{N} log_2(1 + p_{r,n}^{m,k}\gamma_{r,n}^{m,k})}, \tag{6.14}$$

After substituting Eqns. (6.13) and (6.14) into Eqn. (6.12d), we get

$$\tau_1^{m,k} = \frac{T\sum_{n=1}^{N} log_2(1+p_{r,n}^{m,k}\gamma_{r,n}^{m,k})}{\sum_{k=1}^{K}\sum_{m=1}^{M}\sum_{n=1}^{N} log_2(1+p_{s,n}^{m,k}\gamma_{s,n}^{m,k}) + \sum_{k=1}^{K}\sum_{m=1}^{M}\sum_{n=1}^{N} log_2(1+p_{r,n}^{m,k}\gamma_{r,n}^{m,k})}, \quad (6.15)$$

$$\tau_2^{m,k} = \frac{T\sum_{n=1}^{N} log_2(1+p_{s,n}^{m,k}\gamma_{s,n}^{m,k})}{\sum_{k=1}^{K}\sum_{m=1}^{M}\sum_{n=1}^{N} log_2(1+p_{s,n}^{m,k}\gamma_{s,n}^{m,k}) + \sum_{k=1}^{K}\sum_{m=1}^{M}\sum_{n=1}^{N} log_2(1+p_{r,n}^{m,k}\gamma_{r,n}^{m,k})}, \quad (6.16)$$

Now, substituting Eqns. (6.15) and (6.16) into the objective function (6.12a), we get

$$\max\left[\frac{2\sum_{k=1}^{K}\sum_{m=1}^{M}\sum_{n=1}^{N} log_2(1+p_{s,n}^{m,k}\gamma_{s,n}^{m,k}) log_2(1+p_{r,n}^{m,k}\gamma_{r,n}^{m,k})}{\sum_{k=1}^{K}\sum_{m=1}^{M}\sum_{n=1}^{N} log_2(1+p_{s,n}^{m,k}\gamma_{s,n}^{m,k}) + \sum_{k=1}^{K}\sum_{m=1}^{M}\sum_{n=1}^{N} log_2(1+p_{r,n}^{m,k}\gamma_{r,n}^{m,k})}\right], \quad (6.17)$$

The above objective function in Eqn. (6.17) can be transformed to

$$\min\frac{1}{2}\Big(\frac{1}{\sum_{k=1}^{K}\sum_{m=1}^{M}\sum_{n=1}^{N} log_2(1+p_{s,n}^{m,k}\gamma_{s,n}^{m,k})} + \frac{1}{\sum_{k=1}^{K}\sum_{m=1}^{M}\sum_{n=1}^{N} log_2(1+p_{r,n}^{m,k}\gamma_{r,n}^{m,k})}\Big), \quad (6.18)$$

The Hessian matrix of the two inner functions $\sum_{k=1}^{K}\sum_{m=1}^{M}\sum_{n=1}^{N} log_2(1+p_{s,n}^{m,k}\gamma_{s,n}^{m,k})$ and $\sum_{k=1}^{K}\sum_{m=1}^{M}\sum_{n=1}^{N} log_2(1+p_{r,n}^{m,k}\gamma_{r,n}^{m,k})$ is negative semi-definite. Hence, they are concave functions. Based on this, we conclude that the equivalent objective function $\min\frac{1}{2}\Big(\frac{1}{\sum_{k=1}^{K}\sum_{m=1}^{M}\sum_{n=1}^{N} log_2(1+p_{s,n}^{m,k}\gamma_{s,n}^{m,k})} + \frac{1}{\sum_{k=1}^{K}\sum_{m=1}^{M}\sum_{n=1}^{N} log_2(1+p_{r,n}^{m,k}\gamma_{r,n}^{m,k})}\Big)$ is a convex function. Moreover, we observe that the constraints (6.12b) and (6.12d) of $\mathcal{RAP}$ are affine and all affine functions are convex functions. The right-hand side of constraint (6.12c) is a differentiable concave function [22], hence, it is a convex constraint, whereas, constraint (6.12e) is also convex [18]. Therefore, $\mathcal{RAP}$ is a convex optimization problem and there is one and only one optimal solution. □

6.4.2 Solution of the Convex Optimization Problem

In this subsection, we present the solution for the $\mathcal{RAP}$ based on Lagrange Multiplier method. The Lagrangian function of the problem is written as:

$$\begin{aligned} L = &\sum_{k=1}^{K}\sum_{m=1}^{M}\sum_{n=1}^{N}\frac{\tau_1^{m,k}}{T}log_2(1+p_{s,n}^{m,k}\gamma_{s,n}^{m,k}) + \sum_{k=1}^{K}\sum_{m=1}^{M}\sum_{n=1}^{N}\frac{\tau_2^{m,k}}{T}log_2(1+p_{r,n}^{m,k}\gamma_{r,n}^{m,k}) \\ &- \sum_{k=1}^{K}\mu_k\Big(\sum_{m=1}^{M}\sum_{n=1}^{N}p_{s,n}^{m,k} - P\Big) \\ &- \sum_{m=1}^{M}\lambda_m\Big(\sum_{k=1}^{K}\sum_{n=1}^{N}p_{r,n}^{m,k} + p_c - P_m(\boldsymbol{p_s}^{(j)}, \boldsymbol{p_m}^{(j)}) - \sum_{k=1}^{K}\sum_{n=1}^{N}\nabla_{p_{s,n}^{m,k}}P_m(\boldsymbol{p_s}^{(j)}, \boldsymbol{p_m}^{(j)})(p_{s,n}^{m,k} - p_{s,n}^{m,k(j)}) - \\ &\sum_{k=1}^{K}\sum_{n=1}^{N}\nabla_{p_{r,n}^{m,k}}P_m(\boldsymbol{p_s}^{(j)}, \boldsymbol{p_m}^{(j)})(p_{r,n}^{m,k} - p_{r,n}^{m,k(j)})\Big) \\ &-\nu(\sum_{k=1}^{K}\tau_1^{m,k} + \sum_{k=1}^{K}\tau_2^{m,k} - T) \\ &- \sum_{k=1}^{K}\sigma_k\Big(\sum_{n=1}^{N}\frac{\tau_1^{m,k}}{T}log_2(1+p_{s,n}^{m,k}\gamma_{s,n}^{m,k}) - \sum_{n=1}^{N}\frac{\tau_2^{m,k}}{T}log_2(1+p_{r,n}^{m,k}\gamma_{r,n}^{m,k})\Big) \end{aligned} \tag{6.19}$$

where μ_k, σ_K, ν,λ_m, $\forall k, \forall m$ are the Lagrangian multipliers corresponding to multiple constraints and $\mu_k \geq 0$, $-1 \geq \sigma_k \geq 1$, $\lambda_m \geq 0$, $\nu \geq 0$. Now, we present the optimal solution of $\mathcal{RAP}$ in Theorem 1 below.

Theorem 1. The optimal values of $\tau_1^{m,k}$, $\tau_2^{m,k}$, $p_{s,n}^{m,k}$, and $p_{r,n}^{m,k}$ are given by

$$\tau_1^{m,k} = \frac{1-\sigma_k}{2}T \tag{6.20}$$

$$\tau_2^{m,k} = \frac{1+\sigma_k}{2}T \tag{6.21}$$

$$p_{s,n}^{m,k} = \Big[\frac{(1-\sigma_k)^2}{2ln(2)[\mu_k - \lambda_m(\nabla_{p_{s,n}^{m,k}}P_m(\boldsymbol{p_s}^{(j)}, \boldsymbol{p_m}^{(j)}))]} - \frac{1}{\gamma_{s,n}^{m,k}}\Big]^+ \tag{6.22}$$

$$p_{r,n}^{m,k} = \Big[\frac{(1+\sigma_k)^2}{2ln(2)\lambda_m[1 - (\nabla_{p_{r,n}^{m,k}}P_m(\boldsymbol{p_s}^{(j)}, \boldsymbol{p_m}^{(j)}))} - \frac{1}{\gamma_{r,n}^{m,k}}\Big]^+ \tag{6.23}$$

Proof. Taking the derivative of Lagrangian function L w.r.t τ_1 and τ_2 yields Eqns. (6.24) and (6.25).

$$\frac{\partial L}{\partial \tau_1^{m,k}} = \frac{1-\sigma_k}{T}\Big(\sum_{k=1}^{K}\sum_{m=1}^{M}\sum_{n=1}^{N} log_2(1+p_{s,n}^{m,k}\gamma_{s,n}^{m,k})\Big) - \nu = 0, \tag{6.24}$$

$$\frac{\partial L}{\partial \tau_2^{m,k}} = \frac{1+\sigma_k}{T}\Big(\sum_{k=1}^{K}\sum_{m=1}^{M}\sum_{n=1}^{N} log_2(1+p_{r,n}^{m,k}\gamma_{r,n}^{m,k})\Big) - \nu = 0, \tag{6.25}$$

We know that the optimization problem is maximized when,

$$\frac{\tau_1^{m,k}}{T}\sum_{m=1}^{M}\sum_{n=1}^{N} log_2(1+p_{s,n}^{m,k}\gamma_{s,n}^{m,k}) = \frac{\tau_2^{m,k}}{T}\sum_{m=1}^{M}\sum_{n=1}^{N} log_2(1+p_{r,n}^{m,k}\gamma_{r,n}^{m,k}), \tag{6.26}$$

Therefore, the following equality holds

$$\frac{\tau_1^{m,k}}{1-\sigma_k} = \frac{\tau_2^{m,k}}{1+\sigma_k}, \tag{6.27}$$

Substituting Eqn. (6.12d) into Eqn. (6.27) gives the optimal solution of $\tau_1^{m,k}$ and $\tau_2^{m,k}$, as presented in Theorem 1. Similarly, taking the derivative of L w.r.t $p_{s,n}^{m,k}$ and $p_{r,n}^{m,k}$ is given as

$$\frac{\partial L}{\partial p_{s,n}^{m,k}} = \frac{(1-\sigma_k)\tau_1^{m,k}\gamma_{s,n}^{m,k}}{T ln(2)(\gamma_{s,n}^{m,k}p_{s,n}^{m,k}+1)} - \mu_k + \lambda_m(\nabla_{p_{s,n}^{m,k}} P_m(\boldsymbol{p_s}^{(j)}, \boldsymbol{p_m}^{(j)})) = 0, \tag{6.28}$$

$$\frac{\partial L}{\partial p_{r,n}^{m,k}} = \frac{(1+\sigma_k)\tau_2^{m,k}\gamma_{r,n}^{m,k}}{T ln(2)(\gamma_{r,n}^{m,k}p_{r,n}^{m,k}+1)} - \lambda_m + \lambda_m(\nabla_{p_{r,n}^{m,k}} P_m(\boldsymbol{p_s}^{(j)}, \boldsymbol{p_m}^{(j)})) = 0, \tag{6.29}$$

Putting the values of $\tau_1^{m,k}$ and $\tau_2^{m,k}$ from Eqns. (6.20) and (6.21) give

$$\frac{\partial L}{\partial p_{s,n}^{m,k}} = \frac{(1-\sigma_k)(1-\sigma_k)T\gamma_{s,n}^{m,k}}{2T ln(2)(\gamma_{s,n}^{m,k}p_{s,n}^{m,k}+1)} - \mu_k + \lambda_m(\nabla_{p_{s,n}^{m,k}} P_m(\boldsymbol{p_s}^{(j)}, \boldsymbol{p_m}^{(j)}))] = 0, \tag{6.30}$$

$$\frac{\partial L}{\partial p_{r,n}^{m,k}} = \frac{(1+\sigma_k)(1+\sigma_k)T\gamma_{r,n}^{m,k}}{2T ln(2)(\gamma_{r,n}^{m,k}p_{r,n}^{m,k}+1)} - \lambda_m + \lambda_m(\nabla_{p_{r,n}^{m,k}} P_m(\boldsymbol{p_s}^{(j)}, \boldsymbol{p_m}^{(j)})) = 0, \tag{6.31}$$

After some simple algebraic manipulations which are skipped for brevity, Eqns. (6.30) and (6.31) can be written as in Theorem 1. □

Now, we adopt the gradient method to update the Lagrange multipliers. The rules of updating multipliers are given as:

$$\sigma_k(i+1) = \Big[\sigma(i)+\epsilon_1(i)\Big(\sum_{n=1}^{N}\frac{\tau_1^{m,k}}{T}log_2(1+p_{s,n}^{m,k}\gamma_{s,n}^{m,k})-\sum_{n=1}^{N}\frac{\tau_2^{m,k}}{T}log_2(1+p_{r,n}^{m,k}\gamma_{r,n}^{m,k})\Big)\Big]_{[-1,1]} \quad (6.32)$$

$$\lambda_m(i+1) = \Big[\lambda_m(i)+\epsilon_2(i)\Big(\sum_{k=1}^{K}\sum_{n=1}^{N}p_{r,n}^{m,k}+p_c-P_m(\boldsymbol{p_s^{(j)}},\boldsymbol{p_m^{(j)}})-\sum_{k=1}^{K}\sum_{n=1}^{N}\nabla_{p_{s,n}^{m,k}}P_m(\boldsymbol{p_s^{(j)}},\boldsymbol{p_m^{(j)}})(p_{s,n}^{m,k}-p_{s,n}^{m,k,(j)}) - \sum_{k=1}^{K}\sum_{n=1}^{N}{}_{p_{r,n}^{m,k}}P_m(\boldsymbol{p_s^{(j)}},\boldsymbol{p_m^{(j)}})(p_{r,n}^{m,k}-p_{r,n}^{m,k,(j)})\Big)\Big]^{+} \quad (6.33)$$

$$\mu_k(i+1) = \Big[\mu(i)+\epsilon_3(i)\Big(\sum_{m=1}^{M}\sum_{n=1}^{N}p_{s,n}^{m,k}-P\Big)\Big]^{+} \quad (6.34)$$

where $\epsilon_1(i)$, $\epsilon_2(i)$, $\epsilon_3(i)$ are the corresponding step sizes [24] at the i^{th} iteration. In order to guarantee the convergence, step sizes must satisfy $\sum_{i=1}^{\infty}\epsilon(i) = \infty$ and $lim_{i\to\infty}\epsilon(i) = 0$ [24, 92].

6.4.3 Iterative Algorithm for Convergence to Optimal Solution

In this subsection, we present an iterative algorithm to obtain the optimal solution of the $\mathcal{RAP}$. Solving $\mathcal{RAP}$ after replacing the right hand side of Eqn. (6.10c) in $\mathcal{RA}-\mathcal{RSP}$ with Eqn. (6.12c) leads to an upper bound of the optimal solution. To tighten this upper bound, we will present an iterative algorithm (presented in Algorithm 7) where intermediate solution is obtained using the Taylor approximation, and then repeated iteratively until convergence. ∇ denotes the derivation calculation and j denotes the iteration index of the algorithm. Since the right hand side of Eqn. (6.10c) in $\mathcal{RA}-\mathcal{RSP}$ is a concave function, the iterative algorithm always converges to the optimal solution w.r.t. the original problem in polynomial-time [24]. In the following, we present the algorithm for the evaluation of the time and power variables obtained in Theorem 1, named as Time and Power Allocation Algorithm (TAP). The algorithm takes the set of relays M, and users K as inputs. The algorithm starts by initializing the outer loop, initial transmission power

Algorithm 7 Time and Power Allocation (TAP) Algorithm

input: set of relays M, and users K

output: Optimal $\tau_1^{m,k}$, $\tau_2^{m,k}$, $p_{s,n}^{m,k}$, $p_{r,n}^{m,k}$ $\forall n, m, k$

1: set $j \leftarrow 0$ and initialize $\boldsymbol{p_s}^{(j)}$, and $\boldsymbol{p_r}^{(j)}$
2: **repeat**
3: $i \leftarrow 0$
4: **repeat**
5: update σ_k, λ_m, μ_k, and according to Eqns. (6.32), (6.33), and (6.34)
6: update $\tau_1^{m,k}$, $\tau_2^{m,k}$, $p_{s,n}^{m,k}$, and $p_{r,n}^{m,k}$ according to Eqns. (6.20), (6.21), (6.22), and (6.23) using the updated Lagrange multipliers
7: $i \leftarrow i + 1$
8: **until** convergence
9: obtain the intermediate values $\boldsymbol{p_s}'^{(j)}$, $\boldsymbol{p_r}'^{(j)}$
10: update $\boldsymbol{p_s}^{(j+1)} = \boldsymbol{p_s}'^{(j)}$, and $\boldsymbol{p_r}^{(j+1)} = \boldsymbol{p_r}'^{(j)}$
11: $j \leftarrow j + 1$
12: **until** convergence
13: obtain the values $\tau_1^{m,k}$, $\tau_2^{m,k}$, $p_{s,n}^{m,k}$, and $p_{r,n}^{m,k}$

values $\boldsymbol{p_s}^{(j)}$, $\boldsymbol{p_r}^{(j)}$ (Line 1). Then, in the inner loop, the algorithm updates the Lagrange multipliers λ_m, σ_k, and μ_k, corresponding to the constraints (Line 5), with the given initial values of the variables. It then calculates the intermediate variables $\tau_1^{m,k}$, $\tau_2^{m,k}$, $p_{s,n}^{m,k}$, and $p_{r,n}^{m,k}$ by using the multiplier values (Line 6). After each iteration, the values of $\boldsymbol{p_s}^{(j)}$, $\boldsymbol{p_r}^{(j)}$ are updated in the outer layer (Line 10). Two steps run until convergence. Note that the outer loop in TAP algorithm is incorporated to handle the constraint (6.12c) involving EH expression, as discussed earlier. In the $\mathcal{RAP}$, constraint (6.12c) is upper bounded by Taylor approximation, so, by updating the values of $\boldsymbol{p_s}^{(j)}$ and $\boldsymbol{p_r}^{(j)}$ iteratively in the outer loop, this approximation will eventually approach the original problem and convergence will be achieved [24].

The computational complexity of TAP is $\mathcal{O}(l_{inner} \times l_{outer})$, where l_{inner} represents the number of iterations in the inner layer, i.e., updating multipliers according to Eqns. (6.32), (6.33), and (6.34). On the other hand, l_{outer} represents the number of iterations in the outer layer, i.e., updating intermediate variables $\boldsymbol{p_s}^{(j)}$, and $\boldsymbol{p_r}^{(j)}$ after the j^{th} iteration.

6.5 Relay Selection Problem

In this section, we present the relay selection problem and propose polynomial-time heuristic relay selection algorithm such that the throughput of the system is maximized. In section 6.4, we discussed the resource allocation problem for a predetermined relay selection i.e., $s^{m,k}$ was known for $m \in \{1, ...M\}$, $k \in \{1, ..., K\}$. The throughput can be further maximized by allocating a suitable relay to each user. A straightforward approach to the relay selection problem, after finding the optimal resource allocation $\mathcal{RAP}$ solution, can be brute-force search algorithm (BFA). In this technique, we enumerate all possible permutations of relay-user allocation and then pick the one that gives the best throughput. The computational complexity of BFA is $O((^{M}C_{K})K!)$, where M and K are the total number of relays and users, respectively. Due to the higher computational complexity of BFA, we propose a heuristic polynomial-time algorithm based on the idea of allocating a relay to user which offers the maximum throughput. The Maximum Throughput Relay Selection Algorithm (MTRSA), as given in Algorithm 8, is described in detail next. The inputs to the algorithm are set of users K, and set of relays M. The outputs are the relay selection set $\mathcal{R}$ and sum throughput R. It starts by initializing an empty relay set $\mathcal{R}$ and sum throughput R as 0 (Line 1). For each user k, the relay that offers the maximum throughput by using the optimal solution of Theorem 1 is selected (Lines 3 and 4). Then, the relay set $\mathcal{R}$ is updated with the selected relay (Line 5), whereas the selected relay is eliminated from the relay set M (Line 6). Algorithm terminates when all the users in the network are being assigned to the best relays. Finally, MTRSA algorithm returns the relay set $\mathcal{R}$ (Line 8) and sum-throughput R (Line 9).

The computational complexity of MTRSA is $O(K \times M)$ for M relays and K users since the algorithm picks one user at each iteration; i.e., K iterations, and determines the relay which offers the maximum throughput, which has $O(M)$ complexity.

6.6 Performance Evaluation

The goal of this section is to evaluate the performance of the proposed MTRSA in comparison to the optimal solution denoted by BFA, previously proposed conventional relay

Algorithm 8 Maximum Throughput Relay Selection Algorithm (MTRSA)

input: set of users K and relays M

output: Relay selection $\mathcal{R}$, sum throughput R

```
R ← ∅, R ← 0,
for k = 1 : |K| do
    Calculate R_{m,k}, R_k, ∀m ∈ M
    i ← argmax_{m∈M} {R_{m,k} + R_k},
    R ← R + {i},
    M ← M-{i},
end for
obtain R,
obtain R ← Σ_{k=1}^{K} {R_{m,k} + R_k}
```

selection algorithms, which are Opportunistic Relay Selection ORS and Partial Relay Selection PRS, and predetermined relay allocation algorithm TAP. The proposed MTRSA aims at maximizing the throughput by allocating a relay to each user which offers the maximum throughput in polynomial-time, as given in Algorithm 7. In BFA, all possible relay-user permutations are enumerated, and then, the best relay with the maximum throughput is selected. In ORS scheme, the relay selection decision is determined by considering the channel of both the hops, i.e., source-to-relay and relay-to-user [94]. It is based on selecting a relay for every user k with the best CNR ratio, i.e., $\max_{m\in\mathcal{M}}$ $\{min(\sum_{n=1}^{N}\gamma_{s,n}^{m,k}), (\sum_{n=1}^{N}\gamma_{r,n}^{m,k})\}$. On the other hand, in PRS algorithm, CSI of only one hop is assumed to be available, i.e., either source-to-relay or relay-to-user [95]. Specifically, in this work, we consider the CNR of the first source-to-relay hop. Relay with the $\max_{m\in\mathcal{M}}$ $\sum_{n=1}^{N}\gamma_{s,n}^{m,k}$ is assigned to its specific user. The TAP determines the throughput of the system for a predetermined relay allocation, as given in Algorithm 1. We also compare the proposed A-FR based FD-MIMO system with the conventional S-FR based FD-MIMO in which the time durations $\tau_1^{m,k}$ and $\tau_2^{m,k}$ for every user k are assumed to be equal, and the FD-MIMO system without self-energy recycling, referred as W-SE.

The simulation results are obtained in MATLAB R2021a and averaged over 1000 random network realizations. The users are uniformly distributed in a circle of 10m. The source is located at the center of the circle and the relays are randomly positioned between the source and users. The attenuation of the links considering large scale statistics are

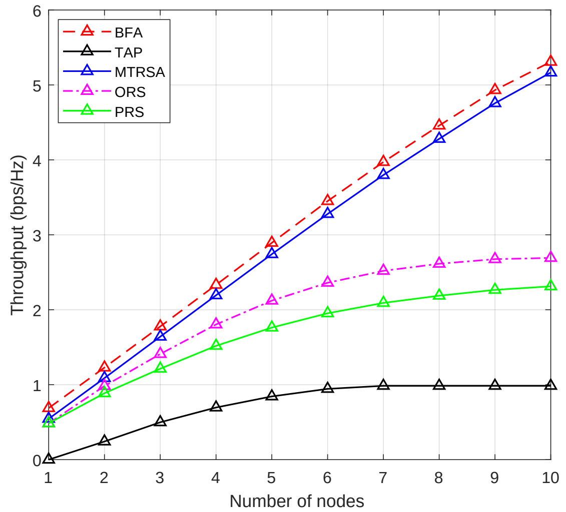

Figure 6.2: Sum throughput of the algorithms for different network sizes.

determined using the path loss model given by [20, 88]

$$PL(d, dB) = PL(d_0, dB) + 10\alpha log_{10}(d/d_0) + Z \tag{6.35}$$

where $PL(d, dB)$ is the path loss in dB at distance d, $d_0 = 1m$ is the reference distance and path loss at this distance is taken as $30dB$, α is the path loss exponent, and is taken as 2.76. Z is a zero mean Gaussian random variable, and its standard deviation is taken as σ=4. For the non-linear EH model based on logistic function, $P_s = 7mW$, $a = 1500$ and $b = 0.0022$ [20]. The small-scale fading has been modeled by using Rayleigh fading with scale parameter Ω set to mean power level obtained from the large-scale path loss model.

6.6.1 Throughput versus Network Size

Fig. 6.2 illustrates the sum-throughput performance of the proposed algorithm MTRSA in comparison to the optimal BFA, ORS, PRS and TAP for different number of nodes in the network for $P = 1dBm$. The throughput increases with the network size for all the algorithms. As the number of nodes increases, the system can find the channels with better conditions to carry the information and energy signals, i.e., befitting from the multi-node diversity. The proposed algorithm MTRSA performs better than the other heuristic algorithms and close to the optimal solution even for higher number of nodes in the network, demonstrating the robustness of the proposed algorithm to network size. The robustness to network size is critical for future generation networks, which are expected to contain a large number of devices or sensors. The throughput performance achieved by the ORS algorithm is better as compared to PRS. It is because the ORS algorithm takes into account the channel characteristics of both the hops of the network, while deciding for the relay allocation, in contrast to PRS which considers only a single-hop. On the other hand, TAP performs the worst as it considers the predetermined relay allocation in the network. Note that the performance gap among the different algorithms increases with the network size showing the significance of multi-node diversity and appropriate relay allocation scheme. For a large network, the proposed MTRSA yields a better throughput improvement with the addition of each node as compared to the other polynomial-time ORS, PRS and TAP algorithms. This trend shows the significance of allocating a relay to each user with the maximum throughput value based on the proposed optimal solution in Theorem 2. In conventional ORS and PRS algorithms, relay selection is performed considering only the channel characteristics, which results in a limited throughput performance as compared to the proposed MTRSA.

Fig. 6.3 compares the sum-throughput performance of the presented A-FR based FD-MIMO system with the conventional S-FR and the system without self-energy recycling W-SE. For the MTRSA, the A-FR system outperforms the S-FR and W-SE. It is because the A-FR system benefits from the better utilization of the system resources. Specifically, the time durations $\tau_1^{m,k}$ and $\tau_2^{m,k}$ for every user k can be adjusted dynamically in A-FR based FD-MIMO, hence, results in better throughput performance. For a network of 8 users, A-FR based MTRSA achieves a throughput ratio of 1.27 and 2.43 over S-FR and W-SE based MTRSA, respectively. The main reason for the significant increase of the throughput in A-FR compared to S-FR is that the S-FR based MTRSA allocates uniform time-slots $\tau_1^{m,k}$ and $\tau_2^{m,k}$ for its source and relays, even when the effective SNR of each relay-user hop is significantly lower than that of the first hop. As a result, the system throughput performance is significantly limited by the bottleneck relay-user link, and the resources allocated for improving throughput is wasted partially. On the other hand, the

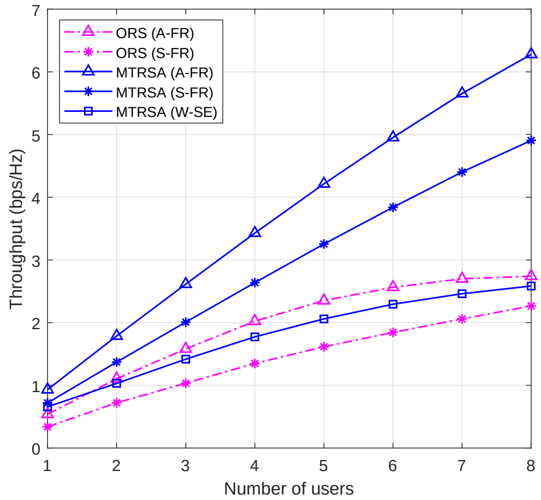

Figure 6.3: Sum throughput of the A-FR based FD-MIMO in comparison to S-FR and W-SE for different network sizes.

W-SE based MTRSA system achieves lower performance gain as it solely harvests energy from the source, thus harvests less energy as compared to A-FR and S-FR based MTRSA systems. Furthermore, for the ORS algorithm specifically, the A-FR performs better than S-FR as expected and achieves a throughput performance ratio of around 1.45 over the S-FR. Note that the static time S-FR protocol of the proposed MTRSA outperforms the dynamic time protocol for the conventional ORS algorithm, which shows the robustness of the proposed MTRSA and the importance of relay selection in the network to achieve better throughput gains. The W-SE based MTRSA performs better than the S-FR based system incorporating conventional ORS scheme. Therefore, it is significant to allocate proper relays to the users in the network.

6.6.2 Throughput versus Transmission Power of the Source

Fig. 6.4 compares the sum-throughput performance of the BFA, MTRSA, ORS, PRS and TAP algorithms for varying source transmission power P values for $K = 5$ users in the network. As P increases, throughput performance of the algorithms increases. It is due to the fact that the relays can harvest more energy with increasing source power P values,

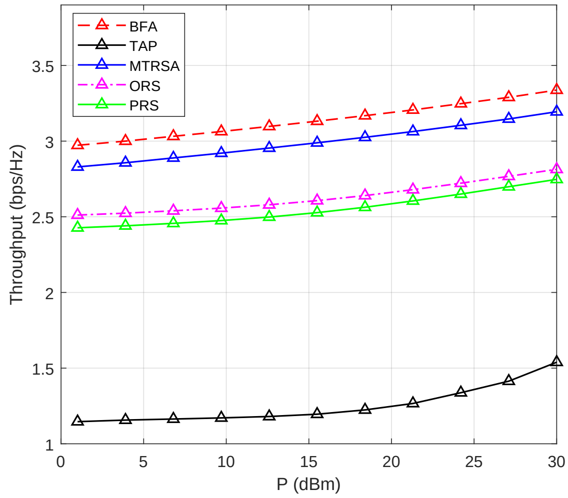

Figure 6.4: Sum throughput of the algorithms for different values of source transmission power P.

which in turn increases the transmission power at the relays, and thus the throughput increases. The proposed MTRSA achieves better throughput performance as compared to the other conventional ORS and PRS algorithms and performs close to the optimal BFA solution, showing the significance of proper relay allocation in the network. Note that the ORS algorithm which considers the channel characteristics of both the hops while selecting a relay performs better than the PRS, which takes into account only a single-hop. TAP algorithm again achieves the lowest throughput performance.

Fig. 6.5 compares the sum-throughput performance of the proposed A-FR based MTRSA with S-FR and W-SE based MTRSA, respectively. We observe that the throughput increases as the power P increases. With the increasing values of P, the relays are able to harvest more energy, which increases the throughput performance of the system. The A-FR based MTRSA achieves the throughput ratio of 1.32 and 2.1 over S-FR and W-SE based MTRSA for the $P = 1$dBm, respectively. The higher performance gain of the A-FR based MTRSA shows the significance of incorporating dynamic time slot based A-FR protocol. Furthermore, the A-FR based MTRSA outperforms conventional ORS for both A-FR and S-FR protocols, showing the robustness of appropriate relay allocation. Note that the static time S-FR protocol based MTRSA performs better than the dynamic time

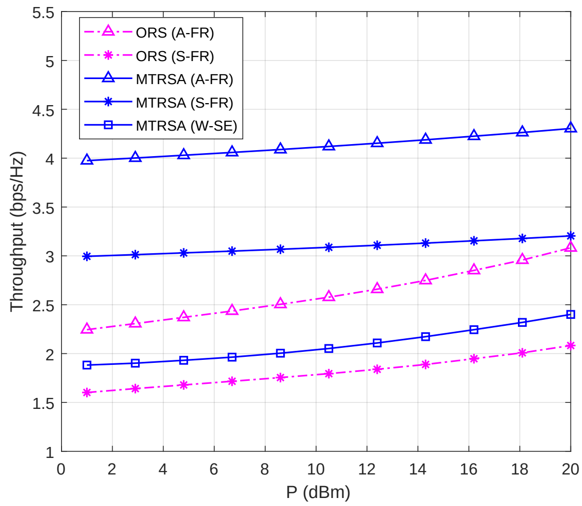

Figure 6.5: Sum throughput of the A-FR algorithm in comparison to S-FR and W-SE for different values of source transmission power P.

A-FR protocol based conventional ORS system. Therefore, it is significant to incorporate dynamic time A-FR protocol along with the robust relay selection which in our case is the proposed MTRSA.

6.7 Conclusion

In this chapter, we have considered an FD-DF MIMO multi-relay-user system with self-energy recycling capability. We have investigated the sum-throughput maximization problem to determine the optimal dynamic time slot durations of the A-FR protocol, transmission powers of the source and relays, and relay selection. The formulated problem is MINLP, which is generally hard to solve for the global optimum. We have provided a solution strategy in which the problem is divided into two sub-problems: resource allocation and relay selection. We have reduced the resource allocation problem for a given relay allocation to a convex problem by using the Taylor series approximation of the harvested power at the relay and presented the optimal solution using convex optimization techniques. For the relay allocation, we have proposed the heuristic polynomial-time algorithm based on the idea of the iterative selection of a relay that offers the maximum throughput rather than only considering the channel conditions in conventional relay selection algorithms. Through extensive simulations, we have observed that the proposed algorithm outperforms previously proposed conventional relay selection algorithms and performs very close to the optimal solution. We have also illustrated that the A-FR based system achieves better throughput performance as compared to the conventional system incorporating uniform time duration S-FR protocol and the FD-MIMO system without self-energy recycling. In the future, we are planning to include scheduling of the users in the problem since it will further improve the throughput performance. The work can also be extended in a multi-cell environment. Beam-forming can also be exploited to improve the energy harvesting rates of the relays to improve the throughput. Furthermore, we will incorporate machine learning techniques to solve the optimization problem in low run-time computational complexity.

Chapter 7

WIRELESS INFORMATION AND ENERGY TRANSFER FOR OUTDOOR TO INDOOR MULTICARRIER SUDAS SYSTEM

In this chapter, we study the resource allocation in an amplify and forward (AF) relay assisted orthogonal frequency division multiple access (OFDMA) system employing a shared UE side distributed antenna (SUDAS). It simultaneously utilizes both unlicensed (in the UE to AF relay link) and licensed frequency bands (AF relay to BS link), hence exploiting the advantages of both MIMO over licensed band with its favorable propagation conditions and mmW band with larger bandwidths, to improve achievable rate of the future 5G communication systems. The users in the system have no energy of their own, so for transmitting information to the base station in the uplink, they first need to harvest energy from the AF relays in the downlink. For this purpose, we present a time switching based MIMO-OFDM (TS) protocol. To explore the system performance limits, we formulate a non-convex optimization problem to maximize the end-to-end achievable information rate of the system. Due to the non-convexity of the problem, we propose a polynomial time algorithm based on the separation of energy harvesting and information transmission problems and optimization of the interactive time variable. Simulation results illustrate that the proposed system achieves a significant performance gain over the conventional systems exploiting only licensed bands. Moreover, the effect of the number of SUDACs (relays) and number of subcarriers on the system performance are also investigated.

7.1 Introduction

Wireless relaying is an efficient technique to provide reliable transmission, high throughput and long coverage as with the exponential growth of wireless traffic, future 5-th generation (5G) wireless communication systems face huge challenges for high data rate and reliability of transmission [81]. Different relaying techniques such as amplify and forward (AF), compress and forward (CF) and decode and forward (DF) have been presented in the literature [96, 97]. Among them, AF is one of the most widely used technique, mostly preferred due to its simplicity. On the other hand, multiple input multiple output (MIMO) systems have received great attention in the past decades as it provide higher rates, reliability and spectrum efficiency. Moreover, orthogonal frequency division multiple access (OFDMA) provides high speed wireless communications because of its resistance to multipath fading and high spectral efficiency. Therefore, recently there has been a lot of interest in combining the concepts of MIMO and OFDMA to pave the way for the transition of existing communication systems to 5G. In [98], a suboptimal resource allocation algorithm design for multiuser MIMO-OFDMA systems is presented. In [99], the performance of multiuser MIMO with limited feedback is investigated. But, the total end to end throughput in [98] and [99] is limited by the system bandwidth which is a scarce resource in licensed frequency bands. Also, small number of antennas at the UEs limits the spatial multiplexing gain offered by MIMO. Therefore, using unlicensed frequency spectrum around 60 GHz is useful as it offers a bandwidth of 7 GHz. The mmWave band can offer high data rates for 5G networks but suffers from the penetration losses which limits its scope for outdoor to indoor scenarios. Moreover, backhauling of this data to a central unit is a problem as the last mile from the central unit to homes cannot support such high data rates except when optical fiber is used which is a very costly solution. Also, finding a suitable location for the BS using mmWave band that is in line-of-sight to all the available UEs is very difficult. Therefore, we propose a solution which combines the advantages of MIMO over a licensed band with its favorable propagation conditions and mmWave band with its larger bandwidths to increase the rate of the system.

In this chapter, we present a SUDAS uplink communication system which resembles a

wireless relay assisted MIMO system and utilizes both licensed and unlicensed frequency bands. SUDAS is a system which translates spatial multiplexing in the mobile band into frequency multiplexing in the mm-wave band. In [100], an efficient resource allocation algorithm design to maximize the end-to-end system throughput for downlink multicarrier transmission with SUDAS is presented. But considering the mobile networks, in which the nodes having a limited lifetime have garnered a great interest on an efficient use of energy in wireless networks so for that purpose, we consider that the users in the system have no energy of their own, and for transmitting the information to the BS, they first harvest energy from the SUDACs (relays) available in the downlink. For EH, we assume that the time switching (TS) based protocol is used. In [101], the authors studied the wireless energy and information transfer for two hop MIMO-OFDM relay networks for a single user, but they considered the relay to be energy harvesting component. On the contrary, we have multiple users in our system and they are the energy harvesting components. In [92], the authors presented a SUDAS system and their objective was to maximize the energy efficiency of the system but there are no energy harvesting components. The contribution of our work is summarized as follows:
We propose a SUDAS communication system which utilizes both licensed and unlicensed frequency bands to increase the information rate of the system. To explore the system performance, we formulate a non convex optimization problem to maximize the end-to-end achievable rate. Due to non convexity of the problem, we divide the main problem into two sub problems namely EH problem and information transmission problem and present an algorithm to solve it optimally.

The rest of the chapter is organized as follows. In section 7.2, we present the model of the proposed SUDAS system and the Time switching based (TS) protocol. In section 7.3, we formulate a non convex optimization problem to maximize the end to end achievable rate of the system. Due to the non-convexity of the problem, it is very difficult to solve. Section 7.4 discuss how to optimize the proposed TS based protocol. In section 7.5, we present numerical results to evaluate the performance gain of our proposed TS based protocol. Section 7.6 summarizes our work.

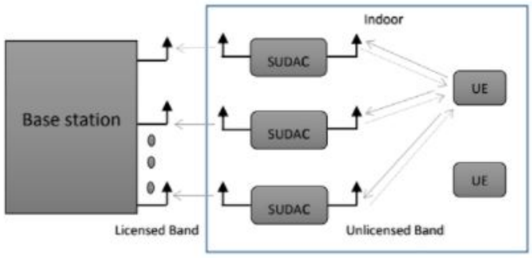

Figure 7.1: SUDAS uplink communication system

7.2 System Model

7.2.1 Physical Layer Uplink SUDAS Model

We consider an OFDMA uplink communication system that consists of K UEs, M SUDACs (relays) and a BS. A SUDAC is a device operating on both licensed and unlicensed frequency bands. We assume that the users have no power of their own, so for communication to the BS, they need to harvest energy from the SUDACs available in the downlink. The UEs transmit the information to SUDACs in the unlicensed band and every SUDAC transmits to the BS in the licensed band. Simultaneous transmission and reception is possible at SUDACs since the two signals are separated in frequency. In the unlicensed band, a huge bandwidth is available. As shown in Fig. 7.1, the UEs are equipped with N_D transmit antennas, transmitting the signals to M SUDACs in the unlicensed band. The BS contains N_T antennas, receiving the signals in the licensed band from the SUDACs. The multicarrier communication system is wideband with N subcarriers. We assume that the channel of both hops are known to their respective transmitter and receiver. The data vector symbol $m_n^k \in \mathbb{C}^{N_s \times 1}$ on subcarrier n from UE k denoted by X_n^k is precoded as

$$X_n^k = W_{1,n}^k m_n^k, \tag{7.1}$$

where $W_{1,n}^k \in \mathbb{C}^{N_D \times N_s}$ is the precoding matrix adopted by UE k on subcarrier n in the unlicensed band.

The signals received at the M SUDACs on subcarrier n for the k-th UE denoted by $y_{S,n}^k$

are

$$y^k_{S,n} = H^k_{1,n} X^k_n + z^k_l \tag{7.2}$$

where $H^k_{1,n}$ is the $(M \times N_D)$ MIMO channel matrix for the first hop between the UE and the M SUDACs. z^k_l is the additive white Gaussian noise(AWGN) vector on subcarrier n with distribution $CN(0, \sigma_Z)$ and $y^k_{S,n} = [y^k_{S1,n}, y^k_{S2,n} .... y^k_{SM,n}]$, where $y^k_{SM,n}$ represents the signal received at SUDAC M.

After receiving the signals from the UE in the unlicensed band, each SUDAC multiplies the received signal by the $(M \times M)$ AF relay gain matrix $W^k_{2,n}$ and forwards the signal vector on subcarrier n to the BS in the licensed band, and $W^k_{2,n} = diag[W^k_{2,n,1}, W^k_{2,n,2} .... W^k_{2,n,M}]$ where;

$$W^k_{2,n,M} = \sqrt{\frac{P^k_{2,n,M}}{P^k_{1,n,M} * \gamma^k_{1,n,M} + \sigma^2_z}} \tag{7.3}$$

Now the signal received at the BS on subcarrier n via the SUDAC denoted by $y^k_{2,n}$ is

$$y^k_{2,n} = H^k_{2,n} W^k_{2,n} H^k_{1,n} W^k_{1,n} m^k_n + H^k_{2,n} W^k_{2,n} z^k_l + n^k_n \tag{7.4}$$

where $H^k_{2,n}$ is the $(N_T \times M)$ MIMO channel matrix between the SUDACs and the BS. n^k_n is the AWGN vector on subcarrier n with distribution $CN(0, \sigma_N)$.

7.2.2 *Singular Value Decomposition*

By doing SVD, we can convert our end to end MIMO channel to N_s parallel channels. We denote the MIMO channel matrix for the first hop as

$$H_{1,n} = U_{1,n} \sum_{1,n} (V_{1,n})^H \tag{7.5}$$

where $U_{1,n} \in \mathbb{C}^{M \times M}$, $(V_{1,n})^H \in \mathbb{C}^{\mathbb{N_D} \times \mathbb{N_D}}$ and $\sum_{1,n}$ is the $(M \times N_D)$ diagonal matrix whose diagonal singular values represent the channel to noise ratio ($\sqrt{\gamma_{1,n,j}}$) on spatial channel j

for subcarrier n, where $j = [1, 2, ..., N_s]$
Similarly, for the second hop, by using SVD

$$H_{2,n} = U_{2,n} \sum_{2,n} (V_{2,n})^H \tag{7.6}$$

where $U_{2,n}$,$(V_{2,n})^H \in \mathbb{C}^{N_T \times N_T}$ and $\mathbb{C}^{M \times M}$ are unitary matrices, and $\sum_{2,n}$ is the $(N_T \times M)$ diagonal matrix with diagonal elements representing the equivalent CNR values for the second hop on the spatial channel j ($\sqrt{\gamma_{2,n,j}}$).

After doing SVD, the MIMO channel is converted to N_s parallel channels where;

$$N_s \leq [Rank(H_{1,n}), Rank(H_{2,n})] \tag{7.7}$$

So, the precoding matrices adopted by the UE and SUDAC as given by theorem 1 in [100] are ,

$$W_{1,n}^k = \hat{V_{1,n}} P_{1,n} \tag{7.8}$$

where $\hat{V_{1,n}}$ consists of the N_s columns of $(V_{1,n})^H$ corresponding to the non-zero singular values of $\sum_{1,n}$ and $P_{1,n}$ is the $(N_s \times N_s)$ power allocation diagonal matrix for the UE to SUDAC(relay) link, $diag(P_{1,n}) = [\sqrt{P_{1,n,1}^k} ...... \sqrt{P_{1,n,N_s}^k}]$ Similarly,

$$W_{2,n}^k = \hat{V_{2,n}} P_{2,n} (\hat{U_{1,n}})^H \tag{7.9}$$

where $\hat{V_{2,n}}$ and $(\hat{U_{1,n}})^H$ are the N_s rightmost columns of $V_{2,n}$ and $U_{1,n}$, $P_{2,n}$ is the diagonal power allocation matrix for the SUDAC to BS link, $diag(P_{2,n}) = [\sqrt{P_{2,n,1}^k} ...... \sqrt{P_{2,n,N_s}^k}]$.
Therefore, the end-to-end rate of the system on subcarrier n denoted by R_n^k is given as

$$R_n^k = \sum_{j=1}^{N_s} \log(1 + SNR_{n,j}^k) \tag{7.10}$$

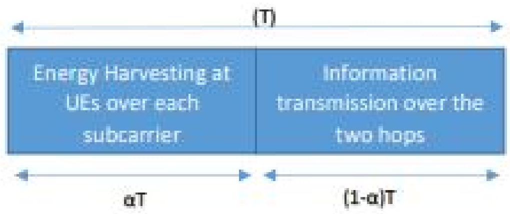

Figure 7.2: Framework of TS protocol

and the SNR can be expressed as in [100];

$$SNR_{n,j}^{k} = \frac{\gamma_{1,n,j} P_{1,n,j}^{k} \gamma_{2,n,j} P_{2,n,j}^{k}}{\gamma_{1,n,j} P_{1,n,j}^{k} + \gamma_{2,n,j} P_{2,n,j}^{k}} \tag{7.11}$$

7.2.3 TS Protocol

The framework of time switching based (TS) protocol is presented in the Fig. 7.2 where the time period T is divided into two phases. The first phase is of duration αT. This phase is used to transfer energy to UEs from the SUDACs available and $\alpha \in [0, 1]$ is the time switching factor. The second phase is of $(1 - \alpha)T$ duration and it is used to transfer information from the UEs to SUDACs and from SUDACs to BS. For simplicity, we normalize the time period T to be 1. In the first phase, only energy is transferred. Thus, the received signal at UE k denoted by $y_{UE,n}^{k}$ is

$$y_{UE,n}^{k} = H_{0,n}^{k} s_{n}^{k} + z_{l}^{k} \tag{7.12}$$

where $H_{0,n}^{k}$ is the $(N_D \times M)$ MIMO channel matrix for the first hop between the M SUDACs and the UE. $y_{UE,n}^{k}$ represents the signal received at UE k for energy harvesting.

The total harvested energy at the UE k over subcarrier n denoted by $E_{harv,n}^{k}$ is given by

$$E_{harv,n}^{k} = \alpha\eta[\sum_{j}(P_{0,n,j}^{k})(\gamma_{0,n,j}^{k})] \tag{7.13}$$

where η describes the converting efficiency of the energy transducer in converting the harvested energy to electrical energy. Here, we assume η to be 1.

7.3 Optimization problem formulation

The optimization problem for the SUDAS assisted MIMO-OFDMA system can be expressed as:

$$\max_{\alpha, m_n^k, P_{1,n,j}^k, P_{2,n,j}^k} \quad \sum_{k=1}^{K}\sum_{n=1}^{n_F}(1-\alpha)m_n^k R_n^k$$

$$s.t$$

$$\sum_{j=1}^{N_s} m_n^k P_{1,n,j}^k \leq \frac{E_{harv,n}^k}{1-\alpha}; \forall k, \forall n \tag{7.14a}$$

$$\sum_{k=1}^{K}\sum_{n=1}^{n_F}\sum_{j=1}^{N_s} m_n^k P_{2,n,j}^k \leq MP_R \tag{7.14b}$$

$$\sum_{k=1}^{K} m_n^k \leq 1; \quad \forall n \tag{7.14c}$$

$$m_n^k \epsilon [0,1]; \quad \forall k, \forall n \tag{7.14d}$$

$$P_{1,n,j}^k \geq 0 \tag{7.14e}$$

$$P_{2,n,j}^k \geq 0 \tag{7.14f}$$

$$0 \leq \alpha \leq 1 \tag{7.14g}$$

where the objective is to maximize the end-to-end achievable information rate. m_n^k, $P_{1,n,j}^k$, $P_{2,n,j}^k$ and α are the decision variables and m_n^k is the subcarrier allocation variable. Moreover, constraints (7.14c) and (7.14d) are imposed to ensure that each subcarrier serves atmost one user. Constraints (7.14a) and (7.14b) are the transmit power constraints of the energy harvesting users and the SUDACs (relays) while constraint (7.14g) shows that the fraction of time in which the users harvest energy is between 0 and 1.

It can be observed that the above problem consists of a non-convex objective function. It is a combinatorial optimization problem with discrete variable m_n^k. Moreover, constraints (7.14a) and (7.14b) are non-linear. Due to these reasons, the problem is very difficult to solve so, we solve it as follows.

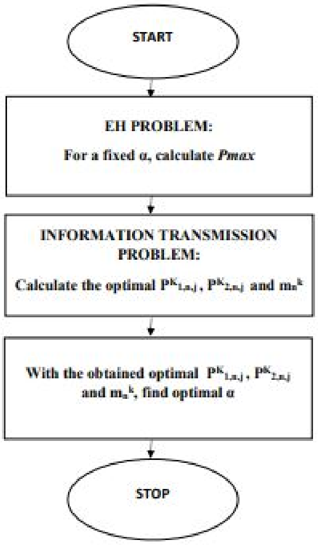

7.4 Optimal Design Of TS Protocol

We know that in the first phase of the TS protocol, only energy is transferred to the UEs from the SUDACs which means we need to deal with $E^{k}_{harv,n}$ only. Based on this, we present the solution of our problem in the flow chart above.

7.4.1 EH Problem

For a given α, we can see from the equation (7.13) that larger $E^{k}_{harv,n}$ means more power available to the UEs to transfer the information. This motivates us that the objective of our EH Problem should be maximize $E^{k}_{harv,n}$, as we need users to harvest more power. For this purpose, we present an algorithm below to find the EH solution. The sub optimal EH

Algorithm 9 SUBOPTIMAL EH ALGORITHM

1. $for\ k = 1, 2, .., K;$
2. $find\ (n) = \max\limits_{n=1,2,...,N} [\gamma^{k}_{0,n,1}]$
3. $assign\ (MP_R)\ to\ [\lambda^{k}_{0,n,1}]\ corresponding\ to\ [\gamma^{k}_{0,n,1}]$
4. end

algorithm is described as follows. We find the best subcarrier for each user (Lines 1-2) and allocate all the power MP_R to the subcarrier with the maximum $\gamma^{k}_{0,n,1}$(Line 3). The power harvested by each user denoted by P_k is therefore given by

$$P_k = \frac{\alpha\eta M P_R(\gamma^k_{0,n,1})}{1-\alpha} \tag{7.15}$$

The total harvested power by all the users in the system denoted by $Pmax$ is

$$Pmax = \sum_{k=1}^{K} P_k \tag{7.16}$$

7.4.2 Information Transmission Problem

After, we find the optimal EH problem solution, the optimization problem is transformed to

$$\max_{m^k_n, P^k_{1,n,j}, P^k_{2,n,j}} \quad \sum_{k=1}^{K}\sum_{n=1}^{n_F} m^k_n R^k_n$$

$$s.t$$

$$\sum_{j=1}^{N_s} m^k_n P^k_{1,n,j} \leq P_{max}; \forall k, \forall n \tag{7.17a}$$

$$\sum_{k=1}^{K}\sum_{n=1}^{n_F}\sum_{j=1}^{N_s} m^k_n P^k_{2,n,j} \leq M P_R \tag{7.17b}$$

$$\sum_{k=1}^{K} m^k_n \leq 1; \quad \forall n \tag{7.17c}$$

$$m^k_n \epsilon [0,1]; \quad \forall k, \forall n \tag{7.17d}$$

$$P^k_{1,n,j} \geq 0 \tag{7.17e}$$

$$P^k_{2,n,j} \geq 0 \tag{7.17f}$$

This transformed problem is similar to the problem in [100], therefore we use the same solution as presented in that work to find the optimal power $P^k_{1,n,j}$, $P^k_{2,n,j}$ and subcarrier allocation m^k_n. We observe that there is a combinatorial constraint (7.17d). To relax this, we adopt a time sharing approach [102] such that m^k_n is a real valued variable between 0 and 1. We note that after adopting time sharing relaxation approach, the optimization problem is jointly concave with respect to the variables. So, we solve it by using iterative resource allocation algorithm based on alternating optimization. Please refer to [100] for the details.

7.4.3 Finding Optimal α

After finding the optimal power and subcarrier allocation variables, we find optimal α. It can be observed that our objective function $[(1-\alpha)m_n^k R_n^k]$ gives 0 when $\alpha = 0$ *or* 1. Means, there exists an optimal value within the interval $(0, 1]$. For finding the optimal value, we use the hill climbing algorithm [103] which has a fast convergence.

7.5 Numerical Results and Discussions

The goal of this section is to evaluate the system performance based on simulations. We assume that there are k UEs located in an indoor environment. The total bandwidth of the licensed band is assumed to be 5 MHz so each subcarrier has a bandwidth of $5 * 10^6/N$ Hz. The distances between the BS and each SUDAC and between each SUDAC and UEs are different as SUDACs (relays) are assumed to be scattered in an indoor environment. Besides this, the path loss effect is also considered, where we assume it to be 3.7 for the licensed and 4.7 for the unlicensed band. For simplicity, we assume that $N_s \leq min[N_T, M, N_D]$. To show the performance gain of our proposed optimal TS scheme, we consider two configurations as benchmarks i.e, TS with fixed $\alpha = 0.1$, and a basic system which utilizes only licensed band.

7.5.1 Performance vs Pmax

Fig. 7.3 illustrates the performance of various schemes for different transmission powers for $N = 8$ subcarriers, $K = 2$ UEs and $M = 8$ SUDACs. It can be seen from the figure that all schemes achieve higher achievable information rate as Pmax increases, this is because higher Pmax will lead to high SNR for the system. It is also shown that the performance of the proposed optimized TS scheme is better than the TS with a fixed α for both the SUDAS and the basic system. Note that we found optimal α to be $214 * 10^{-6}$ for SUDAS system and $20.5 * 10^{-3}$ for the basic system. Besides, it can also be observed that the SUDAS system achieves higher performance gain as compared to the basic system.

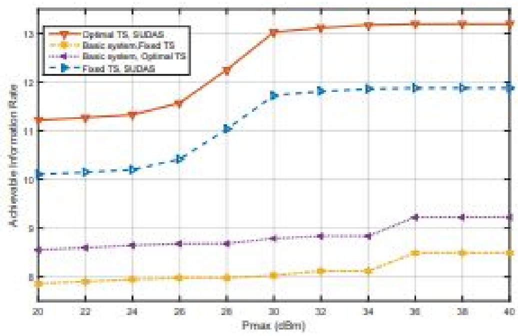

Figure 7.3: Pmax versus Achievable information rate of the system

7.5.2 Performance vs Number of Subcarriers

Fig. 7.4 shows the achievable information rate for different number of subcarriers in the system with P_{max}=20dBm. It can be observed from the figure that as the number of subcarriers increases, the performance of both the SUDAS and basic system increases. However, the increasing rate of both the curves becomes slower with the increment of subcarriers, the reason might be that more subcarriers bring more flexible configuration to increase the system rate but with a fixed system bandwidth, more subcarriers means smaller bandwidth allocated to each subcarrier. So, there is the trade off between the number of subcarriers and system achievable information rate.

7.5.3 Number of SUDACs (Relays) vs α

Fig. 7.5 depicts the number of SUDACs versus α. It is observed that the fraction of time for energy harvesting α descreases as we increase the number of SUDACs, which in turn means higher achievable information rate of the system. From the figure, we can notice that when the number of SUDACs are eight, the fraction of time for EH α is very close to what we have found.

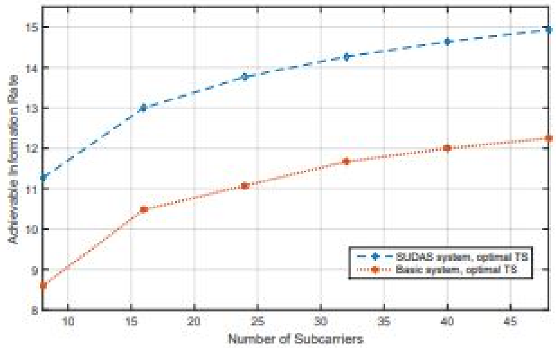

Figure 7.4: Number of subcarriers vs achievable information rate of the system

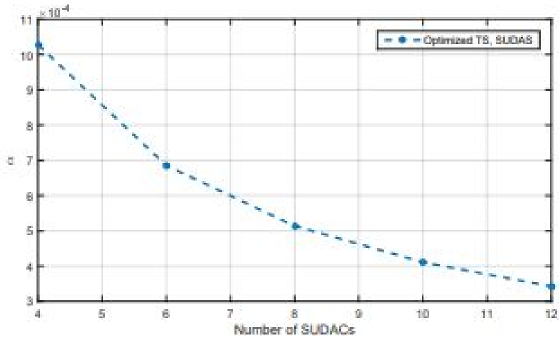

Figure 7.5: Number of SUDACs vs α

7.6 Conclusion

In this chapter, we studied the wireless energy and information transfer in SUDAS assisted multicarrier transmission system, SUDAS is a system which utilizes both licensed and unlicensed bands. For EH, we present the time switching based (TS) protocol. To investigate the system performance, we formulated a non convex optimization problem with the objective of maximizing the achievable rate of the system. For the solution of the problem, we divided the main problem into two sub problems and presented some algorithms. The simulation results suggested that the SUDAS system outperforms the previous systems. Also, the effect of the number of SUDACs and the number of subcarriers on the system performance has been discussed.

Chapter 8

CONCLUSION

In this thesis, we have investigated the resource allocation in full-duplex relay based WPCN and SWIPT networks. We have investigated novel optimization frameworks for the optimization of time allocation, scheduling and relay selection. First, we studied the transmission time minimization and throughput maximization optimization problems through relay selection in an FD-WPCCN, respectively. Incorporating the on-off transmission scheme, we then investigated the transmission time minimization and throughput maximization problems using scheduling and relay selection in FD-WPCCN. Note that we have incorporated a practical non-linear EH model based on logistic function in the above mentioned FD-WPCCN works. For the SWIPT network, we first provided the outage analysis of an FD-DF relay system with a practical non-linear CLC-EH model and presented the optimization problems of outage throughput and EE maximization. Then, we extended the system model to a multi-relay-user FD-MIMO incorporating self-energy recycling, considering a logistic function based non-linear EH model. Self-energy recycling exploits the self-interference that arises due to the FD mode in a very useful manner. We presented the resource allocation and relay selection optimization framework with the objective of maximizing the sum-throughput in a SWIPT FD-DF MIMO system. Finally, we have studied the resource allocation in an AF relay based SWIPT system employing SUDAS and presented an optimization framework for the throughput maximization.

We believe that our studies for different network models of relay based WPCN and SWIPT are very promising for the emerging future wireless communication networks such as IoT and MTC over the 5G communication system. This is due to the similar application requirement and network characteristics of the sensors in WPCN and SWIPT. In future, we plan to incorporate our solutions and findings to realize the dream of attaining perpetual lifetime for more spectrum efficient WPCNs and SWIPTs. Moreover, we will incorporate machine learning schemes to solve the optimization frameworks in a very low run-time computational complexity.

BIBLIOGRAPHY

[1] A. Nosratinia, T. Hunter, and A. Hedayat, "Cooperative communication in wireless networks," *IEEE Communications Magazine*, vol. 42, no. 10, pp. 74–80, 2004.

[2] Y. Zhao, Q. Li, L. Huang, S. Feng, T. Han, and J. Zhang, "Wireless information and power transfer on cooperative multi-path relay channels," in *2016 IEEE/CIC International Conference on Communications in China (ICCC)*, pp. 1–6, 2016.

[3] D. Sui, F. Hu, W. Zhou, M. Shao, and M. Chen, "Relay selection for radio frequency energy-harvesting wireless body area network with buffer," *IEEE Internet of Things Journal*, vol. 5, no. 2, pp. 1100–1107, 2018.

[4] H. Nasir, N. Javaid, M. Imran, M. Shoaib, and M. Anwar, "Simultaneous wireless information and power transfer for buffer-aided cooperative relaying systems," in *2018 14th International Wireless Communications Mobile Computing Conference (IWCMC)*, pp. 845–849, 2018.

[5] Y. Gu, H. Chen, Y. Li, Y.-C. Liang, and B. Vucetic, "Distributed multi-relay selection in accumulate-then-forward energy harvesting relay networks," *IEEE Transactions on Green Communications and Networking*, vol. 2, no. 1, pp. 74–86, 2018.

[6] F. Wang, S. Guo, Y. Yang, and B. Xiao, "Relay selection and power allocation for cooperative communication networks with energy harvesting," *IEEE Systems Journal*, vol. 12, no. 1, pp. 735–746, 2018.

[7] D. Wang, R. Zhang, and X. Cheng, "Full-duplex energy-harvesting relay networks: Capacity-maximizing relay selection," *Journal of Communications and Information Networks*, vol. 3, no. 3, pp. 79–85, 2018.

[8] D. Wang, R. Zhang, X. Cheng, and L. Yang, "Relay selection in two-way full-duplex energy-harvesting relay networks," in *2016 IEEE Global Communications Conference (GLOBECOM)*, pp. 1–6, 2016.

[9] D. Wang, R. Zhang, X. Cheng, L. Yang, and C. Chen, "Relay selection in full-duplex energy-harvesting two-way relay networks," *IEEE Transactions on Green Communications and Networking*, vol. 1, no. 2, pp. 182–191, 2017.

[10] H. Chen, Y. Li, J. Luiz Rebelatto, B. F. Uchôa-Filho, and B. Vucetic, "Harvest-then-cooperate: Wireless-powered cooperative communications," *IEEE Transactions on Signal Processing*, vol. 63, no. 7, pp. 1700–1711, 2015.

[11] Y. Gu, H. Chen, Y. Li, and B. Vucetic, "An adaptive transmission protocol for wireless-powered cooperative communications," in *2015 IEEE International Conference on Communications (ICC)*, pp. 4223–4228, 2015.

[12] A. G. Onalan, E. D. Salik, and S. Coleri, "Relay selection, scheduling, and power control in wireless-powered cooperative communication networks," *IEEE Transactions on Wireless Communications*, vol. 19, no. 11, pp. 7181–7195, 2020.

[13] R. Corless, G. Gonnet, D. E. G. Hare, D. J. Jeffrey, and D. E. Knuth, "On the lambertw function," *Advances in Computational Mathematics*, vol. 5, pp. 329–359, 1996.

[14] M. S. Iqbal, Y. Sadi, and S. Coleri, "Minimum length scheduling for full duplex time-critical wireless powered communication networks," *IEEE Transactions on Wireless Communications*, vol. 19, no. 9, pp. 5993–6006, 2020.

[15] M. Ku, W. Li, Y. Chen, and K. J. Ray Liu, "Advances in energy harvesting communications: Past, present, and future challenges," *IEEE Communications Surveys Tutorials*, vol. 18, no. 2, pp. 1384–1412, 2016.

[16] D. Mishra, S. De, and D. Krishnaswamy, "Dilemma at rf energy harvesting relay: Downlink energy relaying or uplink information transfer?," *IEEE Transactions on Wireless Communications*, vol. 16, no. 8, pp. 4939–4955, 2017.

[17] M. A. Hossain, R. Md Noor, K. L. A. Yau, I. Ahmedy, and S. S. Anjum, "A survey on simultaneous wireless information and power transfer with cooperative relay and future challenges," *IEEE Access*, vol. 7, pp. 19166–19198, 2019.

[18] X. Kang, C. K. Ho, and S. Sun, "Full-duplex wireless-powered communication network with energy causality," *IEEE Transactions on Wireless Communications*, vol. 14, no. 10, pp. 5539–5551, 2015.

[19] X. Li, Q. Tang, and C. Sun, "The impact of node position on outage performance of rf energy powered wireless sensor communication links in overlaid deployment scenario," *Journal of Network and Computer Applications*, vol. 73, pp. 1–11, 2016.

[20] S. A. A. Kazmi, M. S. Iqbal, and S. Coleri, "Total transmission time minimization through relay selection for full-duplex wireless powered cooperative communication networks," *Grieco L.A., Boggia G., Piro G., Jararweh Y., Campolo C. (eds) Ad-Hoc, Mobile, and Wireless Networks. ADHOC-NOW*, vol. 12338, pp. 257–268, 2020.

[21] M. S. Iqbal, S. A. Abbas Kazmi, Y. Sadi, and S. Coleri, "Scheduling and relay selection for full-duplex wireless powered cooperative communication networks," *IEEE 6th International Conference on Computer and Communications (ICCC)*, pp. 188–193, 2020.

[22] E. Boshkovska, D. W. K. Ng, N. Zlatanov, and R. Schober, "Practical non-linear energy harvesting model and resource allocation for swipt systems," *IEEE Communications Letters*, vol. 19, no. 12, pp. 2082–2085, 2015.

[23] B. C. Nguyen, T. M. Hoang, L. T. Dung, and T. Kim, "Impacts of nonlinear energy harvesting and residual self-interference on the performance of full-duplex decode-and-forward relay system," *IEEE Access*, vol. 9, pp. 42333–42344, 2021.

[24] Z. Wei, S. Sun, X. Zhu, D. In Kim, and D. W. K. Ng, "Resource allocation for wireless-powered full-duplex relaying systems with nonlinear energy harvesting efficiency," *IEEE Transactions on Vehicular Technology*, vol. 68, no. 12, pp. 12079–12093, 2019.

[25] R. Pabst, B. H. Walke, D. C. Schultz, P. Herhold, H. Yanikomeroglu, S. Mukherjee, H. Viswanathan, M. Lott, W. Zirwas, M. Dohler, H. Aghvami, D. D. Falconer, and G. P. Fettweis, "Relay-based deployment concepts for wireless and mobile broadband radio," *IEEE Communications Magazine*, vol. 42, no. 9, pp. 80–89, 2004.

[26] O. Ozel, K. Tutuncuoglu, J. Yang, S. Ulukus, and A. Yener, "Transmission with energy harvesting nodes in fading wireless channels: Optimal policies," *IEEE Journal on Selected Areas in Communications*, vol. 29, no. 8, pp. 1732–1743, 2011.

[27] H. Ju and R. Zhang, "Throughput maximization in wireless powered communication networks," *IEEE Transactions on Wireless Communications*, vol. 13, no. 1, pp. 418–428, 2014.

[28] S. A. A. Kazmi, M. S. Iqbal, and S. Coleri, "Relay selection and throughput maximization for full duplex wireless powered cooperative communication networks," *IEEE International Symposium on Personal, Indoor and Mobile Radio Communications, PIMRC*, pp. 1–1, 2021.

[29] R. Morsi, D. S. Michalopoulos, and R. Schober, "Performance analysis of near-optimal energy buffer aided wireless powered communication," *IEEE Transactions on Wireless Communications*, vol. 17, no. 2, pp. 863–881, 2018.

[30] R. Morsi, D. S. Michalopoulos, and R. Schober, "On-off transmission policy for wireless powered communication with energy storage," in *2014 48th Asilomar Conference on Signals, Systems and Computers*, pp. 1676–1682, 2014.

[31] M. S. Iqbal, Y. Sadi, and S. Coleri, "Optimal on-off transmission schemes for full duplex wireless powered communication networks," in *2020 IEEE International Black Sea Conference on Communications and Networking (BlackSeaCom)*, pp. 1–6, 2020.

[32] X. Xie, J. Chen, and Y. Fu, "Outage performance and qos optimization in full-duplex system with non-linear energy harvesting model," *IEEE Access*, vol. 6, pp. 44281–44290, 2018.

[33] E. Hossain and M. Hasan, "5g cellular: key enabling technologies and research challenges," *IEEE Instrumentation Measurement Magazine*, vol. 18, no. 3, pp. 11–21, 2015.

[34] E. V. D. Meulen, "Three-terminal communication channels," *IEEE Communications Magazine*, vol. 3, pp. 120–154, 1971.

[35] R. Pabst, B. Walke, D. Schultz, P. Herhold, H. Yanikomeroglu, S. Mukherjee, H. Viswanathan, M. Lott, W. Zirwas, M. Dohler, H. Aghvami, D. Falconer, and G. Fettweis, "Relay-based deployment concepts for wireless and mobile broadband radio," *IEEE Communications Magazine*, vol. 42, no. 9, pp. 80–89, 2004.

[36] S. Sudevalayam and P. Kulkarni, "Energy harvesting sensor nodes: Survey and implications," *IEEE Communications Surveys Tutorials*, vol. 13, no. 3, pp. 443–461, 2011.

[37] T. D. Ponnimbaduge Perera, D. N. K. Jayakody, S. K. Sharma, S. Chatzinotas, and J. Li, "Simultaneous wireless information and power transfer (swipt): Recent

advances and future challenges," *IEEE Communications Surveys Tutorials*, vol. 20, no. 1, pp. 264–302, 2018.

[38] Y. Chen, "Energy-harvesting af relaying in the presence of interference and nakagami-*m* fading," *IEEE Transactions on Wireless Communications*, vol. 15, no. 2, pp. 1008–1017, 2016.

[39] A. A. Nasir, X. Zhou, S. Durrani, and R. A. Kennedy, "Throughput and ergodic capacity of wireless energy harvesting based df relaying network," in *2014 IEEE International Conference on Communications (ICC)*, pp. 4066–4071, 2014.

[40] A. A. Nasir, X. Zhou, S. Durrani, and R. A. Kennedy, "Relaying protocols for wireless energy harvesting and information processing," *IEEE Transactions on Wireless Communications*, vol. 12, no. 7, pp. 3622–3636, 2013.

[41] H. Lee, C. Song, S.-H. Choi, and I. Lee, "Outage probability analysis and power splitter designs for swipt relaying systems with direct link," *IEEE Communications Letters*, vol. 21, no. 3, pp. 648–651, 2017.

[42] R. Tao, A. Salem, and K. A. Hamdi, "Adaptive relaying protocol for wireless power transfer and information processing," *IEEE Communications Letters*, vol. 20, no. 10, pp. 2027–2030, 2016.

[43] A. Gupta, K. Singh, and M. Sellathurai, "Time-switching eh-based joint relay selection and resource allocation algorithms for multi-user multi-carrier af relay networks," *IEEE Transactions on Green Communications and Networking*, vol. 3, no. 2, pp. 505–522, 2019.

[44] C. Zhong, H. A. Suraweera, G. Zheng, I. Krikidis, and Z. Zhang, "Wireless information and power transfer with full duplex relaying," *IEEE Transactions on Communications*, vol. 62, no. 10, pp. 3447–3461, 2014.

[45] M. Mohammadi, B. K. Chalise, H. A. Suraweera, C. Zhong, G. Zheng, and I. Krikidis, "Throughput analysis and optimization of wireless-powered multiple antenna full-duplex relay systems," *IEEE Transactions on Communications*, vol. 64, no. 4, pp. 1769–1785, 2016.

[46] H. Liu, K. J. Kim, K. S. Kwak, and H. Vincent Poor, "Power splitting-based swipt with decode-and-forward full-duplex relaying," *IEEE Transactions on Wireless Communications*, vol. 15, no. 11, pp. 7561–7577, 2016.

[47] H. Liu, K. J. Kim, K. S. Kwak, and H. V. Poor, "Qos-constrained relay control for full-duplex relaying with swipt," *IEEE Transactions on Wireless Communications*, vol. 16, no. 5, pp. 2936–2949, 2017.

[48] G. Chen, P. Xiao, J. R. Kelly, B. Li, and R. Tafazolli, "Full-duplex wireless-powered relay in two way cooperative networks," *IEEE Access*, vol. 5, pp. 1548–1558, 2017.

[49] J. Guo, S. Zhang, N. Zhao, and X. Wang, "Performance of swipt for full-duplex relay system with co-channel interference," *IEEE Transactions on Vehicular Technology*, vol. 69, no. 2, pp. 2311–2315, 2020.

[50] G. Nauryzbayev, M. Abdallah, and K. M. Rabie, "Outage probability of the eh-based full-duplex af and df relaying systems in $\alpha - \mu$ environment," pp. 1–6, 2018.

[51] Y. Liu, Z. Wen, N. C. Beaulieu, D. Liu, and X. Liu, "Power allocation for swipt in full-duplex af relay interference channels using game theory," *IEEE Communications Letters*, vol. 24, no. 3, pp. 608–611, 2020.

[52] A. A. Nasir, H. D. Tuan, T. Q. Duong, and H. V. Poor, "Full-duplex mimo-ofdm communication with self-energy recycling," *arXiv:1903.09921. [Online]*, 2019.

[53] C. Li, W. Wen, P. Wu, and M. Xia, "Wirelessly-powered full-duplex af mimo relay systems based on antenna switching," *IEEE Communications Letters*, vol. 23, no. 9, pp. 1640–1643, 2019.

[54] E. Boshkovska, D. W. K. Ng, N. Zlatanov, A. Koelpin, and R. Schober, "Robust resource allocation for mimo wireless powered communication networks based on a non-linear eh model," *IEEE Transactions on Communications*, vol. 65, no. 5, pp. 1984–1999, 2017.

[55] R. Morsi, E. Boshkovska, E. Ramadan, D. W. K. Ng, and R. Schober, "On the performance of wireless powered communication with non-linear energy harvesting," pp. 1–5, 2017.

[56] K. Xiong, B. Wang, and K. J. R. Liu, "Rate-energy region of swipt for mimo broadcasting under nonlinear energy harvesting model," *IEEE Transactions on Wireless Communications*, vol. 16, no. 8, pp. 5147–5161, 2017.

[57] E. Boshkovska, X. Chen, L. Dai, D. W. K. Ng, and R. Schober, "Max-min fair beamforming for swipt systems with non-linear eh model," pp. 1–6, 2017.

[58] J.-M. Kang, I.-M. Kim, and D. I. Kim, "Mode switching for swipt over fading channel with nonlinear energy harvesting," *IEEE Wireless Communications Letters*, vol. 6, no. 5, pp. 678–681, 2017.

[59] S. Wang, M. Xia, and Y.-C. Wu, "Space-time signal optimization for swipt: Linear versus nonlinear energy harvesting model," *IEEE Communications Letters*, vol. 22, no. 2, pp. 408–411, 2018.

[60] J.-M. Kang, I.-M. Kim, and D. I. Kim, "Wireless information and power transfer: Rate-energy tradeoff for nonlinear energy harvesting," *IEEE Transactions on Wireless Communications*, vol. 17, no. 3, pp. 1966–1981, 2018.

[61] J. T. L. S. Xiaobo Bai, Jingfeng Shao, "Power-splitting scheme for nonlinear energy harvesting af relaying with direct link," *Wireless Communications and Mobile Computing*, vol. 2018, 2018.

[62] S. Gautam, E. Lagunas, S. Chatzinotas, and B. Ottersten, "Relay selection and resource allocation for swipt in multi-user ofdma systems," *IEEE Transactions on Wireless Communications*, vol. 18, no. 5, pp. 2493–2508, 2019.

[63] S. Pejoski, Z. Hadzi-Velkov, and R. Schober, "Optimal power and time allocation for wpcns with piece-wise linear eh model," *IEEE Wireless Communications Letters*, vol. 7, no. 3, pp. 364–367, 2018.

[64] Y. Dong, M. J. Hossain, and J. Cheng, "Performance of wireless powered amplify and forward relaying over nakagami-*m* fading channels with nonlinear energy harvester," *IEEE Communications Letters*, vol. 20, no. 4, pp. 672–675, 2016.

[65] J. Zhang, G. Pan, and Y. Xie, "Secrecy outage performance for wireless-powered relaying systems with nonlinear energy harvesters," *Frontiers Inf Technol Electronic Eng 18*, no. 4, pp. 246–252, 2017.

[66] J. Zhang and G. Pan, "Outage analysis of wireless-powered relaying mimo systems with non-linear energy harvesters and imperfect csi," *IEEE Access*, vol. 4, pp. 7046–7053, 2016.

[67] K. Wang, Y. Li, Y. Ye, and H. Zhang, “Dynamic power splitting schemes for non-linear eh relaying networks: Perfect and imperfect csi,” pp. 1–5, 2017.

[68] A. Cvetkovic and V. Blagojevic, “Performance analysis of nonlinear energy-harvesting df relay system in interference limited nakagami-*m* fading environment,,” vol. 39, no. 6, pp. 803–812, 2017.

[69] X. Xu, A. Özçelikkale, T. McKelvey, and M. Viberg, “Simultaneous information and power transfer under a non-linear rf energy harvesting model,” pp. 179–184, 2017.

[70] B. Clerckx and E. Bayguzina, “Waveform design for wireless power transfer,” *IEEE Transactions on Signal Processing*, vol. 64, no. 23, pp. 6313–6328, 2016.

[71] B. Clerckx, “Wireless information and power transfer: Nonlinearity, waveform design, and rate-energy tradeoff,” *IEEE Transactions on Signal Processing*, vol. 66, no. 4, pp. 847–862, 2018.

[72] S. Wang, M. Xia, K. Huang, and Y.-C. Wu, “Wirelessly powered two-way communication with nonlinear energy harvesting model: Rate regions under fixed and mobile relay,” *IEEE Transactions on Wireless Communications*, vol. 16, no. 12, pp. 8190–8204, 2017.

[73] P. N. Alevizos and A. Bletsas, “Sensitive and nonlinear far-field rf energy harvesting in wireless communications,” *IEEE Transactions on Wireless Communications*, vol. 17, no. 6, pp. 3670–3685, 2018.

[74] K. M. Rabie, B. Adebisi, and M.-S. Alouini, “Half-duplex and full-duplex af and df relaying with energy-harvesting in log-normal fading,” *IEEE Transactions on Green Communications and Networking*, vol. 1, no. 4, pp. 468–480, 2017.

[75] L. Shi, Y. Ye, R. Q. Hu, and H. Zhang, “System outage performance for three-step two-way energy harvesting df relaying,” *IEEE Transactions on Vehicular Technology*, vol. 68, no. 4, pp. 3600–3612, 2019.

[76] W. Yang, W. Cao, T. Chung, and J. Morris, “Applied numerical methods using matlab,” *Hoboken, NJ, USA: Wiley*, 2005.

[77] X. Lu, P. Wang, D. Niyato, D. I. Kim, and Z. Han, "Wireless networks with rf energy harvesting: A contemporary survey," *IEEE Communications Surveys Tutorials*, vol. 17, no. 2, pp. 757–789, 2015.

[78] Z. Hadzi-Velkov, I. Nikoloska, H. Chingoska, and N. Zlatanov, "Opportunistic scheduling in wireless powered communication networks," *IEEE Transactions on Wireless Communications*, vol. 16, no. 6, pp. 4106–4119, 2017.

[79] X. Li, X. Zhou, C. Sun, and D. W. K. Ng, "Online policies for throughput maximization of energy-constrained wireless-powered communication systems," *IEEE Transactions on Wireless Communications*, vol. 18, no. 3, pp. 1463–1476, 2019.

[80] J. Chen, L. Zhang, Y.-C. Liang, X. Kang, and R. Zhang, "Resource allocation for wireless-powered iot networks with short packet communication," *IEEE Transactions on Wireless Communications*, vol. 18, no. 2, pp. 1447–1461, 2019.

[81] J. Laneman, D. Tse, and G. Wornell, "Cooperative diversity in wireless networks: Efficient protocols and outage behavior," *IEEE Transactions on Information Theory*, vol. 50, no. 12, pp. 3062–3080, 2004.

[82] A. S. Ibrahim, A. K. Sadek, W. Su, and K. J. R. Liu, "Cooperative communications with relay-selection: when to cooperate and whom to cooperate with?," *IEEE Transactions on Wireless Communications*, vol. 7, no. 7, pp. 2814–2827, 2008.

[83] A. Sendonaris, E. Erkip, and B. Aazhang, "User cooperation diversity. part i. system description," *IEEE Transactions on Communications*, vol. 51, no. 11, pp. 1927–1938, 2003.

[84] Z. Ding, I. Krikidis, B. Sharif, and H. V. Poor, "Wireless information and power transfer in cooperative networks with spatially random relays," *IEEE Transactions on Wireless Communications*, vol. 13, no. 8, pp. 4440–4453, 2014.

[85] S. Atapattu, H. Jiang, J. Evans, and C. Tellambura, "Time-switching energy harvesting in relay networks," pp. 5416–5421, 2015.

[86] G. Amarasuriya, E. G. Larsson, and H. V. Poor, "Wireless information and power transfer in multiway massive mimo relay networks," *IEEE Transactions on Wireless Communications*, vol. 15, no. 6, pp. 3837–3855, 2016.

[87] K.-H. Liu and T.-L. Kung, “Performance improvement for rf energy-harvesting relays via relay selection,” *IEEE Transactions on Vehicular Technology*, vol. 66, no. 9, pp. 8482–8494, 2017.

[88] S. A. A. Kazmi and S. Coleri, “Optimization of full-duplex relaying system with non-linear energy harvester,” *IEEE Access*, vol. 8, pp. 201566–201576, 2020.

[89] D. Hwang, K. C. Hwang, D. I. Kim, and T. Lee, “Self-energy recycling for rf powered multi-antenna relay channels,” *IEEE Transactions on Wireless Communications*, vol. 16, no. 2, pp. 812–824, 2017.

[90] Y. Zeng and R. Zhang, “Full-duplex wireless-powered relay with self-energy recycling,” *IEEE Wireless Communications Letters*, vol. 4, no. 2, pp. 201–204, 2015.

[91] A. A. Nasir, H. D. Tuan, T. Q. Duong, and H. V. Poor, “Mimo-ofdm-based wireless-powered relaying communication with an energy recycling interface,” *IEEE Transactions on Communications*, vol. 68, no. 2, pp. 811–824, 2020.

[92] D. W. K. Ng, M. Breiling, C. Rohde, F. Burkhardt, and R. Schober, “Energy-efficient 5g outdoor-to-indoor communication: Sudas over licensed and unlicensed spectrum,” *IEEE Transactions on Wireless Communications*, vol. 15, no. 5, pp. 3170–3186, 2016.

[93] Y. Rong and Y. Hua, “Optimality of diagonalization of multi-hop mimo relays,” *IEEE Transactions on Wireless Communications*, vol. 8, no. 12, pp. 6068–6077, 2009.

[94] M. Soysa, H. A. Suraweera, C. Tellambura, and H. K. Garg, “Partial and opportunistic relay selection with outdated channel estimates,” *IEEE Transactions on Communications*, vol. 60, no. 3, pp. 840–850, 2012.

[95] B. K. Chalise, L. Vandendorpe, Y. D. Zhang, and M. G. Amin, “Local csi based selection beamforming for amplify-and-forward mimo relay networks,” *IEEE Transactions on Signal Processing*, vol. 60, no. 5, pp. 2433–2446, 2012.

[96] M. Souryal and B. Vojcic, “Performance of amplify-and-forward and decode-and-forward relaying in rayleigh fading with turbo codes,” vol. 4, pp. IV–IV, 2006.

[97] B. Rankov and A. Wittneben, “On the capacity of relay-assisted wireless mimo channels,” pp. 323–327, 2004.

[98] T. F. Maciel and A. Klein, "On the performance, complexity, and fairness of suboptimal resource allocation for multiuser mimo–ofdma systems," *IEEE Transactions on Vehicular Technology*, vol. 59, no. 1, pp. 406–419, 2010.

[99] S. Schwarz, R. W. Heath, and M. Rupp, "Multiuser mimo in distributed antenna systems with limited feedback," pp. 546–551, 2012.

[100] M. Breiling, D. W. K. Ng, C. Rohde, F. Burkhardt, and R. Schober, "Resource allocation for outdoor-to-indoor multicarrier transmission with shared ue-side distributed antenna systems," pp. 1–7, 2015.

[101] K. Xiong, P. Fan, C. Zhang, and K. B. Letaief, "Wireless information and energy transfer for two-hop non-regenerative mimo-ofdm relay networks," *IEEE Journal on Selected Areas in Communications*, vol. 33, no. 8, pp. 1595–1611, 2015.

[102] C. Y. Wong, R. Cheng, K. Lataief, and R. Murch, "Multiuser ofdm with adaptive subcarrier, bit, and power allocation," *IEEE Journal on Selected Areas in Communications*, vol. 17, no. 10, pp. 1747–1758, 1999.

[103] S. Russel and P. Peter, "Artificial intelligence: A modern approach, 2nd ed. upper saddle river, nj, usa: Prentice-hall,," pp. 111–114, 2003.